# ANALYTICAL ESTIMATION OF THE EFFECTIVE DISCHARGE OF SMALL URBAN STREAMS

By

**Asif Quader**
M.Sc.

Faculty of Engineering
Department of Civil Engineering

A Thesis
Submitted to the School of Graduate Studies
in Partial Fulfillment of the Requirements
for the Degree

Doctor of Philosophy

McMaster University
Hamilton, Ontario, Canada
September 2007

Doctor of Philosophy (2007)
(Civil Engineering)

McMaster University
Hamilton, Ontario

| | |
|---|---|
| TITLE: | Analytical Estimation of the Effective Discharge of Small Urban Streams |
| AUTHOR: | Asif Quader |
| SUPERVISOR: | Dr. Yiping Guo |
| NUMBER OF PAGES: | 195 pages (I-XI, 1-185) |

# Abstract

Regardless of the design approach, the success or failure of stream restoration projects, especially in small urban streams is dependent on the accurate estimation of the channel-forming discharge. Among the different types of channel-forming discharges, effective discharge $(Q_e)$ is the only one that incorporates sediment transport mechanics in its estimation process. This thesis primarily focuses on $Q_e$, paying special attention to the different $Q_e$ estimation techniques and the different parameters involved in the quantification of $Q_e$.

Of the two existing methods of determining $Q_e$, the analytical approach is dependent on the goodness of fit between the frequency distribution pattern of the flow series and the assumed probability distribution function (pdf) and also the sediment rating curve. Frequency distribution pattern of daily streamflow data are conventionally approximated by lognormal pdfs. However, the flow characteristics of urban streams often have a definite percentage of zero flows throughout the year resulting in a low mean and high variance. That is why the conventional lognormal pdf often results in a poor fit which affects the analytical estimation of discharge such as $Q_e$ and half discharge $(Q_{1/2})$ from the pdf. Therefore, mixed exponential and gamma distributions were introduced as a part of this research which improved the overall fit and provided a more accurate way of determining $Q_e$ and $Q_{1/2}$.

$Q_e$ is dependent on a large number of variables (hydrological and sedimentological). Global sensitivity analysis of $Q_e$ using results from continuous hydrological modeling revealed that this channel-forming discharge is highly sensitive primarily to the sediment and then to the hydrological characteristics. The results also revealed that only when the exponent of the sediment rating curve is within a certain range can $Q_e$ and discharges corresponding to different recurrence intervals $(Q_t)$ be used analogously.

The determination technique of discharge indices such as $Q_e$ and $Q_{1/2}$ are data and analysis intensive. As a result, in the case of degraded streams with little or no streamflow data their applicability becomes restricted. As a part of this research, the analytical probabilistic approach was applied to eradicate the problem associated with lack of data. But before developing the analytical probabilistic approach for the estimation of $Q_e$ and $Q_{1/2}$, the existing probabilistic method of determining peak discharge was applied in a practical design problem. Encouraged by the results, the analytical probabilistic approach was applied for determining the probability of exceedence of streamflows. The advantage of the derived analytical probabilistic flow duration relationship is that it allows the construction of flow duration curves directly from watershed hydrological and climatological data, which are readily available as compared to streamflow data at daily or even smaller time steps, especially for small urban streams. The derived analytical probabilistic flow duration relationship sets up the foundation for determining different discharge indices.

# Acknowledgements

First of all, I would like to thank my Supervisor, Dr. Yiping Guo, who introduced me to this interesting field of stream restoration. I thank him for his support, guidance, and a keen interest in my work on a continuous basis. He has allowed me to develop my skills as a researcher. For that, I am sincerely grateful. I would also like to thank my Ph.D Supervisory Committee members, Dr. Brian Baetz and Dr. James Smith for their continuous support, interest and guidance during my committee meetings. Their advice and encouragement substantially aided the progress of my research. I would like to thank Dr. Jery R. Stedinger of Cornell University for allowing me to build on his ingenious approach of determining half discharge. I gratefully acknowledge the financial support provided by the Natural Sciences and Engineering Research Council of Canada (NSERC), the Ontario Graduate Scholarship for Science and Technology (OGSST), Ontario Graduate Scholarship (OGS), and the Department of Civil Engineering at McMaster University. The atmosphere and the work environment in the Department of Civil Engineering are amazing and conducive to creative research work.

My special thanks and heartfelt appreciation goes out to my loving wife, Shazia Nishat, my son Arian Quader, and my daughter Afia Quader. There presence in my life and throughout my work has always been a blessing. I do regret the times when I was selfishly absorbed in work instead of taking care of my children. Shazia in spite of being a Ph.D candidate herself has always efficiently fulfilled her duties towards the family and given me sufficient time to complete my work. For that I am entirely indebted to her. I would like to thank my parents and my brother for their strong support, encouragement, and patience. Finally, I would like to thank my Creator, the most Gracious and Merciful, the sole Sustainer and Provider. Whatever good we see in this world is because of Him and whatever evil we witness is what our hands have wrought.

**This thesis is dedicated to my wife and children.**

# Publication List

This thesis consists of the following papers:

***Paper I:***

Quader, A., Guo, Y., and Stedinger, J. R., "Analytical Estimation of Effective Discharge using Mixed Exponential Distribution Models.", submitted to the Canadian Journal of Civil Engineering in March 2007.

***Paper II:***

Quader, A., Guo, Y., and Stedinger, J. R., "Effective and f-load Discharges for Streams with Mixed Gamma Distributions.", to be submitted to the ASCE Journal of Hydrologic Engineering.

***Part III:***

Quader, A., and Guo, Y., "Hydrological and Sedimentological Parameters Affecting Effective Discharge of Small Urban Streams.", submitted to the ASCE Journal of Hydrologic Engineering in July, 2007.

***Part IV:***

Quader, A., and Guo, Y., "Peak Discharge Estimation for Urban Catchments using Analytical Probabilistic and Design Storm Approaches." ASCE Journal of Hydrologic Engineering (2006), 11(1), pp: 46-54.

***Part V:***

Guo, Y., and Quader, A., "Analytical Flow-Duration Relationships Derived from Watershed and Climate Characteristics.", Submitted to the ASCE Journal of Hydrologic Engineering in June, 2007.

Thesis related paper (included in ***Appendix A***)

Quader, A., Guo, Y., Bui, T., 2006. Discussion of "Analytical Solutions for Estimating Effective Discharge" by Peter Goodwin (2004), ASCE Journal of Hydraulic Engineering, 132(1), pp: 112-114.

## Co-Authorship

This thesis was prepared in accordance with the regulation of a 'Sandwich' thesis format by the School of Graduate Studies at McMaster University and was co-authored.

**Chapter 2: Analytical Estimation of Effective Discharge using Mixed Exponential Distribution Models**
**by: A. Quader, Y. Guo, and J. R. Stedinger**

The mathematical derivation and statistical analysis was performed by A. Quader in consultation with Y. Guo and J. R. Stedinger. The paper was written by A. Quader and edited by both Y. Guo and J. R. Stedinger.

**Chapter 3: Effective and f-load Discharges for Streams with Mixed Gamma Distributions**
**by: A. Quader, Y. Guo and J. R. Stedinger**

The idea of utilizing a mixed gamma distribution was proposed by J. R. Stedinger. The mathematical derivation using the original concept of J. R. Stedinger was performed by A. Quader through consultation with Y. Guo. The post derivation comparisons and statistical analyses were performed by A. Quader. The paper was written by A. Quader and edited by Y. Guo and J. R. Stedinger.

**Chapter 4: Hydrological and Sedimentological Parameters Affecting Effective Discharge of Small Urban Streams**
**by: A. Quader and Y. Guo**

The hydrologic modeling and post simulation data analysis were performed by A. Quader with consultation with Y. Guo. The paper was written by A. Quader and edited by Y. Guo.

**Chapter 5: Peak Discharge Estimation for Urban Catchments using Analytical Probabilistic and Design Storm Approaches**
**by: A. Quader and Y. Guo**

The application of stormwater models and data analysis were conducted by A. Quader with consultation with Y. Guo. The paper was written by A. Quader and edited by Y. Guo.

**Chapter 6: Analytical Flow-Duration Relationships Derived from Watershed and Climate Characteristics**
**by: Y. Guo and A. Quader**

The mathematical derivation, hydrologic modeling, and data analysis were performed by A. Quader in consultation with Y. Guo. The original idea and overall procedures for the mathematical derivation came from Y. Guo. The paper was written by A. Quader and edited by Y. Guo.

# Contents

# Chapter 1

## Thesis Summary

## 1.1 Introduction

This chapter summarizes the research that was conducted in this thesis. It also presents the context and motivation for undertaking this research. The primary motivation behind this research is to address some of the key issues in the emerging field of stream restoration, which is practiced throughout Europe and North America. The primary focus of this thesis is the channel-forming discharge. Therefore, this chapter carefully scrutinizes the different procedures of stream restoration and how the channel-forming discharge is connected to each and every one of them. Without a priori knowledge of stream restoration it would be very difficult to delve into and gain an appreciation of this important parameter known as the 'Channel-forming discharge'. In this chapter, the concept of restoration and to be more specific, 'stream restoration' is discussed. The existing practices and the outcome of some of these restoration projects are reviewed. The important role played by the channel-forming discharge in these restoration activities is explained. Finally, a summary of the papers included in this thesis is presented.

## 1.2 Context and Motivation

Throughout history streams and rivers have acted as an important life line for communities, towns, cities and even civilizations. These streams and rivers nourish and support the natural environment around its banks and in its flow path. Numerous aquatic and terrestrial species rely on these watercourses for their growth and survival. The hydraulic (flow depth, velocity, cross-sectional area etc.) and morphometric (sinuosity, amplitude, pool/riffle sequence etc.) characteristics of these watercourses create an environment that is conducive to a healthy and sound ecosystem. Even during dry periods when the streamflow is significantly low, the water stored in the pools protects certain aquatic species from different predators. Thus these streams play an important role in the

life cycle of different species. At the same time these streams also maintain a symbiotic relationship with native vegetation of the surrounding area. As the streams maintain a well-balanced ground water table, the plants and vegetation in return keeps the water temperature low by providing adequate shading during dry periods. A healthy biodiversity in or around watercourses serves as an important indicator of the health of the stream or its "degree of naturalness".

However, the flow pattern and the resulting hydraulic and morphometric characteristics of a stream are strongly influenced by the upstream catchment characteristics. The rapid growth of urbanization changes the landuse pattern of upstream catchments significantly. Increase in the amount of impervious area has forced streams to accommodate high runoff volume over a short period of time. This abnormal flow pattern not only changes the form and shape of the streams but also negatively influences the aquatic and terrestrial habitat that relies on the stream. Urban development strips a stream of its naturalness and forces different species to abandon the natural environment of the stream and seek shelter elsewhere. At one point, these streams become void of all naturalness and act only as a water conveyance pathway or ditch. This unhealthy transformation of natural streams is most noticeable in streams located in an urban environment, commonly known as urban streams.

In addition to substantial changes in landuse pattern, factors such as global climate change also has deleterious effect on these urban streams. As streams are exposed to high runoff volumes more and more frequently, it changes the shape and form of these streams, causing undercutting of the bed and banks, rapid erosion, and excessive sedimentation. In order to improve the overall condition of the stream and to return a stream back to its natural condition, stream restoration/rehabilitation projects have to be implemented. From either a social, political, economic or environmental perspective, these rehabilitation projects are of utmost importance. Urban streams and their rehabilitation are the focal point of this research.

The Society of Ecological Restoration (SER)'s Primer of Ecological Restoration identifies the goal of restoration as a process that assists the recovery of an ecosystem that has been degraded, damaged, or destroyed (Davis and Slobodkin 2004). Human activities, e.g., urbanization and agriculture, have diverse and far-reaching effects (Rose and Peters 2001; Lee and Heaney 2003; Palmer and Allan 2006; Davis et al. 2003). By changing the landscape and replacing it with hard surfaces, natural replenishment of ground water tables decreases and streams become flashy. Flashy streams cause flooding of the surrounding area, destroying property and lives. Heavy rainfall during the summer can cause an influx of warm water (as the water flows over the impervious surface that retains heat) into the stream, which destroys fish and bottom dwelling organisms. In addition to the destruction of aquatic and terrestrial habitat, the hydraulic and morphometric characteristics of these streams also change significantly. Nowadays this phenomenon has become so common that more than one third of the rivers in the U.S. are listed as impaired (US EPA 2000). Specially, the condition of streams that are in direct or indirect contact with urban areas is of serious concern. These streams known as 'urban streams' usually have small drainage areas and cannot be treated the same way as large streams or rivers. This thesis focuses on the flow characteristics of these small urban streams.

Urban streams are markedly different from rural streams as the former ones are subject to numerous infrastructure constraints. Urban streams also experience a wide range of flow regime, from high peaks of short duration to low baseflows. Furthermore, the bankfull indicators are more difficult to locate in urban streams because of degraded stream banks and fast-changing hydrologic conditions. Urban streams are also exposed to more structures, e.g., culverts, bridges etc., which alter the flow hydraulics. Finally, changing sediment regime because of land development in the upstream catchment is another characteristic of these urban streams. To address the special needs of urban streams 'Urban Stream Restoration Subcommittee' was formed in the summer of 2001, for the sole purpose of promoting awareness of planning, design and monitoring of urban stream restoration projects (ASCE RRS. 2003).

In order to improve the overall condition of these urban streams, stream restoration measures are undertaken, which aim at assisting the establishment of improved hydrologic, geomorphic, and ecological processes in a degraded watershed system (Wohl et al. 2005). Urban stream restoration is an evolving field where most of the projects were undertaken within the last decade (Andrews 1987; Kondolf et al. 2001; Morris and Moses 1999; Ness and Joy 2002; Neizgoda and Johnson 2007; Bhuiyan et al. 2007). Attempt to develop a comprehensive database of these restoration projects has not been successful. Most of these restoration databases are highly fragmented and often rely on *ad hoc* or volunteer data entry, except for the National River Restoration Science Synthesis (NRRSS) database. The NRRSS database reports a synthesis of information on 37,099 restoration projects from seven geographic regions across the U.S. According to the NRRSS database, the U.S. has spent over $1 billion dollars in average per year on river and stream restoration, since 1990 (Bernhardt et al. 2005). In spite of this huge expenditure, the success rate of these restoration projects is minimal. The primary reasons behind this poor performance are: (1) Many projects do not have clearly defined goals or the goals set forth are ambiguous [In the NRRSS database 20% of the projects had no listed goals (Bernhardt et al. 2005)]; (2) Failure to conduct an accurate preliminary assessment of the stream; (3) The lack of monitoring effort in the post-project phase [In the NRRSS database only 10% of project records indicated that any form of monitoring occurred (Bernhardt et al. 2005)]. In spite of the low success rate, there is a growing demand for stream restoration projects at both local and federal level. At the same time environmentalists as well as the general public are gradually realizing the importance of watershed management. Schlapfer and Witzig (2006) showed that the demand for river restoration projects is dependent on population density, mean income, and the 'naturalness' of the river. The remarkable growth in urban stream and subwatershed restoration can be attributed to factors such as new regulatory mandates, increased municipal restoration capability, growth in urban watershed organizations, and increased public demand for cleaner and greener neighborhoods (Schueler 2004).

## 1.3 Stream Restoration Techniques

Natural stable streams maintain their dimension, pattern, and profile over time. They migrate slowly across the landscape over long periods of time, while maintaining their shape and form. Naturally stable channels transport sediment load supplied by the watershed with no net aggradation or degradation. The product of sediment load and size are considered to be proportional to the product of stream slope and discharge, as shown in Eqn. (1.1),

$$(\text{Sediment load} \times \text{Sediment size}) \propto (\text{Stream slope} \times \text{Stream discharge}) \qquad (1.1)$$

Eqn. (1.1) shows that natural streams maintain a balance between the flow pattern and the supplied sediment load. This balance enables a stream to remain in equilibrium with stable form and shape over time. From Eqn. (1.1) it can be inferred that change in any one of the parameter disrupts the dynamic equilibrium of the stable stream, forcing the stream to adjust its hydraulic and morphometric characteristics that may result in a new equilibrium. Urbanization alters the watershed characteristics and the rate at which water moves across the catchment, thus disrupting this dynamic equilibrium. Urban development significantly alters the detention and retention characteristics of a catchment. Thus changing the magnitude, duration, and frequency of stream discharge, resulting in accelerated stream erosion or aggradation.

The underlying principle of natural channel design is to use the stable natural channel as a blue print and make appropriate adjustments and modifications to the degraded stream so that it would mimic the natural stable channel as closely as possible. It is a geomorphic approach to stream restoration that seeks to re-establish the dynamic equilibrium necessary for a riverine system to function on a self-sustaining basis (Abbey and Snyder 2001). Natural channel design looks holistically at the watershed impact. These impacts are investigated from a physical (flow and velocity; erosion and sediment transport) and water chemistry (pH, oxygen demand, nutrients, and temperature) perspective. Different government and private organizations adopt the concept of natural channel design with varying intermediate steps. These natural channel design

methodologies are systematically described in different manuals published by these organizations. Some of these restoration manuals are published by North Carolina Stream Restoration Institute and North Carolina Sea Grant (NCSRI and NCSG 2001), Keystone Stream Team (2002), Center for Watershed Protection [Schueler and Brown 2004; Schueler 2004], Ontario Ministry of Natural Resources (OMNR 1994), and stream restoration specialists, e.g. Rosgen (1994). In addition to the abovementioned manuals, there exists a significant literature, which addresses the issues of stream restoration from hydraulic, hydrological and ecological perspectives (FISRWG 1998; Soar and Thorne 2001; Watson et al. 1999; Shields et al. 2003; MDEWMA 2000 etc.). Furthermore, there are manuals (DCR and DSWC 2004; Biedenharn et al. 1997) that primarily focus on structural aspects of channel stabilization. Channel stabilization involves processes such as stabilization of bed and banks, grade control, flow deflection, flow diversion, etc.

The stream rehabilitation procedures outlined in these manuals or different text books (Rosgen 1996; Riley 1998) can be broadly categorized into analog, empirical and analytical (Skidmore et al. 2002; DCR and DSWC 2004; FISRWG 1998). All three approaches are nowadays practiced for the purpose of stream rehabilitation. The underlying principle between the analog and the empirical approach are the same. Both approaches are based on observed conditions. The analog approach uses the detailed hydraulic geometry of a dynamically stable reach as the design template. Instead of just one template, the empirical approach is dependent on data sets of quantified measurements from a large number of streams. The streams in both the empirical and analog approach must exist in similar environment and be dynamically stable. In both approaches regional curves are developed that express the morphometric characteristics of the stream as a function of the bankfull discharge or catchment area. As the regional curves determined in the empirical approach are dependent on statistically analyzed data sets, it is considered more theoretically sound than the analog approach.

In comparison to the analog and empirical approaches, the analytical approach is based on physically based equations and models. These physically based equations are the continuity equation, flow resistance equation, and sediment transport equation. The

analytical approach can be used without the analog or empirical approaches or can be used for their validation. The analytical design method can prove to be very useful when there are infrastructures, site constraints, and continuously changing land development patterns; a notable aspect of urban streams.

Depending on the category of the approach that is taken, each restoration manual lists a number of design steps. However, even within the same category no two restoration manuals have identical design steps. The primary reason behind this is that each restoration project is unique. Therefore based on the needs and necessities of the project, restoration engineers have made the required changes to the conventional design steps. This is not only true for the analog and empirical approaches but applicable to the analytical approach as well. Table 1.1 lists the principal design steps that are observed in analog/empirical and analytical categories.

**Table 1.1:** Primary design steps used in analog/empirical and analytical approaches

| Design steps | |
|---|---|
| Analog/Empirical | Analytical |
| 1. Determination of restoration goals | 1. Determination of restoration goals |
| 2. Stream evaluation and classification/stability assessment | 2. Preliminary design |
| 3. Channel management and design | 3. Analysis |
| 4. Implementation/construction | 4. Implementation/construction |
| 5. Monitoring | 5. Monitoring |

Table 1.1 shows that regardless of the scope or scale, most restoration projects share three common design steps, which are initial determination of the goals of the project, implementation/construction of the project based on the design specifications and finally, post project monitoring. However, two intermediate steps between the analog/empirical and analytical approaches are different. In all three categories these intermediate steps (2 and 3) dictate the success or failure of the project.

In the analog/empirical approach the second design step is stability assessment or stream evaluation and classification. This step provides the foundation for design and the basis for prediction of system response (Shields et al. 2003). In Rosgen's (1994) stream classification system, the bankfull stage is used for determining the entrenchment and width-to-depth ratio. The entrenchment, width-to-depth ratio, sinuosity, channel slope, and material are used as the primary delineative criteria in Rosgen's multi-level assessment technique. Therefore inaccurate estimation of the bankfull discharge at such a preliminary stage could result in an erroneous assessment of the stream, leading to abolition of the proposed geometric pattern, accompanied by severe aggradation and degradation of streambed and banks. Kondolf et al. (2001) described this type of erroneous design, which ultimately led to the entire reconstructed meandering channel getting washed off in a 0.9 km reach of Uvas creek, California. Similar erroneous determination of the bankfull stage causing damage to a number of restoration projects in southern Ontario were reported by Ness and Joy (2002).

The most important design step in the analytical approach is the preliminary design, followed by analysis. The primary objective of preliminary design is the computation of stable channel morphology which aims at meeting the specified goals of the restoration project. Geomorphic assessment is the first step of preliminary design which examines the climate, geology, geography, and hydrology of the basin. The second stage of preliminary design is to determine the channel-forming discharge based on the data collected from geomorphic assessment. The channel-forming discharge and geomorphic assessment are often combined together to determine the hydraulic geometry and initial dimension, pattern and profile of the degraded stream (DCR and DSWC 2004). Notably in the analog/empirical approach the bankfull discharge is considered to be highly important because it is assumed as the channel-forming discharge. In theory designing a channel to convey the channel-forming discharge should minimize the potential for excessive erosion and sedimentation (Doyle et al. 2007). The channel-forming discharge is also important in assessment of dynamic equilibrium, meander formulas, and flood plain design (Goodwin 2004). Therefore, accurate estimation of the

channel-forming discharge ($Q_{cf}$) in reality paves the way for a successful stream restoration project.

## 1.4 Channel-Forming Discharge

The channel-forming discharge is a single representative discharge that if maintained indefinitely would produce channel geometry as the long term hydrograph. It is a unique flow that over a prolonged period would theoretically yield the same hydraulic and morphometric characteristics that is shaped by the natural sequence of flows (Soar and Thorne 2001). This representative discharge forms the shape and size of channel. The existence of channel-forming discharges has proved to be extremely popular amongst hydrologists, engineers and ecologists, involved in stream rehabilitation projects.

Currently there are four types of channel-forming discharges:

1. Bankfull discharge $(Q_b)$ : The discharge corresponding to the maximum conveyance capacity of the stream, without overflowing the banks is $Q_b$. In analog/empirical approaches, $Q_b$ is considered as one of the most important design parameters. However, in urban streams with continuously changing landuse patterns and infrastructures, identification of $Q_b$ becomes highly problematic.
2. Effective discharge $(Q_e)$: $Q_e$ is based on the magnitude-frequency concept introduced by Wolman and Miller (1960). Wolman and Miller (1960) indicated that the geomorphic significance of an event is dependent not only on the magnitude of the event but also on its frequency of occurrence. Accordingly $Q_e$ is determined by combining the frequency distribution pattern of the flow series with the sediment rating curve, resulting in the transport effectiveness curve. The discharge corresponding to the peak of the transport effective curve is $Q_e$. $Q_e$ as a channel-forming discharge is the principal focus of this thesis.

3. Discharge with a particular recurrence interval $(Q_t)$: $Q_b$ often have return periods of 1 to 2 years. Under the circumstances where field estimation of $Q_b$ becomes very difficult, discharges corresponding to return periods of 1.5 or 2.5 yrs are considered as the channel-forming discharge. Both Kondolf et al (2001) and Williams (1978) have demonstrated that $Q_t$ generates a poor estimate of $Q_b$. Comparison of $Q_t$ with $Q_e$ has also proved to be unsatisfactory (Pickup 1976). This research demonstrates the circumstances under which $Q_t$ and $Q_e$ can be used analogously.
4. Half discharge $(Q_{1/2})$: Half discharge is a relatively new concept introduced by Vogel et al. (2003). It is defined as a discharge above and below which half the long term sediment load is transported. As far as the applicability is concerned it is still at its infancy. As a part of this research, the concept of half discharge was applied for a number of southern Ontario streams and the results were compared with $Q_e$. Furthermore, a new analytical solution of half discharge from mixed gamma distribution was derived and applied it to another set of southern Ontario streams.

This research focuses on discharge indices such as the effective discharge, half discharge and discharges with particular recurrence intervals. As most of the research work and this thesis centers around the effective discharge, in the next section a detailed description is provided.

## 1.5 Effective Discharge

The effective discharge is defined as the mean of the discharge increment that transports the largest fraction of the annual sediment load over a period of years (Andrews 1980). Pickup and Warner (1976) considers the effective discharge as the range of flows which, over a period of time, transports the most bedload or bed-material load. Among the widely used channel-forming discharges, the effective discharge is the only one that directly (mathematically) utilizes the sediment transport mechanics in its

estimation. The underlying principle of the effective discharge ($Q_e$) is based on the magnitude-frequency concept. In determining $Q_e$, the frequency distribution pattern of the flow series is combined with the sediment rating curve, resulting in the transport effectiveness curve. In Fig. 1.1, Curve a is the frequency distribution pattern of the flow series, Curve b is the sediment rating curve, and the combination of the two results in Curve c, which is the transport effectiveness curve. The discharge corresponding to the peak of Curve c is $Q_e$.

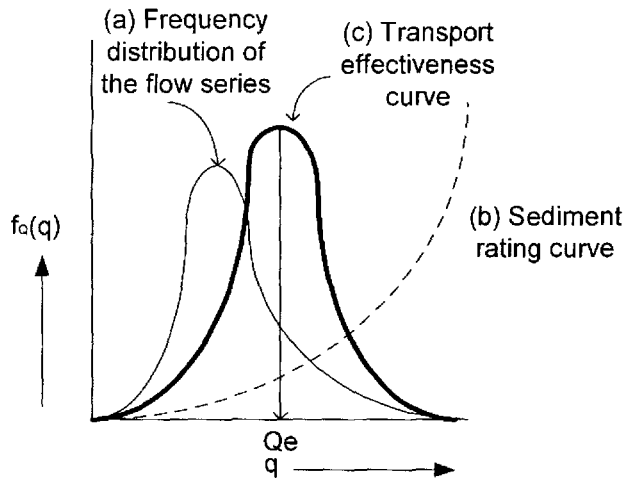


**Fig 1.1:** Determination of $Q_e$ from the transport effectiveness curve approach (Wolman and Miller 1960)

This conventional method of determining $Q_e$ is known as the transport effectiveness curve approach.

The transport effectiveness curve approach is highly sensitive to the size and number of class interval used in the flow frequency analysis. As a result, the magnitude of $Q_e$ changes due to the variation or adjustment of class intervals. Therefore, the transport effectiveness curve approach has received its fair share of criticism (Vogel et al. 2003; Lenzi et al. 2006; Sichingabula 1999; Crowder and Knapp 2005). In order to generate realistic and sensible results from this graphical approach, Biedenharn and Copeland (2000) outlined a fixed set of guidelines that aid the engineer or hydrologist

applying this method. These guidelines were strictly followed in this research whenever $Q_e$ values were determined by the transport effectiveness curve approach. In view of the problem associated with the determination of $Q_e$ from the transport effectiveness curve approach, Nash (1994) introduced the analytical approach.

The analytical approach is a mathematical representation of the transport effectiveness curve approach. The only difference is that $Q_e$ values are directly determined from closed form analytical solutions. As a result, the analytical approach does not require any graphical manipulation for determining a single representative peak. In the analytical approach, the sediment transport mechanics is represented by a power function, as shown in Eqn. (1.2).

$$Q_s = aq^b \tag{1.2}$$

In Eqn. (1.2), $Q_s$ is the quantity of sediment load (kg/sec), q is the flow rate (c.m.s), a and b are the fitting parameters. If $f_Q(q)$ is the frequency distribution function of the flow series, combining $f_Q(q)$ with Eqn. (1.2) results in the transport effectiveness E.

$$E = aq^b \times f_Q(q) \tag{1.3}$$

The peak of the transport effectiveness curve mathematically corresponds to a point where, $dE/dq = 0$. Thus, from $dE/dq = 0$, closed form analytical solution of $Q_e$ can be determined. In the analytical approach, the $f_Q(q)$ term in Eqn. (1.3) must be represented by a standard probability density function (pdf), which best represents the frequency distribution pattern of daily or an even finer temporal resolution streamflow data. Therefore, the accuracy of the analytical solution of $Q_e$ depends on the appropriateness of the sediment rating curve and the goodness-of-fit between the pdf and the frequency distribution pattern of the flow series. A poor fit or an inappropriate sediment rating curve can result in an erroneous determination of $Q_e$. Therefore, following the footsteps of Nash (1994), both Goodwin (2004) and Vogel et al. (2003) have done considerable work on the analytical investigation of $Q_e$. This thesis also includes some interesting

results on the analytical estimation technique of $Q_e$, which will be partially described in this chapter and described in detail in the following chapters.

Regardless of the shortcomings and appropriateness of $Q_e$, most researchers agree that it provides insight into the drivers of current and future destabilization, thus providing the greatest information for channel restoration design (Doyle et al. 2007; Doyle et al. 2005; Copeland et al. 2000). In light of the importance of the effective discharge and other discharge indices, e.g. half discharge ( $Q_{1/2}$ ), discharges with particular recurrence intervals ( $Q_t$ ), the following issues were particularly investigated in this thesis:

1. The analytical estimation of $Q_e$ for small urban catchments by introducing a mixed exponential distribution.
2. The analytical estimation of $Q_{1/2}$ from a mixed gamma distribution as well as its scope of applicability in small urban catchments.
3. The applicability of the analytical probabilistic approach for determining peak discharges of specific recurrence intervals in practical design situations.
4. The identification of critical hydrological and sedimentological parameters affecting $Q_e$.
5. The development of an analytical probabilistic approach for the estimation of $Q_e$.

From the abovementioned list of investigations two questions naturally arise. Firstly, what is the analytical probabilistic approach? And secondly, why is there a need to apply the analytical probabilistic approach in determining $Q_e$? These questions are answered in the following section.

## 1.6 Analytical Probabilistic Approach

The analytical probabilistic approach is based on the rainfall data analysis technique pioneered by Eagleson (1972). According to this technique, a continuous rainfall series is divided into discrete rainfall events based on a minimum time period without any

precipitation, known as the inter-event time definition (IETD). Each rainfall event in the series is characterized by its rainfall volume v, duration t, and interevent time b. Frequency analysis results of each of the rainfall characteristics for the entire rainfall series reveal that the histograms of each of the characteristics can be best represented by exponential pdfs. These exponential pdfs combined with appropriate rainfall-runoff relationships can be used for determining the pdfs of the outputs of interest using the derived probability distribution theory. According to the derived probability distribution theory, the pdf of a dependent variable can be determined from the pdfs of independent variables by using appropriate functional relationships between the dependent and independent variables. A detailed explanation of the analytical probabilistic approach is provided by Adams and Papa (2000).

In order to investigate the applicability of the analytical probabilistic approach in determining the effective discharge, the $Q_e$ estimation technique should be carefully scrutinized. Whether determined from the transport effectiveness curve approach or analytically, it is clear that the determination of $Q_e$ is more data and analysis intensive. Both methods require at least 30 to 40 years of streamflow and sediment transport data. For large streams this type of data might be available but for small urban streams they will be hard to come by. In most small urban streams this type of data are not even collected (Crowder and Knapp 2005). Furthermore, in small urban streams the temporal resolution of the data collected should also be sufficiently high to properly represent short duration high magnitude flow events. In comparison to the streamflow and sediment transport data, it is easier to collect information pertaining to the catchment characteristics. Catchment characteristics such as, the degree of imperviousness, ultimate infiltration capacity of the soil, time of concentration can be determined from the local maps, soil reports or geographic studies of the area. At the same time, instead of streamflow data it may be easier to obtain precipitation information at different temporal resolutions over long periods of time. The analytical probabilistic approach provides the opportunity for utilizing both catchment and meteorological information of the study area and ultimately determining probabilistic expressions of the parameter of interest. From these probabilistic expressions, the variable of interest can be determined. Application of

the analytical probabilistic approach was successful in determining variables of, e.g. peak discharge and runoff volume (Guo and Adams 1998a and 1998b). However, so far, this approach has not been used for determining $Q_e$. In the following section a brief summary of the papers, which are the main part of this sandwich thesis is provided.

## 1.7 Summary of Papers

### 1.7.1 Paper I

*Analytical estimation of effective discharge using mixed exponential distribution models*

The accuracy of the analytical estimation of effective discharge is dependent on the sediment rating curve and the goodness of fit between the frequency distribution pattern of the flow series and the assumed pdf. Conventionally, daily streamflow data are represented by lognormal pdfs. Frequency distribution pattern of selected southern Ontario streams indicate that below a certain drainage area the lognormal pdf does not accurately represent the frequency distribution pattern of the flow series. This means that for those small streams which are represented by lognormal pdfs, the analytical estimation of $Q_e$ would be erroneous. That is why to better represent the daily streamflow data of small streams below the critical drainage area, a mixed exponential distribution function was introduced. Goodness-of-fit results indicated that small southern Ontario streams are better approximated by the mixed exponential pdf as compared to the lognormal pdf. An analytical estimation of $Q_e$ was also determined from the mixed exponential pdf. The analytically estimated $Q_e$ values determined from mixed exponential and lognormal pdfs were compared with those obtained from transport effectiveness curves for selected southern Ontario streams. In spite of the numerical problems, $Q_e$ values obtained from the transport effectiveness curves can be considered as the most accurate as it takes the entire streamflow into consideration and the streamflow series is not approximated by a standard pdf. The results showed that $Q_e$ values determined from the proposed mixed exponential distribution function were more

accurate than those determined from lognormal pdfs. This was found to be true not only for small but for large streams.

### 1.7.2 Paper II

*Effective discharge and f-load discharge for streams with mixed gamma distribution*

The half discharge ( $Q_{1/2}$ ) is a newly introduced (Vogel et al. 2003) discharge index with limited application. Half discharge is the discharge above and below which half of the long term sediment load is transported. The concept of half discharge can be generalized as f-load discharge $(Q_f)$, which is defined as the discharge above which f fraction of the total sediment load is transported. Although both $Q_f$ and $Q_{1/2}$ are free from the subjectivity of graphical manipulation, a phenomenon that is common in determining $Q_e$ from the transport effectiveness curve approach, the analytical solution of both these discharge indices are dependent on the goodness-of-fit between the assumed pdf and the actual streamflow series. Frequency analysis of southern Ontario streams with a definite percentage of zero flows reveals that the lognormal pdf results in a poor fit. Currently there only exists an analytical solution of $Q_{1/2}$ derived from a lognormal pdf. However, compared to the lognormal pdf, the goodness-of-fit results were found to improve significantly by using a mixed gamma distribution function. Therefore in this study for the first time an analytical solution of half discharge was determined from a mixed gamma distribution. The new analytical expression of $Q_{1/2}$ was used for determining $Q_{1/2}$ values for the selected southern Ontario streams. The results showed that $Q_{1/2}$ values determined from mixed gamma distribution functions provided a more accurate prediction of half discharge compared to other conventional distributions (lognormal and gamma) for the selected streams. A comparative analysis between $Q_f$ and $Q_e$ for different values of the exponent of the sediment rating curve (b) revealed that these two types of discharge indices can be used analogously for an f value of 0.6 and under the circumstances when $b \geq 2$.

### 1.7.3 Paper III

*Hydrological and sedimentological parameters affecting effective discharge of small urban streams*

The effective discharge $Q_e$ is dependent on both watershed hydrological and sedimentological parameters. As $Q_e$ is influenced by a large number of parameters there is a growing need for identifying the most influential parameters affecting this special discharge. This would make the job of the restoration engineer much easier, as from that point the engineer can focus on the most sensitive parameters and adequately manage his/her time and budget in activities such as data collection and field verification. In this study, continuous simulation was used to simulate a wide range of catchment characteristics, resulting in diverse streamflow scenarios. At the same time a wide range of sediment characteristics were simulated. These varying hydrological and sedimentological parameters were used for determining effective discharge and other variables of interest. Global sensitivity analysis of these input (hydrological and sedimentological parameters) and output matrices (effective discharge and discharge with particular recurrence intervals) revealed sensitivity indices of different magnitudes. The results showed that $Q_e$ is highly sensitive to the exponent of the sediment rating curve, moderately sensitive to the storage coefficient and the time of concentration of the watershed. Whereas, discharges with a particular recurrence interval were found to be highly sensitive to the degree of imperviousness, the storage coefficient and the time of concentration of the watershed. The results also showed that $Q_e$ and discharge with different recurrence intervals ($Q_t$) (1.5 and 2.5 yrs) can be used analogously when the values of the exponent of the sediment rating curve are within a certain range. Beyond that range it would not be safe to use $Q_e$ and $Q_{1.5}$ or $Q_{2.5}$ analogously.

### 1.7.4 Paper IV

*Peak Discharge Estimation for Urban Catchments Using Analytical Probabilistic and Design Storm Approaches.*

In this study the analytical probabilistic approach of determining peak discharge $(Q_p)$ was applied for the first time in a practical design problem. The study area was located in the Cataraqui North Neighborhood in the city of Kingston. Peak discharge values at the inlet of a detention pond were determined by using both the analytical probabilistic and the design storm approach. Differences in rainfall data analysis and representation of rainfall input, subcatchment aggregation, and the treatment of the catchment time of concentration between the two approaches were identified as the three main causes contributing to the discrepancy in peak discharge estimates. In spite of the differences, peak discharge estimates from the two approaches were generally comparable for the design case. This study revealed that discrepancies caused by subcatchment aggregation and difference in rainfall data analysis are approximately of the same order of magnitude. Treating the time of concentration as a constant across storms of various magnitudes was found not to contribute to a large discrepancy. However, it was shown that the closer the time of concentration values used in the two approaches, the closer the resultant peak discharge estimates.

Before applying the analytical probabilistic approach for determining $Q_e$, it is necessary to observe the performance of the existing analytical probabilistic expression of peak discharge in practical design problems. This study was primarily conducted with that intention. The observed small errors in determining peak discharge rates resulting from the use of discretized and lumped catchments are illustrative that lumped hypothetical catchments with diverse catchment characteristics may be used for development and verification of the analytic probabilistic approach.

### 1.7.5 Paper V

*Analytical Flow-Duration Relationships Derived from Watershed and Climate Characteristics*

In this study closed form analytical expressions for the determination of the probability of exceedence of streamflow rates were determined. In determining these closed-form analytical expressions both rainfall characteristics of the locality and a modified event-

based rainfall-runoff transformation function were utilized. The probability of exceedence within the analytical expressions derived in this study is in fact the percentage of time a streamflow rate is exceeded. Thus using these closed-form analytical expressions of the probability of exceedence, flow duration curves can be easily constructed. The principal difference between the conventional flow duration curves and those derived from closed form analytical expressions is that the former ones are determined directly from streamflow data. Whereas those obtained from the derived closed form analytical expressions are based on watershed and rainfall characteristics. Therefore, in stream restoration projects of small urban catchments where streamflow data are mostly unavailable, the derived analytical expressions of the probability of exceedence can be utilized for determining the flow duration curves. These derived analytical probability of exceedence expressions were tested by comparing the resulting flow duration curve with that obtained from continuous streamflow data obtained from continuous simulation of hypothetical test catchments with identical physiographic characteristics. The two flow duration curves were found to conform well to each other, which indicate that the simplifying assumptions invoked in the derivation process are generally acceptable for small urban streams.

# References:


1. Abbey, K. and Snyder, C., 2001. "Citizen monitoring and natural stream channel design projects." *Monitoring Matters*, 4(3), 1-3.
2. Adams, B. J., and Papa, F., 2000. *Urban Stormwater Management Planning with Analytical Probabilistic Models*. John Wiley Sons, Inc. Printed in the U.S.A.
3. Andrews, E.D. 1980. "Effective and bankfull discharges of streams in the Yampa River basin, Colorado and Wyoming." *Journal of Hydrology*, 46, 311-330.
4. Andrews, B. 1987. "Restoring the sinuosity of artificially straightened stream channels." *Environmental Geology Water Science*, 10(1), 33-41.
5. ASCE River Restoration Subcommittee (RRS) on Urban Stream Restoration, 2003. "Urban Stream Restoration." *Journal of Hydraulic Engineering*, 129(7), 491-493.

6. Bernhardt, E. S., Palmer, M. A., Allan, J. D., Alexander, G., Barnas, K., Brooks, S., Carr, J., Clayton, S., Dahm, C., Follstad-Shah, J., Galat, D., Gloss, S., Goodwin, P., Hart, D., Hassett, B., Jenkinson, R., Katz, S., Kondolf, G. M., Lake, P. S., Lave, R., Meyer, J. L., O'Donnell, T. K. O., Pagano, L., Powell, B., Sudduth, E., 2005. "Synthesizing U.S. River Restoration Efforts." *Science*, 308, 636-637.
7. Bhuiyan, F., Hey, R. D., Wormleaton, P. R., 2007 "Hydraulic evaluation of W-weir for river restoration." *Journal of Hydraulic Engineering*, 133(6), 596-609.
8. Biedenharn, D. S., Elliott, C. M., Watson, C. C., 1997. *The WES Stream Investigation and Streambank Stabilization.* U.S. Army Engineer, Waterways Experiment Station (WES), Vicksburg, Mississippi.
9. Biedenharn, D.S., and Copeland, R.R., 2000. *Effective discharge calculation*, ERDC/CHL HETN-II-4 US Army Corps of Engineers, Vicksburg, MS.
10. Copeland, R. R., Bidenharn, D. S., Fischenich, J. C., 2000. *Channel-Forming Discharge.* ERDC/CHL CHETN-VIII-5, U.S. Army Corps of Engineers.
11. Crowder, D. W. and Knapp, H. V., 2005. "Effective discharge recurrence interval of Illinois streams." *Geomorphology,* 64, 167-184.
12. Davis, M. A. and Slobodkin, L. B., 2004. "The science and values of restoration ecology." *Restoration Ecology*, 12(1), 1-3.
13. Davis, N. M., Weaver, V., Lydy, M. J. 2003. "An assessment of water quality, physical habitat and biological integrity of an urban stream in Wichita, Kansas, prior to restoration improvements (Phase I)." Archives of Environmental Contamination and Toxicology, 44, 351-359.
14. Department of Conservation and Recreation and Division of Soil and Water Conservation (DCR and DSWC), 2004. *The Virginia Stream Restoration and Stabilization Best Management Practices Guide*. Richmond, Virginia, U.S.A.
15. Doyle, M. W., Stanley, E. H., Strayer, D. L., Jacobson, R. B., 2005. "Effective discharge analysis of ecological processes in streams." *Water Resources Research*, 41, W11411, doi: 10.1029/2005WR004222, 2005.

16. Doyle, M. W., Shields, D., Boyd, K. F., Skidmore, P. B., Dominick, D., 2007. "Channel-forming discharge selection in river restoration design." *Journal of Hydraulic Engineering*, 133(7), 831-837.
17. Eagleson, P.S., (1972). "Dynamics of Flood Frequency." *Water Resources Research*, 8(4), 878-897.
18. Federal Interagency Stream Restoration Working Group (FISRWG) 1998. *Stream Corridor Restoration: Principles, Processes, and Practices*. National Technical Information Service, U.S. Department of Commerce, Springfield, VA.
19. Goodwin, P. 2004. "Analytical solutions for estimating effective discharge." *Journal of Hydraulic Engineering*, 130(8), 729-738.
20. Guo, Y. and Adams. B. J., (1998a). "Hydrologic Analysis of Urban Catchments with Event-based Probabilistic Models 1. Runoff Volume." *Water Resources Research*, 34(12), 3421-3431.
21. Guo, Y. and Adams. B. J., (1998b). "Hydrologic Analysis of Urban Catchments with Event-based Probabilistic Models 2. Peak Discharge Rate." *Water Resources Research,* 34(12), 3433-3443.
22. Keystone Stream Team, 2002. *Guidelines for Natural Stream Channel Design for Pennsylvania Waterways*. Prepared by the Alliance for the Chesapeake Bay. Electronic copies of this document are available online at www.canaanvi.org/nscdguidelines.
23. Kondolf, G. M., Smeltzer, M. W., and Railsback, S. F. 2001. "Design and performance of a channel reconstruction project in a coastal California gravel-bed stream." *Environmental Management*, 28(6), 761-776.
24. Lee, J. G., and Heaney, J. P., 2003. "Estimation of urban imperviousness and its effect on stormwater systems." *Water Resources Planning and Management*, 129(5), 419-426.
25. Lenzi, M. A., Mao, L., Comiti, F., (2006) "Effective discharge for sediment transport in a mountain river: computational approaches and geomorphic effectiveness." *Journal of Hydrology*, 326, 257-276.

26. MDEWMA, Maryland Department of Environment and Water Management Administration, 2000. *Maryland's Waterway Construction Guidelines*. Maryland Department of the Environment.
27. Morris, S. and Moses, T. 1999. "Urban stream rehabilitation: a design and construction case study." *Environmental Management*, 23(2), 165-177.
28. Nash, D.B., 1994. "Effective sediment-transporting discharge from Magnitude-Frequency analysis." *Journal of Geology,* 102, 79-95.
29. Ness, R., and Joy, D.M. 2002. "Performance of natural channel designs in southwestern Ontario." *Canadian Water Resources Journal*, 27(3), 293-315.
30. Niezgoda, S. L. and Johnson, P. A., 2007. "Case study in cost-based risk assessment for selecting a stream restoration design method for a channel relocation project." *Journal of Hydraulic Engineering*, 133(5), 468-481.
31. North Carolina Stream Restoration Institute and North Carolina Sea Grant (NCSRI and NCSG), 2001. *Stream Restoration A Natural Channel Design Handbook.* Raleigh, NC.
32. Ontario Ministry of Natural Resources (OMNR), 1994. *Natural Channel Systems: An Approach to Management and Design.* Prepared by the Ontario Ministry of Natural Resources, Toronto, ON, Canada.
33. Palmer, M. A., and Allan, J. D., 2006. "Policy recommendations to enhance the effectiveness of river restoration." *National Academy of Science Journal: Issues in Science and Technology*, 40-48.
34. Pickup, G., and Warner, R.F. 1976. "Effects of hydrologic regime on magnitude and frequency of dominant discharge." *Journal of Hydrology*, 29, 51-75.
35. Pickup, G., 1976. "Adjustment of stream-channel shape to hydrologic regime." *Journal of Hydrology*, 30, 365-373.
36. Riley, A. L., 1998. *Restoring Streams in Cities: A Guide for Planners, Policymakers and Citizens*. Island Press, Washington D.C.
37. Rose, S. and Peters, N. E., 2001. "Effects of urbanization on the streamflow in the Atlanta area (Georgia, U.S.A.): a comparative hydrological approach." *Hydrological Processes*, 15, 1441-1457.
38. Rosgen, D. L., 1994. "A classification of natural rivers." *Catena*, 22, 169-1999.

39. Rosgen, D. L., 1996. *Applied River Morphology*. Wildland Hydrology Books, Pagosa Springs, CO.
40. Schlapfer, F., and Witzig, P-J., 2006. "Public support for river restoration funding in relation to local river ecomorphology, population density, and mean income." *Water Resources Research*, 42, W12412, doi: 10.1029/2006WR004940, 2006.
41. Schueler, T. and Brown, K., 2004. *Urban Stream Repair Practices, version 1*. Urban Subwatershed Restoration Manual No. 4, Prepared by Center for Watershed Protection, Elicott city, MD, U.S.A.
42. Schueler, T., 2004. *An Integrated Framework to Restore Small Urban Watersheds*. Urban Subwatershed Restoration Manual No. 1, Prepared by Center for Watershed Protection, Elicott City, MD, U.S.A.
43. Shields Jr, F.D., Copeland, R.R., Klingeman, P.C., Doyle, M.W., Simon, A. 2003. "Design for stream restoration." *Journal of Hydraulic Engineering*, 129(8), 575-584.
44. Sichingabula, H. M., 1999. "Magnitude-frequency characteristics of effective discharge for suspended sediment transport, Fraser River, British Columbia, Canada." *Hydrological Processes*, 13, 1361-1380.
45. Skidmore, P. B., Shields, F. D., Doyle, M. W., Miller, D. E., 2002. "*A categorization of approaches to natural channel design.*" Proc. ASCE River Restoration Conference, Reno, NV.
46. Soar, P. J. and Thorne, C. R., 2001. *Channel Restoration Design for Meandering Rivers*. ERDC/CHL CR-01-1, U.S. Army Corps of Engineers, Engineer Research and Development Center, Washington, D. C.
47. U.S. Environmental Protection Agency (EPA) 2000. National Water Quality Inventory. EPA pub: 841-R-02-001, Washington D.C.
48. Vogel, R. M., Stedinger, J. R., Hooper, R. P., 2003. "Discharge indices for water quality loads." *Water Resources Research*, 39(10), doi: 10.1029/2002WR001872, 2003.
49. Watson, C. C., Biedenharn, D. S., and Scott, H. S., 1999. *Channel Rehabilitation: Processes, Design, and Implementation*. U.S. Army Engineer, Engineer Research and Development Center, Vicksburg, Mississippi.

50. Williams, G.P. 1978. "Bank-full discharge of rivers." *Water Resources Research*, 14(6), 1141-1154.

51. Wohl, E., Angermeier, L., Bledsoe, B., Kondolf, M., MacDonnell, L., Merritt, D. M., Palmer, M. A., Poff, N. L., Tarboton, D., 2005. "River restoration." *Water Resources Research*, doi: 10.1029/2005WR003985. 41.

52. Wolman, M.G., and Miller, J.P. 1960. "Magnitude and frequency of forces in geomorphic processes." *Journal of Geology*, 68, 54-74.

# Chapter 2

## Analytical Estimation of Effective Discharge Using Mixed Exponential Distribution Models

Asif Quader, Yiping Guo, and Jery R. Stedinger

**Abstract:** The effective discharge $Q_e$ of a channel reach is defined as the discharge that transports the largest fraction of the sediment load over a period of years. The accuracy associated with the analytical estimation of $Q_e$ depends on the goodness of fit between the stream flow series and the adopted probability density function as well as the accuracy of the sediment transport rating curve. Streamflow data from selected Ontario streams indicate that below a certain drainage area, the commonly used lognormal probability density function does not provide a good fit for observed streamflows. As such, a mixed exponential flow frequency distribution model is proposed and a formula for the resulting $Q_e$ is derived. The results from this new $Q_e$ formula were compared with those obtained using a number of well-tested distribution functions and those from empirical sediment transport effectiveness curves. These comparisons indicate that the new analytical solution provides better estimates of $Q_e$ for large as well as small streams.

**Keywords:** Effective discharge, stream restoration, flow duration curve, flow distribution model, half discharge

## 2.1 Introduction

Urbanization causes degradation of water quality, physical habitat and biotic integrity of downstream river reaches. This has necessitated stream restoration projects in Europe (Andrews 1987; Poudevigne et al. 2002) and North America (Kondolf et al. 2001; Morris and Moses 1999; Jackson and Haveren 1984; Ness and Joy 2002; Downs and Kondolf 2002; Scholz and Booth 2001). The objectives of these restoration projects range from aesthetic improvement to protection and enhancement of aquatic and terrestrial habitat. Despite the widely varying nature of these objectives, the first step of a restoration project is always stability assessment. Such an assessment involves the identification of current watershed conditions and the potential of the stream. This stability assessment acts as the foundation of design and allows the prediction of system response. Discharges at a river reach vary widely with time, however, usually a single discharge known as the channel-forming discharge is used as the representative value for stability assessment and channel design (Shields et al. 2003).

The channel-forming discharge is believed to govern the shape and form of a channel. It represents the overall effect of the whole range of discharges experienced by the stream (Pickup and Warner 1976). The channel-forming discharge is defined as the single representative discharge that if maintained indefinitely would produce channel geometry as the long term hydrograph (Shields et al. 2003). The effective discharge ($Q_e$) is computed as the range of intermediate discharges that transports the largest fraction of the annual sediment load over a period of years (Andrews 1980). $Q_e$, bankfull discharge ($Q_b$), and discharge with a particular recurrence interval ($Q_t$) have all been considered as the possible channel-forming discharges. Most private organizations and government agencies, e.g., the Ontario Ministry of Natural Resources (OMNR 1994), North Carolina Stream Restoration Institute (Doll et al. 2003), and Keystone Stream Team (2002), use $Q_b$ as the channel-forming discharge. However, the lack of correlation of $Q_b$ with sediment transport rate, the high degree of uncertainty associated with the field estimation of $Q_b$ (Riley 1972; Woodyer 1968; Williams 1978), and the over prediction of

$Q_b$ for deeply incised urbanized streams have resulted in $Q_b$ being gradually replaced by $Q_e$ as the channel-forming discharge. The U.S. Army Corps of Engineers (USACE) recommends that both $Q_e$ and $Q_b$ be used and crosschecked against each other to ensure better estimation of the channel-forming discharge (Copeland et al. 2000).

Among the currently used channel-forming discharges, the effective discharge is the only one that connects sediment load with channel geometry. The definition of $Q_e$ originates from the 'magnitude-frequency concept' introduced by Wolman and Miller (1960). According to this concept, the effectiveness of a geomorphic process is the product of its magnitude and its frequency of occurrence. In determining $Q_e$, the frequency distribution of the flows is combined with the sediment transport equation, resulting in the transport effectiveness curve. The discharge corresponding to the peak of the transport effectiveness curve is denoted $Q_e$. $Q_e$ values determined from the peak of the transport effectiveness curves have received their fair share of criticism, because the estimation technique is highly sensitive to the size or number of class intervals used in the flow frequency analysis (e.g., Vogel et al. 2003). In spite of the criticisms, the transport effectiveness curve approach continues to be used for determining $Q_e$. Examples include sites in the Cumberland basin, in eastern New South Wales, in Australia (Pickup and Warner 1976), in the Yampa river basin located in northwest Colorado and southwest Wyoming (Andrews 1980), a number of U.S. Geological Survey (USGS) and U.S. Forest Service (USFS) stream gauges (Emmett and Wolman 2001), 55 streams located throughout the U.S. in a wide variety of settings (Nash 1994), the Red river in northern Idaho and the Russian river in California (Goodwin 2004).

In comparison to the transport effectiveness curve approach, analytical approaches for estimating $Q_e$ are relatively new. Pioneered by Nash (1994), the analytical approach is based on the mathematical interpretation of the 'magnitude-frequency concept'. The key to the analytical approach is the analytical frequency distribution models fitted to the stream flow series. Different frequency distribution models and the advantages and disadvantages of the analytical approach were

investigated by Goodwin (2004) and Vogel et al. (2003). Nash (1994) reports that the analytical approach does not work well for small streams. Goodwin (2004) and Vogel et al. (2003) focused only on large streams, with drainage areas exceeding 200 $km^2$. Since stream restoration projects are mostly implemented for small streams, further investigation of the analytical approach for $Q_e$ estimation for small streams is called for.

This paper proposes the use of a mixed exponential flow distribution model for determining analytically the value of $Q_e$. The proposed approach was applied to 25 streams located in the province of Ontario with drainage areas ranging from 0.58 to 1550 $km^2$. This wide range of drainage areas is necessary for the verification of the proposed methodology, because the size of the drainage basin significantly influences flow characteristics. The analytically estimated $Q_e$ values based on the mixed exponential distribution models were compared to analytically estimated $Q_e$ values based on other frequency distribution models and those obtained from the empirical transport effectiveness curve.

## 2.2 Existing Methods for Estimating Effective Discharge

The process of removal and deposition of sediment defines channel morphology. According to Wolman and Miller (1960), the stream power required for the movement of sediment is related both to the magnitude of the flow event and to its frequency of occurrence, a concept commonly referred to as the 'magnitude-frequency concept'. Transport effectiveness of individual flows is defined as the product of sediment load transported by the flow and its frequency of occurrence. For a river reach, a transport effectiveness curve can be constructed by plotting estimated effectiveness (sediment load times frequency of that flow rate) versus flow. The peak of the transport effectiveness curve is the single flow or a range of flows that transports on average the largest fraction of sediment load over a year. $Q_e$ is thus defined as the flow that transports the largest fraction of sediment load. The transport effectiveness curve approach and the analytical

approach (Nash 1994; Goodwin 2004; Vogel et al. 2003) are the two existing methods of estimating $Q_e$ based on the magnitude-frequency concept.

### 2.2.1 Transport Effectiveness Curve Approach

In practice, using the transport effectiveness curve approach, the range of possible flow at a river reach is divided into a number of equal intervals and the frequency distribution pattern of flows at the river reach among these intervals is determined from the observed flow series. Sediment transport equations are used to calculate the sediment load carried by a specific discharge. Quite often complex sediment transport equations are simplified as sediment rating curves fitted by simple power functions. For the mean discharge within an interval, the rate of sediment transported by this mean discharge is multiplied by the frequency of occurrence of discharges within that interval. This product is plotted as a single bar in the sediment transport histogram. All the individual bars covering the entire flow range constitute the bed material load histogram (if bedload is predominant), or approximately the transport effectiveness curve. $Q_e$ is graphically determined using the transport effectiveness curve.

In applying the transport effectiveness curve approach, two types of problems may arise. Firstly, the peak of the transport effectiveness curve could be located in the first class interval and secondly, the curve may contain multiple peaks. If $Q_e$ is located in the first class interval, Biedenharn and Copeland (2000) suggest that the size of the class intervals should be reduced or the number of class intervals should be increased. The problem of multiple peaks can be dealt with by increasing the size of the class interval or reducing the number of class intervals within the specific range of the flow series. These guidelines set forth by the U.S. Army Corps of Engineers (USACE) allows hydrologists and practicing engineers to deal with the problems associated with the transport effectiveness curves more efficiently. These guidelines were followed in this study in the application of the transport effectiveness curve approach for determining $Q_e$. The advantage of the transport effectiveness curve approach is that in estimating $Q_e$, the flow

frequency distribution pattern is based on the actual flow series for a particular period of record. It is not based on an assumed probability density function (pdf) fitted to the flows of the site. As the actual flow series is used, it is considered more accurate than the analytical approach which employs an assumed probability density function (pdf). However, if the adopted pdf fits the flow series well, then by smoothing the sampling variation in the histogram from the available flow series, the analytical method should actually yield a more precise result. This illustrates the classical tradeoff between bias resulting from the use of a distribution that does not match the actual flow distribution; versus variance or imprecision that comes with a histogram with too many small intervals, resulting in an effective discharge estimator with a large sampling variance.

### 2.2.2 Analytical Approach

An analytical solution of $Q_e$ was first derived by Nash (1994) by assuming that daily streamflows follow approximately lognormal frequency distributions. Goodwin (2004) adopted the same methodology but incorporated additional stream flow frequency distribution patterns. In the analytical approach used by both Nash (1994) and Goodwin (2004), standard analytical pdfs, e.g., lognormal, gamma, normal, etc, denoted in general as f(Q), is used to represent the frequency distribution of flow series. The sediment rating curve is expressed as a power function of flow rate Q ($m^3$/sec), as shown in Eqn. (2.1).

$$Q_d = \alpha Q^{\beta} \tag{2.1}$$

Where $Q_d$ is the sediment transport rate (kg/sec), and $\alpha$ and $\beta$ are the fitting parameters. The transport effectiveness (E) of the stream is the product of f(Q) and $Q_d$, i.e.

$$E = f(Q) \cdot Q_d \tag{2.2}$$

$Q_e$ is the Q value where E attains its maximum; $Q_e$ can be identified by differentiating E with respect to Q and equating that derivative to zero:

$$\frac{\partial E}{\partial Q} = \alpha \frac{\partial \left[ f(Q) \times Q^{\beta} \right]}{\partial Q} = 0 \tag{2.3}$$

For example, if f(Q) follows a lognormal pdf, the value of $Q_e$ is given by (Goodwin 2004),

$$Q_e = e^{\mu_y + \sigma_y^2 (\beta - 1)} \tag{2.4}$$

where $\mu_y$ and $\sigma_y$ are the mean and the standard deviation of the log-transformed flows at the stream reach, respectively. Based on Eqn. (2.3), $Q_e$ values may be estimated for any type of flow frequency distribution. Eqn. (2.3) also shows that $Q_e$ is independent of $\alpha$.

The advantage of the analytical approach is that based on the flow characteristics and the exponent of the sediment rating curve (expressed as a power function), $Q_e$ can be conveniently computed. The analytical approach does not require elaborate computation and histogram construction for estimating $Q_e$. However, the performance of the analytical approach depends on how well the fitted distribution describes the frequency pattern of flows.

For the 55 streams investigated by Nash (1994), it was found that for small drainage areas the analytically estimated $Q_e$ values were not in good agreement with $Q_e$ values estimated using the transport effectiveness curve approach. Although Goodwin (2004) found that the $Q_e$ values determined from empirical transport effectiveness curves and the analytical approach (with lognormal as the flow distribution) are in close agreement, the drainage areas of the two rivers (937 and 294 $km^2$) investigated by Goodwin (2004) are quite large. The agreements between $Q_e$ values obtained analytically and from transport effectiveness curves for large drainage basins but not for small drainage basins, and the goodness of fit between commonly used flow distribution and observed flows from small streams, necessitate further investigation of the analytical approach.

## 2.3 Selection and Analysis of Streams with Various Drainage Areas

To determine the influence of the size of the drainage basin on the frequency distribution pattern of flows, daily stream flow data from streams located in Ontario were extracted from the HYDAT CD. The HYDAT CD released by Environment Canada contains hydrometric data for over 2900 active stations and 5100 discontinued sites across Canada (HYDAT, 2001). The following two criteria were used for the selection of streams: (1) streams with a wide range of drainage areas; and (2) streams for which daily flow data were available for at least 10 years. Based on these two criteria, 22 streams, tabulated in Table 2.1 and also shown in Fig. 2.1 were selected. The numbering system adopted in Fig. 2.1 follows the stream numbers of the first column in Table 2.1.

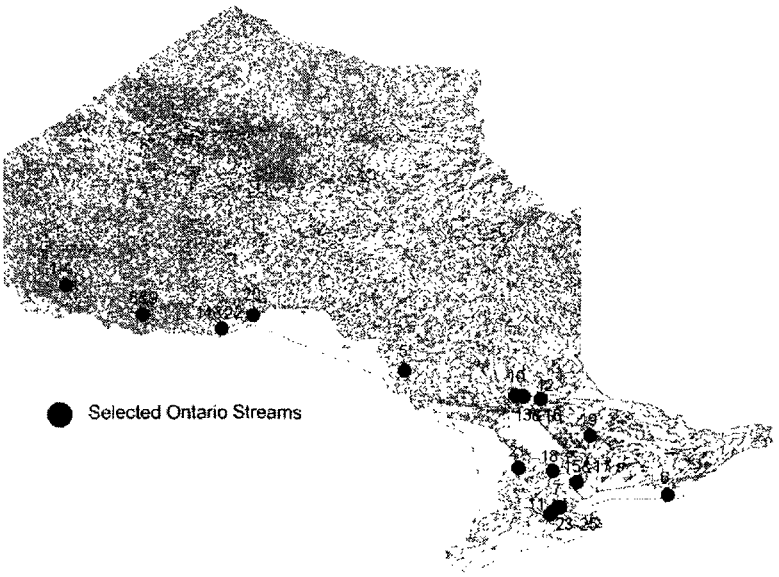


**Fig 2.1:** Location of the selected Ontario streams

Fig. 2.1 shows that a number of streams are located extremely close to one another (based on latitude and longitude); there a single dot was used to represent these multiple streams. For the selected streams, the first 22 as listed in Table 2.1 have no sediment information. The drainage area of these streams ranged from 0.58 to 1,550 $km^2$. The names, stream ID, drainage area, and the coordinates of the gauging stations of these streams are all presented in Table 2.1.

**Table 2.1:** Name, location, and characteristics of the selected Ontario streams

| No. | Name | Stream ID | Latitude | Longitude | Flow record | A ($km^2$) |
|---|---|---|---|---|---|---|
| 1 | Lake 114 outlet near Kenora | 05PD014 | 49°40'10"N | 93°45'45"W | 1971-1994 | 0.58 |
| 2 | Lake 223 outlet near Kenora | 05QD017 | 49°41'56"N | 93°42'50"W | 1975-1995 | 2.6 |
| 3 | Lake 239 outlet near Kenora | 05PD023 | 49°39'28"N | 93°43'36"W | 1970-1995 | 3.9 |
| 4 | Lake 240 outlet near Kenora | 05PD015 | 49°38'52"N | 93°43'34"W | 1969-1995 | 7.25 |
| 5 | Norberg Creek above Batchawana River | 02BF005 | 47°4'8"N | 84°26'7"W | 1980-2000 | 11.5 |
| 6 | Bloomfield Creek at Bloomfield | 02HE001 | 43°59'26"N | 77°13'6"W | 1969-1992 | 13.9 |
| 7 | Black Creek below Acton | 02HB024 | 43°37'46"N | 80°0'41"W | 1987-2001 | 18.5 |
| 8 | Eye River near Hardtack Lake near Atikokan | 05PB021 | 48°55'30"N | 91°39'44"W | 1985-1994 | 19.8 |
| 9 | Eye River near Coulson Lake near Atikokan | 05PB022 | 48°53'40"N | 91°40'3"W | 1985-1993 | 27.9 |
| 10 | Moose Creek at Levack | 02CF013 | 46°38'8"N | 81°23'25"W | 1981-2001 | 40 |
| 11 | Alder Creek near New Dundee | 02GA030 | 43°22'19"N | 80°33'6"W | 1965-2001 | 49.7 |
| 12 | Junction Creek at Sudbury | 02CF005 | 46°29'20"N | 80°59'45"W | 1958-1996 | 89.1 |
| 13 | Whitson River at Val Caron | 02CF008 | 46°36'36"N | 81°1'59"W | 1960-2001 | 179 |
| 14 | Neebing River near Thunder Bay | 02AB008 | 48°22'56"N | 891828W | 1953-2001 | 187 |
| 15 | Boyne River at Earl Rowe Park | 02ED102 | 44°9'6"N | 79°54'8"W | 1967-2001 | 211 |
| 16 | Whitson River at Chelmsford | 02CF007 | 46°34'56"N | 81°11'59"W | 1960-2001 | 272 |
| 17 | Nottawasaga River near Alliston | 02ED101 | 44°6'38"N | 79°53'21"W | 1967-2001 | 334 |
| 18 | Beaver River near Clarksburg | 02FB009 | 44°31'20"N | 80°28'0"W | 1957-2001 | 572 |
| 19 | Magnetawan River near Burk's Fall | 02EA006 | 45°37'3"N | 79°23'17"W | 1915-1998 | 650 |
| 20 | Wolf River at Highway No. 17 | 02AC001 | 48°49'19"N | 88°32'7"W | 1971-2001 | 736 |
| 21 | Sauble River at Sauble Falls | 02FA001 | 44°40'10"N | 81°15'10"W | 1957-2001 | 927 |
| 22 | Pigeon River at Middle Falls | 02AA001 | 48°0'44"N | 89°36'58"W | 1921-1999 | 1550 |
| 23 | O.A.C Farm Gauge No. 5 at Guelph | 02GA032 | 43°31'53"N | 80°18'18"W | 1969-1984 | 2.51 |
| 24 | East Canagagigue Creek near Floradale | 02GA035 | 43°39'4"N | 80°34'20"W | 1974-1984 | 27.7 |
| 25 | Canagagigue Creek near Floradale | 02GA036 | 43°40'12"N | 80°35'48"W | 1974-1984 | 17.9 |

In Table 2.1, a stream ID which starts with the number 02 is part of the St. Lawrence River drainage system. A stream ID which starts with the number 05 is a part of the Nelson River drainage system. In addition to flow data, HYDAT CD also contains water level, suspended sediment concentration, and particle size analysis results for bedload. As far as the sediment load is concerned, there are three major problems that prohibit the extensive use of sediment transport rate from HYDAT CD for estimating $Q_e$.

Firstly, for most rivers suspended sediment load is available for less than 10 years. Secondly, the drainage areas for those rivers for which at least 10 years of suspended sediment load is available are more than 100 $km^2$. Thirdly, no sediment information is available for the streams that are a part of the Nelson River drainage system. Only three streams were found in the entire database of the St. Lawrence River drainage system for which suspended sediment information was available for at least 10 years and the drainage area of the streams were also less than 100 $km^2$. These three streams are listed in Table 2.1 after the first 22 streams, and thus have numbers 23-24-25. The stream ID of these streams are 02GA032, 02GA035 and 02GA036. In the following subsections, a brief discussion of the sediment rating curves and different flow frequency distributions used for the selected streams are provided.

### 2.3.1 Sediment Rating Curve

Sediment rating curves were developed for the three streams for which sediment transport information was available. These sediment rating curves are shown in Fig. 2.2 The least squares method was used to fit the power function in Eqn. (2.1) to the data. The values of $\beta$ for streams 02GA032, 02GA035 and 02GA036 were 5.15, 1.58 and 1.75, respectively. Fig. 2.2(a), as well as the high value of $\beta$ for stream 02GA032, indicates that a high threshold discharge needs to be exceeded for the mobilization of sediment particles. Figs. 2.2(a)–2.2(c) display the fitted power functions later used for determining $Q_e$.

Dickinson and Green (1988) show that the volume of sediment transported in Ontario streams can be determined from consideration of the annual suspended sediment load only. They also found that daily suspended sediment load fluctuates more widely than daily average flows. The wide fluctuation of daily suspended sediment load is due to the higher threshold discharge required to mobilize sediment particles. This characteristic of sediment transport in Ontario streams can be described by sediment rating curves that

(a)

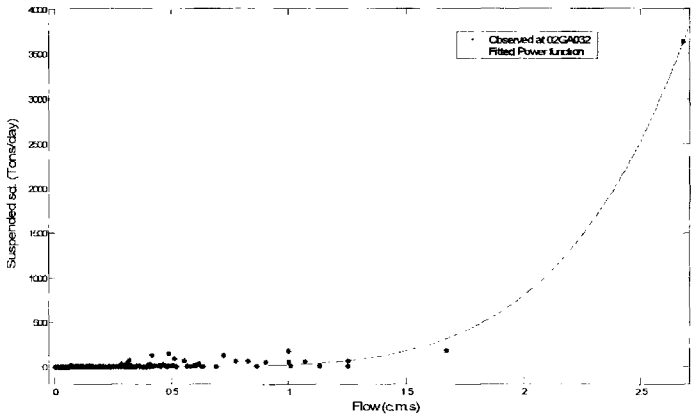


(b)

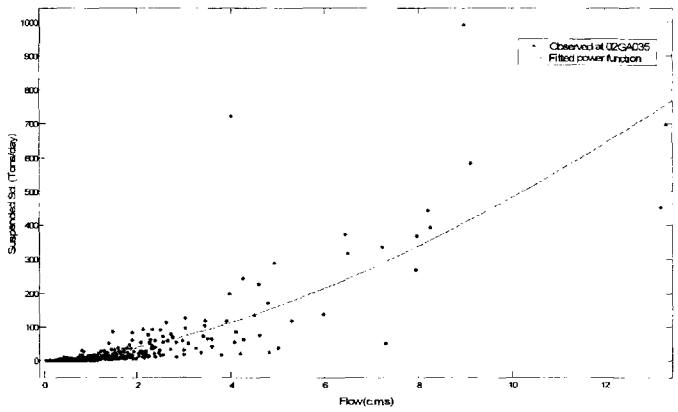


(c)

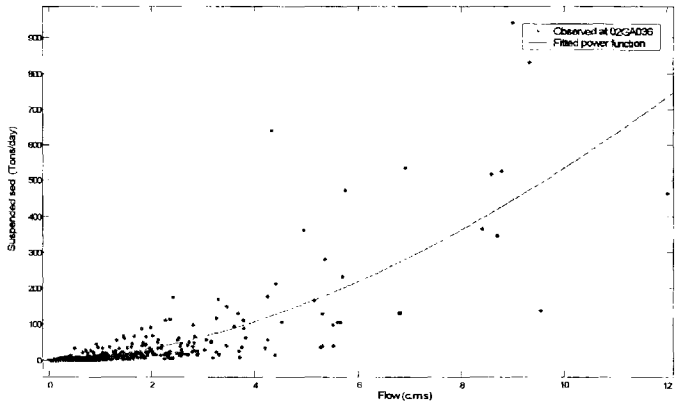


**Fig 2.2:** Sediment rating curves for streams (a) 02GA032, (b) 02GA035 and (c) 02GA036

have a large exponent and a low value of the coefficient in Eqn. (2.1). The value of $\beta$ for streams for which no sediment information was available was assumed to be 2. Nash (1994) reported $\beta$ values ranging from 1.23 to 3.02 for suspended sediment load. Goodwin (2004) reported $\beta$ values of 1.68 and 1.86 for the Red river and the Russian river. Vogel et al. (2003) reported a $\beta$ value of 1.84 for the Susquehanna River at Harrisburg, Pennsylvania. Thus, by assuming a reasonable $\beta$ value of 2 for streams without sediment information, it would be possible to determine $Q_e$ both analytically and from empirical transport effectiveness curves. As the value of $\alpha$ does not influence the analytical solution of $Q_e$, a typical value of 0.1 was assumed for streams without sediment information. The assumed $\alpha$ and $\beta$ values are used for comparative study purposes only. They should not be used to determine the actual $Q_e$ values for the corresponding stream gauge locations.

### 2.3.2 Flow Frequency Distribution Models

In addition to a sediment rating curve the analytical solution for $Q_e$ also depends on the theoretical pdf fitted to the streamflows. The accuracy of the analytical solution depends on the goodness of fit between the assumed analytical distribution and the frequency distribution of the actual flow series. If the stream flow data does not fit the assumed distribution well, the analytical solution of $Q_e$ would be inaccurate.

Lognormal, gamma and exponential distributions have been used to represent the frequency distributions of daily streamflow data (Nash 1994; Goodwin 2004; Limbrunner et al. 2000). The gamma distribution was used because the frequency analysis of many small streams revealed only a recession limb, instead of a rising and a recession limb that is typically found for large streams. The exponential (E) distribution was chosen for the same reason, and is a special case of the gamma with $\alpha_g = 1$. The gamma distribution (G) has a pdf given by:

$$f(Q) = \frac{1}{\beta_g^{\alpha_g}\Gamma(\alpha_g)} Q^{\alpha_g - 1} e^{-Q/\beta_g} \qquad (2.5)$$

where $\Gamma(\alpha_g)$ is the gamma function, and $\alpha_g$ and $\beta_g$ are distribution parameters. The lognormal distribution (LN) has a pdf of

$$f(Q) = \frac{1}{Q\sigma_y\sqrt{2\pi}} e^{\frac{-(\ln Q - \mu_y)^2}{2\sigma_y^2}} \tag{2.6}$$

where $\mu_y$ and $\sigma_y$ are the mean and standard deviation of log-transformed Q values. The exponential distribution has a pdf of

$$f(Q) = \lambda e^{-\lambda Q} \tag{2.7}$$

where $\lambda$ is the single parameter.

Combining the pdfs for the gamma (G) and exponential (E) distributions with Eqn. (2.1), the $Q_e$ values were found to be (Goodwin 2004):

$$Q_e = \beta_g[\beta + (\alpha_g - 1)], \text{ for gamma distribution.} \tag{2.8}$$

$$Q_e = \beta/\lambda, \text{ for exponential distribution.} \tag{2.9}$$

$Q_e$ for the lognormal distributions is reported in Eqn. (2.4).

Using the method of moment (MOM), the theoretical distribution functions can be fit to observed flow series for a site. For lognormal distribution using the relationship that $\mu_y = 0.5\ln[\mu^2/(1+CV^2)]$ and $\sigma_y^2 = \ln[1+CV^2]$ (Stedinger et al. 1993; Haan 1977), where CV is the coefficient of variation and $\mu$ is the mean of the flow series, Eqn. (2.4) can be written:

$$Q_e = \mu\left(1+CV^2\right)^{(\beta-1.5)} \tag{2.10}$$

For the gamma distribution, Eqn. (2.8) can be written

$$Q_e = \mu[1+CV^2(\beta-1)] \tag{2.11}$$

where $\mu$ and CV are again the mean and coefficient of variation of the flow series.

An alternative to the MOM is the method of maximum likelihood (MLE). To gain an appreciation of the possible difference between the two, both estimators were used with the LN distribution. Since the log transformation of zero flows is undefined, the

MLE was used with lognormal distributions only for those streams which do not have zero flows. For small streams with zero flow or low-outlier problems, use of more sophisticated methodologies may be investigated in the future. To be consistent in this study, all zero flows were included in the analyses with all distributions. Only MOM was used for distributions other than LN.

## 2.4 The Mixed Exponential Distribution Model

To improve the accuracy of $Q_e$ estimators for small streams, an alternative flow frequency distribution model may be required. To this end, the flow data from the 25 selected streams were used to determine their respective flow duration curves (FDC). A FDC plots flow versus the percent (or fraction) of time that flow value is exceeded during the entire period of record. FDCs provide a summary of flow characteristics for a specific period of record (Quimpo et al. 1983). If a FDC can be fitted by an analytical function, denoted as $P(Q > q)$, this function is the complement of the cumulative distribution function (CDF) of daily streamflows. That is

$$P(Q > q) = 1 - F(Q \le q) \tag{2.12}$$

where $F(Q \le q)$ is the CDF of daily stream flow.

To compare flow characteristics of different streams, the discharge per unit area of the basin, known as the specific discharge (or specific flow) is sometimes used to construct specific flow duration curves (SFDCs). In a SFDC, instead of plotting the original discharge values, the specific discharge is plotted against the percentage of the time that the specific discharge is exceeded. In this study, to incorporate the influence of basin area and to permit the comparison of streams with varying sizes, the SFDCs were constructed using the observed stream flows of the 25 selected streams. By placing the resulting 25 SFDCs together as shown in Fig. 2.3 (the shaded area), one can see that the

SFDCs of the 25 streams are clustered in a narrow band of approximately exponential shape bounded by the SFDCs of streams 02GA030 and 02BF005.

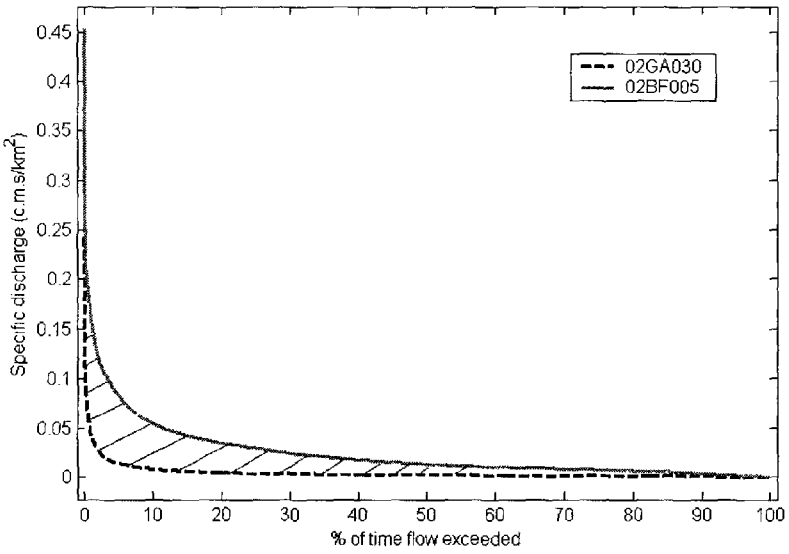


**Fig 2.3:** Bounded region of the SFDCs for the selected 25 Ontario streams

This indicates that the distributions of small and large streams looks very much like an exponential distribution. However, exponential distributions have only one distribution parameter and cannot account for the occurrence of zero flows, which are common in small streams.

Thus we propose that the distribution of daily stream flows from Ontario streams be described by a two-parameter mixed exponential distribution (MED) (Johnson et al. 1994):

$$f(Q) = \begin{cases} (1-\gamma)\delta(Q) & Q = 0 \\ \gamma\lambda e^{-\lambda Q} & Q > 0 \end{cases} \tag{2.13}$$

where $\gamma$ and $\lambda$ are distribution parameters; and $\delta(Q)$ is the Dirac delta function of Q. $\gamma$ should always be less than unity; $1-\gamma$ accounts for the probability of the occurrence of zero flows or flows close to the baseflow level. The mean $\mu$ and variance $\sigma^2$ of this distribution are

$$\mu = \frac{\gamma}{\lambda} \tag{2.14}$$

$$\sigma^2 = \frac{2\gamma - \gamma^2}{\lambda^2} \tag{2.15}$$

The values of $\gamma$ and $\lambda$ can be obtained from the population moments using

$$\lambda = \frac{2\mu}{\mu^2 + \sigma^2} \tag{2.16}$$

$$\gamma = \frac{2\mu^2}{\mu^2 + \sigma^2} \tag{2.17}$$

Using the magnitude-frequency concept, Eqn. (2.13) is combined with Eqn. (2.1). Setting to zero the derivative respect to Q of the resultant expression for E yields for $Q_e$

$$Q_e = \frac{\beta(\mu^2 + \sigma^2)}{2\mu} = \frac{\mu\beta}{2}(1 + CV^2) \tag{2.18}$$

For a specific river reach, the $\mu$ and $\sigma^2$ in Eqn. (2.18) can be estimated by the sample mean and variance calculated from the observed flows. For $\beta = 2$, the analytical expressions for $Q_e$ using G and MED distributions [Eqn.s (2.11) and (2.18)] both reduce to $Q_e = \mu(1 + CV^2)$, resulting in the same $Q_e$ values. However, this is not true for other $\beta$ values.

## 2.5 Results and Discussion

### 2.5.1 Goodness of Fit of Alternative Distribution Models

A goodness of fit analysis was performed comparing the FDC of daily streamflows and alternative flow frequency distribution models. Using the method of moment, the four alternative distribution models were fitted to the flow data for the 25 Ontario streams. In addition to the method of moment, the maximum likelihood estimator was also used for the lognormal distribution. The Kolmogorov-Smirnov (K-S) test statistic was calculated for each river for each distribution. The K-S test can provide bounds within which every observation on a probability plot should lie if the sample is

drawn from the assumed distribution (Stedinger et al. 1993). If the test statistic is larger than a critical value which is dependent on the sample size and significance level, the assumed theoretical distribution would be rejected. In this study, the test statistic, which is the maximum difference between the flow exceedence frequencies estimated from observed daily streamflow data and that calculated using the fitted theoretical distribution, was compared between rivers but not against a critical value. This is to provide a relative comparison of the goodness of fit between alternative distribution models and the observed flow data.

Table 2.2 lists the K-S test statistics for lognormal (fitted by both MOM and MLE), gamma, mixed exponential and exponential distributions. As mentioned previously, the LN-MLE was not applied to streams containing zero flows and the K-S test statistics for these streams are blank in Table 2.2. In that table, the 25 selected streams are placed in descending order according to their drainage areas. It was found that below a drainage area of about 10 $km^2$, the gamma and mixed exponential distributions provided a consistently better fit than lognormal and simple exponential distributions. The maximum difference for the gamma distribution ranged from 0.07-0.36 for streams with drainage areas less than 10 $km^2$. Two flow records, namely, O.A.C Farm Gauge No. 5 at Guelph (02GA032) with a drainage area of 2.51 $km^2$ and the Eye River near Hardtack Lake near Atikokan (05PB021) with a drainage area of 19.8 $km^2$ had poorer fits not only with G and MED but also with LN (fitted with either MOM or MLE) and E distributions.

Above drainage areas of 10 $km^2$, the average maximum difference for LN (MOM), G, MED and E were 0.23, 0.23, 0.29 and 0.49 respectively. Although these average values indicate that the LN (MOM) and G fit the best, careful scrutiny of Table 2 reveals that this is less consistent as compared to those rivers with drainage areas less than 10 $km^2$. Table 2.2 shows that for streams such as 02AC001, the LN (MLE) outperforms all other distributions, and in streams 02CF007 and 02FB009, the LN (MLE) provides a better fit than LN (MOM). This is in agreement with Stedinger (1980) who demonstrated that for random data generated from continuous simulation and fitted to LN distributions

with both MOM and MLE, MLE outperforms MOM in terms of goodness of fit. But the relative performance of the two methods is also dependent on the sample size. In streams 02EA006, 02HB024, and 02FB009, the E distribution performs the best or at least as good as the best distribution even though it has but a single parameter.

**Table 2.2:** Goodness of fit test results

| | | K-S Test Statistics | | | | |
|---|---|---|---|---|---|---|
| Stream ID | A ($km^2$) | LN-MLE | LN-MOM | G | MED | E |
| 05PD014 | 0.58 | | 0.20 | 0.10 | 0.16 | 0.57 |
| 02GA032 | 2.51 | | 0.36 | 0.36 | 0.36 | 0.58 |
| 05QD017 | 2.6 | | 0.25 | 0.10 | 0.13 | 0.42 |
| 05PD023 | 3.9 | | 0.18 | 0.07 | 0.13 | 0.26 |
| 05PD015 | 7.25 | | 0.25 | 0.05 | 0.13 | 0.40 |
| 02BF005 | 11.5 | | 0.22 | 0.19 | 0.23 | 0.37 |
| 02HE001 | 13.9 | | 0.18 | 0.29 | 0.40 | 0.67 |
| 02GA036 | 17.9 | | 0.24 | 0.19 | 0.20 | 0.64 |
| 02HB024 | 18.5 | 0.27 | 0.23 | 0.23 | 0.23 | 0.23 |
| 05PB021 | 19.8 | 0.27 | 0.29 | 0.29 | 0.39 | 0.66 |
| 02GA035 | 27.7 | 0.69 | 0.30 | 0.38 | 0.50 | 0.81 |
| 05PB022 | 27.9 | | 0.37 | 0.37 | 0.37 | 0.40 |
| 02CF013 | 40 | | 0.18 | 0.15 | 0.18 | 0.24 |
| 02GA030 | 49.7 | | 0.24 | 0.40 | 0.52 | 0.84 |
| 02CF005 | 89.1 | 0.18 | 0.22 | 0.10 | 0.20 | 0.55 |
| 02CF008 | 179 | 0.17 | 0.14 | 0.19 | 0.29 | 0.57 |
| 02AB008 | 187 | 0.36 | 0.28 | 0.22 | 0.36 | 0.70 |
| 02ED102 | 211 | 0.50 | 0.22 | 0.38 | 0.43 | 0.55 |
| 02CF007 | 272 | 0.23 | 0.28 | 0.17 | 0.28 | 0.51 |
| 02ED101 | 334 | 0.45 | 0.14 | 0.21 | 0.26 | 0.36 |
| 02FB009 | 572 | 0.11 | 0.15 | 0.16 | 0.12 | 0.11 |
| 02EA006 | 650 | 0.26 | 0.24 | 0.08 | 0.08 | 0.06 |
| 02AC001 | 736 | 0.19 | 0.19 | 0.31 | 0.41 | 0.61 |
| 02FA001 | 927 | 0.34 | 0.22 | 0.15 | 0.20 | 0.31 |
| 02AA001 | 1550 | 0.30 | 0.30 | 0.13 | 0.23 | 0.47 |
| $A<10\ km^2$ (avg.)[1] | | | 0.24 | 0.15 | 0.19 | 0.43 |
| $A>10\ km^2$ (avg.)[2] | | | 0.23 | 0.23 | 0.30 | 0.49 |

Notes

1: The average of the K-S test statistics for all streams with drainage areas $< 10\ km^2$.

2: The average of the K-S test statistics for all streams with drainage areas $> 10\ km^2$.

These results indicate that for small streams a more suitable distribution may be the gamma (G) or the mixed exponential distribution (MED). However, for large

drainage basins, no obvious conclusions are apparent; other distribution such as the 3-parameter distributions may be attractive.

## 2.5.2 Comparison of $Q_e$ Estimated Using Different Approaches

The main objective of this study is to derive and test the applicability of the proposed analytical approach for computing $Q_e$, especially for small streams. Using Eqn. (2.18), the mean and standard deviation of the flows computed from the observed flow series and the fitted or assumed $\beta$ values, we determined the $Q_e$ values for the 25 selected streams. Similarly, the $Q_e$ values were also analytically estimated using gamma, exponential and lognormal (fitted by both MOM and MLE) flow frequency distributions. The $Q_e$ values were not determined by the LN distribution with MLE for streams with zero flows. These streams were the same as those for which the K-S test statistics under LN-MLE were not shown in Table 2.2. $Q_e$ values were also determined using transport effectiveness curves (TEC). Table 2.3 reports the various $Q_e$ values. As noted above, for $\beta = 2$, $Q_e$ values for G and MED are the same.

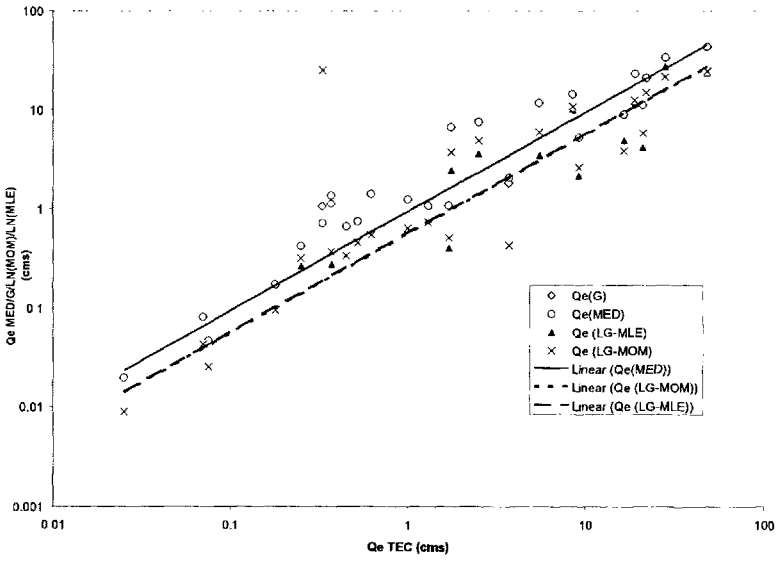


**Fig 2.4:** Comparison of effective discharge between $Q_e$ (G) vs $Q_e$ (TEC); $Q_e$ (MED) vs $Q_e$ (TEC); $Q_e$ (LN-MLE) vs $Q_e$ (TEC); $Q_e$ (LN-MOM) vs $Q_e$ (TEC)

The accuracy of analytically estimated $Q_e$ values using lognormal and mixed exponential distributions was evaluated by comparing them with $Q_e$ values determined from the empirical transport effectiveness curve. In Fig. 2.4, $Q_e$ values estimated analytically are plotted against those determined from transport effectiveness curves for the selected streams.

**Table 2.3:** Magnitudes and frequencies of $Q_e$ computed using different methods

| Stream ID | $Q_e$[1] | | | | | | $Q_{1/2}$ | P(Q>q) | $T_r$ (yr)[4] |
|---|---|---|---|---|---|---|---|---|---|
| | TEC | LN-MLE | LN-MOM | G | MED | E | Emp.[2] | (%)[3] | |
| 05PD014 | 0.025 | | 0.01 | 0.02 | 0.02 | 0.01 | 0.03 | 10 | 1.07 |
| 02GA032[5] | 0.33 | | 25.00 | 1.07 | 0.72 | 0.13 | 0.89 | 1.7 | 1.14 |
| 05QD017 | 0.075 | | 0.03 | 0.05 | 0.05 | 0.03 | 0.07 | 3.1 | 1.8 |
| 05PD023 | 0.07 | | 0.04 | 0.08 | 0.08 | 0.05 | 0.12 | 15 | 1.04 |
| 05PD015 | 0.18 | | 0.10 | 0.17 | 0.17 | 0.11 | 0.26 | 20 | 1.05 |
| 02BF005 | 0.52 | | 0.46 | 0.75 | 0.75 | 0.55 | 1.24 | 17 | <1.05 |
| 02HE001 | 0.45 | | 0.33 | 0.67 | 0.67 | 0.34 | 1.13 | 9 | <1.04 |
| 02GA036[5] | 3.7 | | 0.43 | 1.86 | 2.10 | 0.42 | 3.71 | 0.7 | 1.38 |
| 02HB024 | 0.25 | 0.27 | 0.32 | 0.42 | 0.42 | 0.48 | 0.60 | 40 | <1.07 |
| 05PB021 | 1.7 | 0.40 | 0.51 | 1.09 | 1.09 | 0.48 | 1.83 | 2.7 | 1.08 |
| 02GA035[5] | 0.37 | 0.28 | 0.37 | 1.14 | 1.38 | 0.51 | 2.24 | 20 | <1.06 |
| 05PB022 | 1 | | 0.64 | 1.27 | 1.27 | 0.64 | 1.82 | 12 | <1.11 |
| 02CF013 | 1.3 | | 0.74 | 1.09 | 1.09 | 1.00 | 1.48 | 10 | 1.08 |
| 02GA030 | 0.62 | | 0.54 | 1.42 | 1.42 | 0.41 | 3.76 | 8 | <1.03 |
| 02CF005 | 9.2 | 2.20 | 2.66 | 5.29 | 5.29 | 2.67 | 9.67 | 2 | 1.09 |
| 02CF008 | 5.5 | 3.51 | 5.99 | 11.81 | 11.81 | 6.07 | 15.80 | 9 | 1.05 |
| 02AB008 | 16.5 | 4.97 | 3.88 | 9.06 | 9.06 | 3.33 | 14.97 | 1.5 | 1.48 |
| 02ED102 | 1.75 | 2.48 | 3.75 | 6.76 | 6.76 | 4.17 | 12.03 | 50 | <1.04 |
| 02CF007 | 21 | 4.23 | 5.87 | 11.38 | 11.38 | 6.05 | 21.20 | 2 | 1.24 |
| 02ED101 | 2.5 | 3.68 | 4.97 | 7.68 | 7.68 | 6.43 | 15.24 | 80 | <1.06 |
| 02FB009 | 8.5 | 10.17 | 10.90 | 14.50 | 14.50 | 16.39 | 19.25 | 31 | <1.02 |
| 02EA006 | 22 | 15.52 | 15.11 | 21.08 | 21.08 | 21.66 | 28.30 | 14 | 1.01 |
| 02AC001 | 19 | 12.04 | 12.56 | 23.07 | 23.07 | 13.67 | 33.43 | 9 | 1.05 |
| 02FA001 | 28 | 27.34 | 21.54 | 33.89 | 33.89 | 27.37 | 47.00 | 15 | <1.02 |
| 02AA001 | 48 | 23.92 | 24.86 | 43.50 | 43.50 | 28.40 | 60.15 | 7 | 1.04 |

Notes

1: All $Q_e$ values are expressed in the units of $m^3$/sec.

2: $Q_{1/2}$ values determined based on the empirical approach (Vogel et al. 2003).

3: The percentage of time $Q_e$ (from transport effectiveness curve (TEC)) is equaled or exceeded, determined from the flow duration curves.

4: The recurrence interval of $Q_e$ (TEC) determined from the maximum annual flow series.

5: Actual sediment transport data available for the three streams.

A linear regression analysis between the true values (assumed to be those from transport effectiveness curves) and the analytically estimated values based on mixed exponential distribution models indicates an $R^2$ value of 0.89 and a slope of 0.94. Thus, $Q_e$ values from the proposed analytical solution are fairly close to those estimated from transport effectiveness curves. Regression of $Q_e$ values based on lognormal distributions fitted by MOM and MLE (only streams without zero flows) on $Q_e$ values from transport effectiveness curves yielded $R^2$ values of just 0.44 and 0.72, respectively, and slopes of 0.56 and 0.57, respectively. The root mean square error (RMSE) between the mixed exponential estimates and those determined from transport effectiveness curves was 3.7. This is lower than RMSEs of 8.4 and 7.0 for LN-MOM and E estimates. Surprisingly, as shown in Fig. 2.4 this good performance for the mixed exponential estimates is true for small streams and for large streams with drainage areas exceeding 100 $km^2$ .

These results may be partially explained from the goodness of fit analyses illustrated in Figs. 2.5(a) and (b). Fig. 2.5(a) shows an example of a small drainage basin, and Fig. 2.5(b) shows an example of a large drainage basin. In the upper portion of Figs. 2.5(a) and 2.5(b), FDCs generated from the fitted distributions are compared to those empirically determined from the flow data. In the lower portion of Figs. 2.5(a) and 2.5(b), the transport effectiveness histograms constructed from observed flows and sediment rating curves are plotted. In both Figs. 2.5(a) and 2.5(b), the transport effectiveness histograms are vertically aligned to the FDCs so that the relative location of $Q_e$ within the flow range can be identified. The K-S test statistics indicate that the mixed exponential distribution performs better than the lognormal distribution for small streams but not for large streams. However, in Fig. 2.5(b) one can see that for large streams, the mixed exponential distribution and other distributions are in good conformance for the

(a)

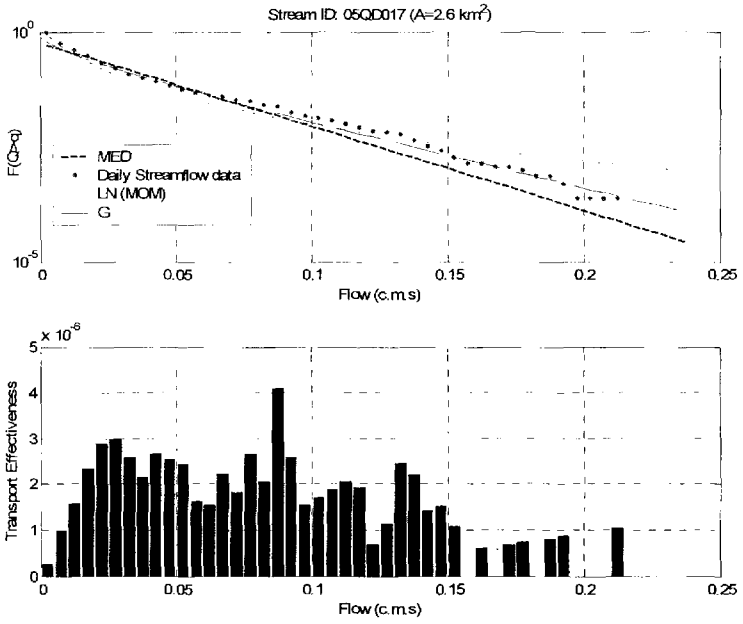


(b)

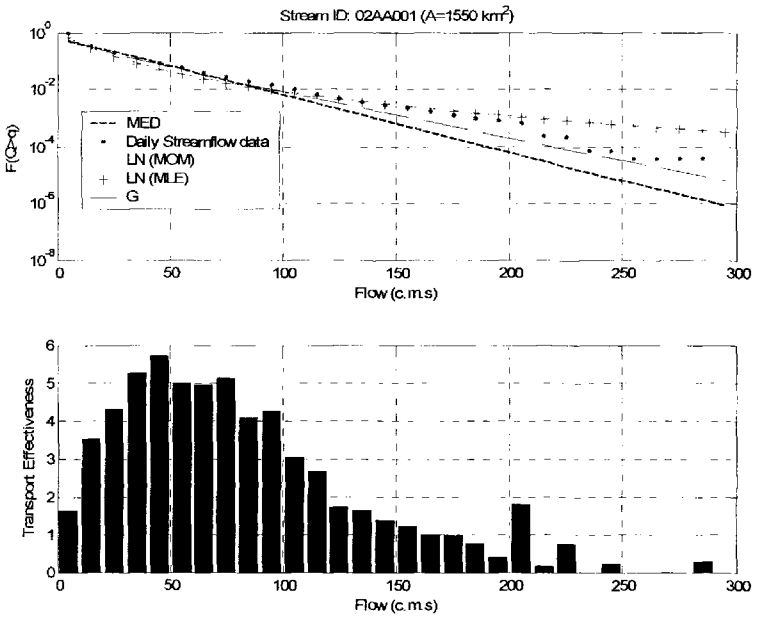


**Fig 2.5:** FDCs and the transport effectiveness histogram for (a) small stream; and (b) large stream

low to moderate flow ranges. Fig. 2.5(b) also shows that the $Q_e$ value determined from the TEC approach is located within the low to moderate flow range. If this is true for other large streams, the proposed analytical solution should perform well.

For small streams, Fig. 2.5(a) shows that MED closely fits the empirical FDC for the low to moderate flow range; and at the extremely high flow range the level of conformance between MED and the empirical FDC is better than LN and almost as good as G. Therefore, whether $Q_e$ is an extreme or low to moderate event, the proposed analytical solution would work well for small streams.

Overall, this study shows that when using estimators of $Q_e$ based upon a fitted distribution, a user should be very cautious in selecting and fitting that distribution function. Tables 2.2 and 2.3 together reveal that the goodness of fit test results coincide with the best comparison results between analytical $Q_e$ solutions and those from transport effectiveness curves for most of the streams except for 05PB021, 02BF005, 02GA032, and 02GA030. For these four streams in the computation of $Q_e$ using the transport effectiveness curve approach, the size of the class interval needed to be adjusted multiple times to come up with a single distinguishable peak because the value was not well defined. A half discharge would be a more stable estimator in this case.

### 2.5.3 Comparison with half-discharge

In light of the problems associated with the determination and interpretation of $Q_e$, Vogel et al. (2003) introduced the concept of half-discharge. The half-discharge $(Q_{1/2})$ of a stream is that discharge above and below which half the total long-term load is transported. It can be determined either theoretically using flow distribution and sediment transport models or empirically using measured flow and sediment transport data. Vogel et al. (2003) provides a detailed description of both methods. To gain more understanding, $Q_{1/2}$ values determined empirically are included in Table 2.3. $Q_e$ (MED)

correlates well with $Q_{1/2}$ (empirical), with an $R^2$ of 0.99, whereas $Q_e$ (LN-MOM) does not correlate as well with an $R^2$ of 0.56. The slopes of the two regression lines are 1.42 between $Q_{1/2}$ and $Q_e$ (MED), and 1.71 between $Q_{1/2}$ and $Q_e$ (LN-MOM), respectively. The $Q_e$ (LN-MOM) value for the stream 02GA032 is extremely high partially because of an unusually high $\beta$ value. The resulting data point affects regression results significantly. Performing the same regression analysis without this data point for $Q_e$ (LN-MOM) and $Q_{1/2}$, $R^2$ increased to 0.95. Inclusion and exclusion of the same data point does not change the regression results between $Q_e$ (MED) and $Q_{1/2}$. The high correlation between $Q_e$ (MED) and $Q_{1/2}$ further supports the application of the derived analytical solution based on mixed exponential distribution models.

### 2.5.4 The Characteristics of Effective Discharge

Characteristics such as the percentage of time $Q_e$ is exceeded and its recurrence interval can enhance our understanding of the frequency of such events. Pickup and Warner (1976) used the flow duration curve and found that for Cumberland Basin streams, the $Q_e$ value is exceeded 3-5 times a year. For streams within the Yampa River basin, flows equaled or exceeded $Q_e$ within a range of 0.4 to 3% of the time per year (Andrews 1980). In most studies, the recurrence intervals ($T_r$) of $Q_e$ estimated from annual maximum flow series were reported to range from 1.15-3.26 years (Emmett and Wolman 2001; Pickup and Warner 1976; Andrews 1980).

In this study, annual maximum flow series were used to determine the annual return period of $Q_e$ estimated from transport effectiveness curves. Table 2.3 reveals that the recurrence intervals of $Q_e$ for all the streams are less than 2 years. For 10 streams, the $T_r$ values of $Q_e$ were less than the recurrence interval of the smallest discharge from their respective annual maximum flow series. For those steams the recurrence intervals were reported as less than those corresponding to the smallest peak discharge in the annual maximum flow series. For these streams it is more appropriate to rely on the probability

of exceedence (or percentage of time $Q_e$ is exceeded) as determined from FDCs to get an idea of the frequency of occurrence of their $Q_e$'s. The fact that 10 out of 25 streams have $Q_e$'s with $<1.11$ year recurrence interval indicates that the conventional notion of $T_r$ values between the range of 1.15-3.26 years for $Q_e$ does not always hold true.

Table 2.3 also reports the fraction of times $Q_e$ is equaled or exceeded using the FDC of each stream under investigation, constructed from the daily streamflow data for the entire historical period. The FDCs for the selected streams indicate that $Q_e$ is exceeded from 0.7 to 80% of the time. This suggests that percentage of time of exceedence alone cannot be used for the identification of effective discharge.

## 2.6 Conclusions and Recommendations

Analytical solution for $Q_e$ require that the frequency distribution pattern of the flow series be approximated by some reasonable function. In the past, a lognormal distribution has often been used to represent the frequency distribution of the flow series. Analysis of the FDCs (flow duration curves) of 25 Ontario streams indicates that below a drainage area of 10 $km^2$, the flow exceedence probabilities are better described by gamma or the proposed mixed exponential distribution. The analytically estimated $Q_e$ values based on the lognormal, gamma and mixed exponential distributions were compared with those obtained from the empirical transport effectiveness curves and with empirical half-discharge values.

This study found that the analytically estimated $Q_e$ values based on the mixed exponential distribution provide better results in comparison to lognormal pdf, for small and large streams. However, the K-S goodness of fit test statistic indicates that the mixed exponential model only provides a good fit for small streams, but not for large streams. Closer visual inspection showed that mixed exponential models for large streams still fit well flows at the low to moderate range. $Q_e$ values determined from transport effectiveness curves are also located in the low to moderate flow range. That is why $Q_e$

values based upon the mixed exponential distribution performed well for both large and small drainage basins. A high correlation between the proposed analytical solution of $Q_e$ with half-discharge values for all 25 streams provides additional support of the reliability of this solution.

The results highlight the importance of good statistical analyses before utilization of the analytical solutions for $Q_e$. The nature of streamflows is highly unpredictable and is strongly dependent on the climate conditions and upstream catchment characteristics. The conventional notion that lognormal and gamma distribution functions fit the daily streamflow data well is not always true. Therefore, relying on analytical solutions based upon these distribution functions may result in poor estimates of $Q_e$. Practicing engineers should use with care the statistical tools at their disposal for fitting the streamflow data to various distribution functions, including 3-parameter distributions. Proper treatment of zero and near zero flows is another challenge. In future studies, probability models that are specifically structured to address zero-flows and censored data may be examined and fitting procedures developed for these models may be utilized (Griffis et al. 2004; Kroll and Stedinger 1996).

# References:


1. Andrews, B. 1987. Restoring the sinuosity of artificially straightened stream channels. Environmental Geology Water Science, **10**(1): 33-41.
2. Andrews, E.D. 1980. Effective and bankfull discharges of streams in the Yampa River basin, Colorado and Wyoming. Journal of Hydrology, **46**: 311-330.
3. Annable, W.K. 1996. Morphologic relationships of rural watercourses in southern Ontario and selected field methods in fluvial geomorphology. Ontario Ministry of Natural Resources, Printed in Ontario, Canada.
4. Biedenharn, D.S., and Copeland, R.R. 2000. Effective discharge calculation. U.S. Army Corps of Engineers, ERDC/CHL HETN-II-4.
5. Copeland, R.R., Biedenharn, D.S., and Fischenich, J.C. 2000. Channel-forming discharge. U.S. Army Corps of Engineers, ERDC/CHL CHETN-VIII-5.

6. Dickinson, W.T., and Green, D.R. 1988. Characteristics of sediment loads in Ontario streams. Canadian Journal of Civil Engineering, **15**: 1067-1079.
7. Doll, B.A., Grabow, G.L, Hall, K.R., Halley, J., Harman, W.A., Jennings, G.D, Wise, D.E. 2003. Stream restoration: a natural channel design handbook, Prepared by the North Carolina Stream Restoration Institute, NC State University. A copy of this handbook can be downloaded from www.bae.ncsu.edu.
8. Downs, P.W., and Kondolf, G.M. 2002. Post-project appraisals in adaptive management of river channel restoration. Environmental Management, **29**(4): 477-496.
9. Emmett, W.W., and Wolman, M.G. 2001. Effective discharge and gravel-bed rivers. Earth Surface, Processes and Landform, **26**: 1369-1380.
10. Fennessey, N. and Vogel, R.M. 1990. Regional flow-duration curves for ungauged sites in Massachusetts. Water Resources Planning and Management, **116**(4): 530-549.
11. Goodwin, P. 2004. Analytical solutions for estimating effective discharge. Journal of Hydraulic Engineering, **130**(8): 729-738.
12. Griffis, V.W., Stedinger, J.R., Cohn, T.A., 2004. Log Pearson type 3 quantile estimators with regional skew information and low outlier adjustments. Water Resources Research, **40**, W07503, doi: 10.1029/2003WR002697, 2004.
13. Haan, C.T. 1977. Statistical methods in hydrology. Printed by the Iowa State University Press, Iowa.
14. HYDAT, 2001. HYDAT CD-ROM user's manual. Printed by Environment Canada.
15. Jackson, W.L., and Haveren, B.P. 1984. Design for a stable channel in coarse alluvium for riparian zone restoration. Water Resources Bulletin, **20**(5): 695-703.
16. Johnson, N.L., Kotz, S., and Balakrishnan, N., 1994. Continuous univariate distributions. Vol. 1, 2nd Edition, John Wiley and Sons, NY, U.S.A.
17. Keystone Stream Team, 2002. Guidelines for natural stream channel design for Pennsylvania Waterways. Prepared by the Alliance for the Chesapeake Bay. Electronic copies of this document are available at www.canaanvi.org/nscdguidelines.

18. Kondolf, G.M., Smeltzer, M.W., and Railsback, S.F. 2001. Design and performance of a channel reconstruction project in a coastal California gravel-bed stream. Environmental Management, **28**(6): 761-776.
19. Kroll, C.N., and Stedinger, J.R., 1996. Estimation of moments and quantiles using censored data. Water Resources Research, **32**(4): 1005-1012.
20. Limbrunner, J.F., Vogel, R.M., Brown, L.C. 2000. Estimation of harmonic mean of a lognormal variable. Journal of Hydrologic Engineering, **5**(1): 59-66.
21. Mimikou, M. and Kaemaki, S. 1985. Regionalization of flow duration characteristics. Journal of Hydrology, **82**: 77-91.
22. Morris, S. and Moses, T. 1999. Urban stream rehabilitation: a design and construction case study. Environmental Management, **23**(2):165-177.
23. Nash, D.B. 1994. Effective sediment-transporting discharge from magnitude-frequency analysis. Journal of Geology, **102**: 79-95.
24. Ness, R., and Joy, D.M. 2002. Performance of natural channel designs in southwestern Ontario. Canadian Water Resources Journal, **27**(3): 293-315.
25. Ontario Ministry of Natural Resources. 1994. Natural channel system: an approach to management and design. Abbreviated as *OMNR*, Ministry of Natural Resources, Natural Resources Information Center, Toronto, ON. Printed in Ontario, Canada.
26. Pickup, G., and Warner, R.F. 1976. Effects of hydrologic regime on magnitude and frequency of dominant discharge. Journal of Hydrology, **29**: 51-75.
27. Poudevigne, J., Alard, D., Leuven, R.S.E.W., Nienhuis, P.H. 2002. A Systems approach to river restoration: a case study in the lower Seine Valley, France. River Research and Applications, **18**: 239-247.
28. Quimpo, R.G., Alejandrino, A.A., and McNally, T.A. 1983. Regionalized flow duration for Philippines. Journal of Water Resources Planning and Management, **109**(4): 320-330.
29. Riley, S.J., 1972. A comparison of morphometric measures of bankfull. Journal of Hydrology, **17**: 23-31.

30. Scholz, J.G., and Booth, D.B. 2001. Monitoring urban stream: strategies and protocols for humid-region lowland systems. Environmental Monitoring and Assessment, **71**: 143-164.
31. Searcy, J.K. 1959. Flow-duration curves. Water Supply Paper 1542-A, U.S. Geological Survey, Weston, VA.
32. Shields Jr, F.D., Copeland, R.R., Klingeman, P.C., Doyle, M.W., Simon, A. 2003. Design for stream restoration. Journal of Hydraulic Engineering, **129**(8):575-584.
33. Singh, R.D., Mishra, S. K., and Chowdhary, H. 2001. Regional flow-duration models for large number of ungauged Himalayan catchments for planning microhydro projects. Journal of Hydrologic Engineering, **6**(4): 310-316.
34. Stedinger, J.R., Vogel, R.M., and Foufoula-Georgiou, E. 1993. Handbook of Hydrology. Editor in Chief, Maidment, D.R. Printed and bound by R.R. Donnelley and Sons Company. Printed in the United States of America.
35. Stedinger, J.R. 1980. Fitting log normal distributions to hydrologic data. Water Resources Research, **16**(3): 481-490.
36. Vogel, R.M., Stedinger, J.R., and Hooper, R.P. 2003. Discharge indices for water quality loads. Water Resources Research, **39**(10): 1-9.
37. Williams, G.P. 1978. Bank-full discharge of rivers. Water Resources Research, **14**(6) : 1141-1154.
38. Wolman, M.G., and Miller, J.P. 1960. Magnitude and frequency of forces in geomorphic processes. Journal of Geology, **68**: 54-74.
39. Woodyer, K.D. 1968. Bankfull frequency in rivers. Journal of Hydrology, **6**: 114-142.
40. Yu, P-S and Yang, T-C. 1996. Synthetic regional flow duration curve for southern Taiwan. Hydrological Processes, **10**: 373-391.

# NOTATIONS

The following symbols are used in this paper:

A= drainage area of the watershed ($km^2$)

CV= coefficient of variation of sample data

E= sediment-transport effectiveness of the stream

$F(Q \leq q)$= cumulative distribution function of daily streamflow

$f(Q)$= probability density function of stream flow

$P(Q>q)$= exceedence probability distribution function of daily stream flow

$Q$= stream flow rate ($m^3$/sec)

$Q_b$= bankfull discharge ($m^3$/sec)

$Q_e$= effective discharge ($m^3$/sec)

$Q_s$= sediment transport rate (tons/day)

$Q_t$= discharge with a particular recurrence interval ($m^3$/sec)

$\alpha$ = coefficient of the sediment rating curve

$\alpha_g$ = parameter of the gamma pdf

$\beta$ = exponent of the sediment rating curve

$\beta_g$ = parameter of the gamma pdf

$\sigma$ = standard deviation of the flow series

$\sigma_y$ = standard deviation of the logarithm of discharge

$\mu$ = mean of the flow series

$\mu_y$ = mean of the logarithm of discharge

$\gamma$ = parameter of the mixed exponential model

$\delta(Q)$= Dirac delta function

$\lambda$ = parameter of the exponential and mixed exponential model

# Chapter 3

## Effective and f-load Discharges for Streams with Mixed Gamma Flow Distributions

Asif Quader, Yiping Guo, Jery R. Stedinger

### Abstract

Goodness-of-fit tests of selected southern Ontario streams with a definite percentage of zero flows indicate that the conventional lognormal probability density functions do not approximate well the frequency distribution of the flow series. Therefore, mixed gamma and mixed lognormal distributions were proposed as alternatives. The analytical solutions of effective discharge, half-load discharge and f-load discharges were derived based on mixed gamma distributions. For the selected small streams in southern Ontario, the half-load discharge values from mixed gamma distributions were found to be more accurate than those determined from lognormal and mixed lognormal distributions. At the same time, it was found that analytical solutions of half-load discharge based on mixed gamma distributions are less sensitive to the exponent of the sediment rating curve for the selected streams. It was also found that when the exponent of the sediment rating curve is equal to or greater than 2, effective discharge of small southern Ontario streams is approximately equal to f-load discharges with an f of 0.6.

**Keywords:** effective discharge, half discharge, stream restoration

## 3.1 Introduction

The magnitude-frequency concept (Wolman and Miller 1960) states that the significance of a geomorphic event is dependent not only on the magnitude of the event but also on its frequency of occurrence. Effective discharge ($Q_e$) is defined as the increment of discharge that transports the largest sediment load over a period of years (Andrews 1980; Emmett and Wolman 2001). As $Q_e$ transports the maximum amount of sediment load and links sediment load with channel geometry, it is hypothesized that it does most of the work in forming a channel. That is why in stream restoration projects $Q_e$ is often considered as the channel-forming discharge. Using observed long-term streamflow series, $Q_e$ can be determined graphically from the peak of the transport effectiveness curve (Wolman and Miller 1960). However, this transport effectiveness curve approach for the determination of $Q_e$ has been criticized for its inaccuracy and application of $Q_e$ in river restoration has been criticized for its lack of theoretical support (e.g., Vogel et al. 2003; Sichingabula 1999; Lenzi et al. 2006).

Nash (1994) and Goodwin (2004) proposed analytical approaches for determining $Q_e$ to improve the accuracy of the TEC approach. The analytical approaches are also based on the principle of 'transport effectiveness', but the frequency distribution pattern of the flow series is represented by a theoretical probability density function (pdf). This allows the determination of $Q_e$ from closed-form mathematical equations. To overcome the difficulty in the determination of $Q_e$ and reduce the ambiguity in the interpretation of $Q_e$, Vogel et al. (2003) introduced the concept of half-load discharge.

Half-load discharge ($Q_{1/2}$) is defined as the value of discharge above and below which half of the long-term sediment load is transported (Vogel et al. 2003). This half-load discharge may be a better discharge index that can be used in river restoration projects. The concept of half-load discharge was also generalized to f-load discharge, i.e., a discharge above which a fraction f of the total sediment load is transported. Similar to

$Q_e$, $Q_{1/2}$ can also be determined graphically (referred to as the empirical approach) and analytically. In the analytical solution of $Q_{1/2}$, the frequency distribution pattern of the flow series is also approximated by a theoretical pdf. Therefore, similar to $Q_e$, the accuracy of the analytical solution of $Q_{1/2}$ depends on how well the selected pdf represents the frequency distribution of the flow series.

Vogel et al. (2003) applied the concept of half-load discharge (referred to as half discharge hereinafter) only for the Susquehanna river at Harrisburg, Pennsylvania, with a drainage area of 55,425 $km^2$. In the analytical solution of $Q_{1/2}$, Vogel et al. (2003) assumed that the daily streamflow data could be best approximated by a lognormal pdf. However, for small streams with small drainage areas, lognormal distribution is probably not the best in representing streamflow frequency distributions (Quader et al. 2007). Often these small streams have zero flows as well. Undertaking restoration projects in small streams can be very difficult because of the lack of streamflow data. A suitable theoretical pdf can in some way compensate for the lack of data. Quader et al. (2007) illustrated that, among the two parameter distribution models, gamma and mixed exponential distributions better approximate the frequency distributions of the daily streamflow series from small streams.

The only analytical solution of $Q_{1/2}$ that is available now is for lognormal streamflow distributions. In this study, mixed gamma and mixed lognormal distributions are introduced to better represent daily streamflows from small drainage areas. Using the mixed gamma and mixed lognormal distributions, analytical expressions for half and f-load discharges were derived. These analytical solutions are then applied to a number of southern Ontario streams. To determine which family of distributions best represent flows from small streams, the analytical results were compared with the half discharge values determined directly from the corresponding streamflow series. To explore if there is a stable relationship between a certain f-load discharge and $Q_e$, a group of different f-load discharges were computed and compared with $Q_e$ for the selected streams.

## 3.2 Calculation of Effective and f-Load Discharges

Conventionally, $Q_e$ is determined as the peak of the transport effectiveness curve (TEC). TEC is developed by combining the sediment rating curve and the frequency distribution of the flow series. For some streams, it may become very difficult to identify a single distinguishable peak from their TECs. For those streams, the size or number of class intervals need to be adjusted repeatedly to identify the peak of their TECs. Biedenharn and Copeland (2000) proposed guidelines for appropriate adjustment procedures. For some streams, even after repeated adjustments following established rules, it may still not be possible to identify a peak from the TEC and thus an estimation of $Q_e$ cannot be made.

In the analytical solution of $Q_e$, the sediment rating curve represented by a simple power function, is combined with a theoretical streamflow pdf, $f_Q(q)$, resulting in the transport effectiveness (E) of the stream. $Q_e$ is the q value where E attains its maximum. Therefore, $Q_e$ can be identified by differentiating E with respect to q and equating that derivative to zero:

$$\frac{\partial E}{\partial q} = a\frac{\partial\left[f_Q(q)\times q^b\right]}{\partial q} = 0 \tag{3.1}$$

In Eqn. (3.1), a and b are the coefficient and exponent of the sediment rating curve (i.e., $L = aq^b$, where L is the sediment load carried by flow rate q).

If streamflows follow a two-parameter LN distribution so that

$$f_Q(q) = \frac{1}{q\sigma_x\sqrt{2\pi}}e^{\frac{-(x-\mu_x)^2}{2\sigma_x^2}} \tag{3.2}$$

where $x = \ln(q)$ and $\mu_x$ and $\sigma_x$ are the mean and standard deviation, respectively, of the log-transformed flow series; the value of $Q_e$ is given by (Goodwin 2004),

$$Q_e = e^{\mu_x+\sigma_x^2(b-1)} \tag{3.3}$$

If $f_Q(q)$ is approximated by a gamma (G) distribution, $Q_e$ is given by (Goodwin 2004),

$$Q_e = \beta[b + (\alpha - 1)] \tag{3.4}$$

where $\alpha$ and $\beta$ are the parameters of the G distribution. A notable aspect of both analytical solutions is that $Q_e$ is always only dependent on the exponent of the sediment rating curve b. The main advantage of the analytical solution of $Q_e$ is that if the distribution parameters and the sediment transport characteristics are known, the $Q_e$ value can always be easily determined.

To compensate for some of the shortcomings of the effective discharge concept, Vogel et al. (2003) proposed the concept of half discharge and related f-load discharges. To make the mathematical derivations more rigorous, sediment loads were described by the following power law model with a stochastic component

$$L = e^a Q^b e^{\varepsilon} = \exp(a + bX + \varepsilon) \tag{3.5}$$

where X=ln(Q), and Q is the streamflow treated as a random variable; L has units of mass per day, a and b are model parameters, $\varepsilon$ is assumed to be normally distributed model errors with zero mean and constant variance $\sigma_\varepsilon^2$. The conditional mean load given $Q = q$, where q denotes a particular value of Q, is

$$E(L|Q = q) = e^a q^b e^{\frac{\sigma_\varepsilon^2}{2}} \tag{3.6}$$

With L defined as a random variable dependent on random variable Q, the expected value of $L(\mu_L)$ can be calculated as

$$\mu_L = \int_0^\infty E(L|Q = q) f_Q(q) dq \tag{3.7}$$

$Q_{1/2}$, according to its definition, can therefore be obtained as follows

$$\int_0^{Q_{1/2}} E[L|Q = q] f_Q(q) dq = \frac{\mu_L}{2} \tag{3.8}$$

where $\mu_L$ is the expected sediment load and $E[L|Q = q]$ is the conditional mean load. As shown in Vogel et al. (2003), the $Q_{1/2}$ value for a LN pdf is

$$Q_{1/2} = \exp(\mu_x + b\sigma_x^2) \tag{3.9}$$

Eqn. (3.9) shows that $Q_{1/2}$ is not dependent on the coefficient of the sediment rating curve either. Clearly, the goodness-of-fit between the frequency distribution of the actual flow series and the theoretical pdf plays a key role in the accurate determination of both effective and half discharges.

The f-load discharge is defined as that discharge above which a fraction f of the long-term sediment load is transported. According to this definition, the f-load discharge can be evaluated through the following equation

$$\frac{E[L|Q < q]}{\mu_L} = 1 - f \tag{3.10}$$

where $E[L|Q < q]$ is the conditional mean load given $Q < q$. Half discharge is therefore a special case of the f-load discharges with f = 0.5. Similar to half discharge, f-load discharges can also be easily calculated if a suitable theoretical pdf can be used to properly represent the frequency distribution of the streamflow series.

## 3.3 Frequency Distribution Patterns of Small Ontario Streams

### 3.3.1 Selection of Streams and Fitting of Theoretical Distributions

Nineteen streams located in the Ontario province with fractions of zero flows ranging from 1 to 40% were selected in this study from HYDAT (2001). The drainage areas of these streams range from 0.34 to 168 $km^2$, with 84% of them less than 20 $km^2$. More details about these streams are presented in Table 3.1. In order to find the suitable distribution function that best fits the daily streamflow data of small streams, different theoretical distributions are fitted to the streamflow data. Goodness-of-fit tests are conducted to determine whether or not a particular set of observations are drawn from a particular family of distributions.

**Table 3.1:** Information about selected southern Ontario streams

| Name of the Stream | Stream ID | Latitude | Longitude | Record | A ($km^2$) | $\gamma$ |
|---|---|---|---|---|---|---|
| Lake 227 Outlet Near Kenora | 05QD008 | 49°41'15"N | 93°41'25"W | 1969-1995 | 0.34 | 0.60 |
| Lake 303 Outlet Near Kenora | 05PD019 | 49°39'35"N | 93°44'38"W | 1970-1995 | 0.54 | 0.64 |
| Northwest Tributary to Lake 239 | 05PD022 | 49°39'57"N | 93°43'40"W | 1970-1995 | 0.56 | 0.67 |
| Lake 226 Outlet Near Kenora | 05QD015 | 49°41'20"N | 93°44'15"W | 1972-1994 | 0.97 | 0.74 |
| Lake 224 Outlet Near Kenora | 05QD018 | 49°41'33"N | 93°46'0"W | 1975-1995 | 0.97 | 0.60 |
| Lake 661 Outlet Near Kenora | 05PD028 | 49°39'30"N | 93°38'0"W | 1983-1995 | 1.25 | 0.72 |
| Lake 470 Outlet Near Kenora | 05PD017 | 49°39'23"N | 93°43'57"W | 1969-2002 | 1.68 | 0.76 |
| O.A.C Farm Gauge No. 5 at Guelph | 02GA032 | 43°31'53"N | 80°18'18"W | 1969-1984 | 2.51 | 0.84 |
| Lake 223 outlet near Kenora | 05QD017 | 49°41'56"N | 93°42'50"W | 1975-1995 | 2.6 | 0.86 |
| Lake 239 outlet near Kenora | 05PD023 | 49°39'28"N | 93°43'36"W | 1970-1995 | 3.9 | 0.70 |
| Fifth Concession Drain near Essex | 02GH013 | 42°12'18"N | 82°47'12"W | 1989-1994 | 3.9 | 0.78 |
| Lake 240 outlet near Kenora | 05PD015 | 49°38'52"N | 93°43'34"W | 1969-1995 | 7.25 | 0.77 |
| Norberg Creek above Batchawana River | 02BF005 | 47°4'8"N | 84°26'7"W | 1980-2000 | 11.5 | 0.99 |
| Bloomfield Creek at Bloomfield | 02HE001 | 43°59'26"N | 77°13'6"W | 1969-1992 | 13.9 | 0.99 |
| Sturgeon Creek near Leamington | 02GH001 | 42°2'44"N | 82°34'29"W | 1971-1992 | 14.2 | 0.99 |
| Canagagigue Creek near Floradale | 02GA036 | 43°40'12"N | 80°35'48"W | 1974-1984 | 17.9 | 0.84 |
| Stoney Creek at Stoney Creek | 02HA022 | 43°13'31"N | 79°45'5"W | 1989-2001 | 20 | 0.94 |
| Collins Creek near Kingston | 02HM005 | 44°15'24"N | 76°36'46"W | 1969-2001 | 155 | 0.99 |
| Twenty Mile Creek above Smithville | 02HA020 | 43°6'54"N | 79°33'56"W | 1989-2001 | 168 | 0.82 |

Note: $\gamma$ is the fraction of non-zero flows.

To fit theoretical distributions to observed data, the estimated value of the distribution parameters can be determined by either the method of moment (MOM) or the method of maximum likelihood (MLE). In fitting LN distributions, because log transformation needs to be applied to the flow data, zero flows make the fitting procedure problematic. Without the removal of zero flows, MLE cannot be applied to flow series containing zero flows. In this analysis, theoretical LN distributions were fitted to observed flow series using the relationships that $\mu_x = 0.5\ln[\mu^2/(1+CV^2)]$ and $\sigma_x^2 = \ln[1+CV^2]$ (Stedinger et al. 1993; Haan 1977), where CV is the coefficient of variation and $\mu$ is the mean of the flow series, respectively; $\mu_x$ and $\sigma_x$ are respectively the mean and standard deviation of the log-transformed flow series. The sample values of CV and $\mu$ are calculated from the streamflow series with zero flows included. The

estimated values of $\mu_x$ and $\sigma_x$ are then calculated using the above relationships. This way, the problem of zero flows is circumvented. The conventional MOM was used in fitting the G distributions to streamflow data. The relative performance of the fitted distributions was assessed next.

### 3.3.2 Visual Inspection and Kolmogorov-Smirnov Test Statistics

In the first round of analysis, exceedence probabilities were determined from daily streamflow data themselves and from fitted LN and G cumulative distribution functions (CDFs). Because all daily flows are included in the analysis, the exceedence probabilities calculated herewith form the flow duration curve of a particular stream. Fig. 3.1 shows the exceedence probabilities obtained from different fitted CDFs and the flow duration curves constructed from the daily streamflow data of two streams. Similar figures were also prepared for all of the 19 streams. Because of space constraint only two streams are shown here. Fig. 3.1 shows that for the two streams, the flow duration curves of daily streamflow data are better approximated by G rather than the LN distributions. This is true for the majority of the other 17 streams. Curves obtained from the two alternative distributions proposed in this paper are also included in these figures. Comments about them will be made later.

Kolmogorvo-Smirnov (K-S) test statistics were determined for each of the fitted CDFs. The magnitude of the K-S test statistics serves as an indicator of the level of performance of the fitted CDFs. The results are summarized in Table 3.2 where the K-S test statistics for the two alternative distributions investigated in this study are also included. Table 3.2 indicates that the G distribution outperforms the LN distribution for the majority of the selected small streams (16 out of 19). Examining the magnitude of the K-S test statistic for our analysis purposes is probably not enough. Because the K-S test statistic is the maximum difference between the fitted theoretical and empirical CDFs, and the location in the distribution spectrum where this maximum difference occurs makes a big difference in our analysis. The maximum difference can occur in the low,

medium, or high flow regions. If it occurs in the high flow region with low exceedence probabilities, large difference in K-S test statistics does not necessarily correspond to

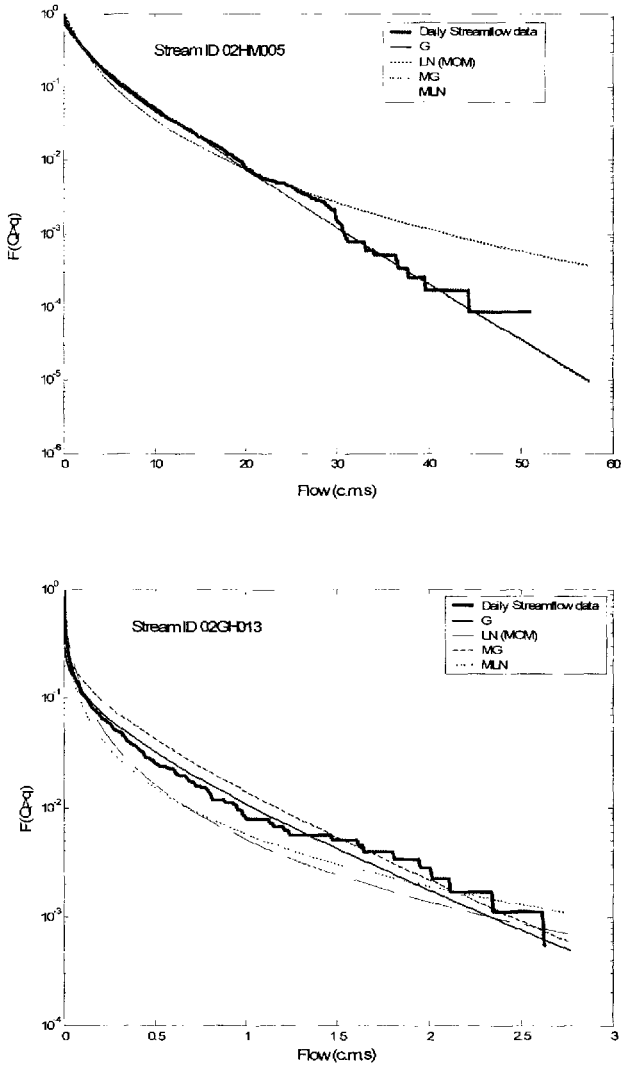


**Fig 3.1:** Exceedence probabilities calculated from daily streamflow data, fitted G, MG, LN and MLN distributions for the selected streams of 02HM005 and 02GH013

large difference in the $Q_e$ and $Q_{1/2}$ values predicted by the two theoretical distribution models. For all the selected 19 streams, the maximum difference occurs near the low flow region with high exceedence probabilities. Verification on the relative goodness-of-fit was necessary to confirm the findings from visual inspection and K-S test statistics.

**Table 3.2:** Values of K-S test statistics

| Stream ID | A ($km^2$) | K-S test statistics | | | |
|---|---|---|---|---|---|
| | | LN | MLN | G | MG |
| 05QD008 | 0.34 | 0.208 | 0.138 | 0.323 | 0.362 |
| 05PD019 | 0.54 | 0.272 | 0.272 | 0.114 | 0.141 |
| 05PD022 | 0.56 | 0.318 | 0.280 | 0.250 | 0.250 |
| 05QD015 | 0.97 | 0.313 | 0.307 | 0.085 | 0.131 |
| 05QD018 | 0.97 | 0.216 | 0.095 | 0.216 | 0.284 |
| 05PD028 | 1.25 | 0.444 | 0.444 | 0.444 | 0.444 |
| 05PD017 | 1.68 | 0.425 | 0.406 | 0.394 | 0.394 |
| 02GA032 | 2.51 | 0.377 | 0.377 | 0.377 | 0.377 |
| 05QD017 | 2.6 | 0.250 | 0.250 | 0.083 | 0.083 |
| 05PD023 | 3.9 | 0.167 | 0.167 | 0.083 | 0.083 |
| 02GH013 | 3.9 | 0.249 | 0.235 | 0.126 | 0.130 |
| 05PD015 | 7.25 | 0.241 | 0.229 | 0.048 | 0.084 |
| 02BF005 | 11.5 | 0.228 | 0.228 | 0.200 | 0.200 |
| 02HE001 | 13.9 | 0.193 | 0.191 | 0.281 | 0.281 |
| 02GH001 | 14.2 | 0.206 | 0.206 | 0.476 | 0.476 |
| 02GA036 | 17.9 | 0.246 | 0.246 | 0.200 | 0.200 |
| 02HA022 | 20 | 0.628 | 0.628 | 0.628 | 0.628 |
| 02HM005 | 155 | 0.363 | 0.363 | 0.111 | 0.111 |
| 02HA020 | 168 | 0.250 | 0.237 | 0.181 | 0.191 |

### 3.3.3 L Moment Diagrams

Originally proposed by Hosking (1990) and discussed in detail by Stedinger et al. (1993), L-moment diagrams illustrate the relationship between the sample estimates of L-kurtosis and L-coefficient of variation to L-skewness. For comparative purposes within the same L-moment diagram, these relationships can also be constructed using different theoretical pdfs. The L-moment diagrams so constructed may be examined to determine the family of theoretical pdfs that best fits the observed data. The advantage of L-moment diagrams over ordinary product moment diagrams is that L-moment ratios are unbiased for all probability distributions, while ordinary product moment ratios are significantly biased (Vogel and Fennessey 1993). In earlier studies, L-moment diagrams were used to evaluate the goodness-of-fit of alternative pdfs to sequences of annual minimum, average and maximum streamflows throughout the U.S. (Vogel and Wilson 1996); to evaluate the goodness-of-fit of alternative pdfs to average daily streamflows (Limbrunner et al. 2000; Vogel and Fennessey 1993); and for regional flood frequency analysis in different countries (Kumar et al. 2003; Kumar and Chatterjee 2005; Daviau et al. 2000; Jingyi and

Hall 2004). Comparison of L moment ratios was used in this study to better determine the family of theoretical distributions that best represent flows from small streams.

To construct L moment diagrams, unbiased estimates of the probability-weighted moments were calculated first. From these unbiased probability-weighted moments, the corresponding L moments were then determined. The theoretical background of the unbiased probability-weighted moments is available in Hosking (1990) and Stedinger et al. (1993). L-coefficient of variation is the ratio between the $2^{nd}$ and $1^{st}$ L moments, L-skewness is the ratio between the $3^{rd}$ and $2^{nd}$ L moments, and L-kurtosis is the ratio between the $4^{th}$ and $2^{nd}$ L moments.

Fig. 3.2(a) shows the relationship between the L-coefficient of variation and L-skewness of the selected 19 Ontario streams (i.e., individual data points). In determining the L moment ratios for the selected streams, the entire streamflow series including zero flows were taken into consideration. Polynomial approximations of the theoretical relationships between L-coefficient of variation and L-skewness for LN distributions was shown to be (Vogel and Wilson 1996)

$$\tau_2 = 1.16008\tau_3 - 0.05325\tau_3^2 - 0.10501\tau_3^4 - 0.00103\tau_3^6 \qquad (3.11)$$

That for G distributions was shown to be

$$\tau_2 = 1.74139\tau_3 - 2.59736\tau_3^3 + 2.09911\tau_3^4 - 0.35948\tau_3^6 \qquad (3.12)$$

Where $\tau_2$ and $\tau_3$ represent the L-coefficient of variation and L-skewness, respectively. Based on these approximations, the L moment ratios for these two types of distributions were plotted in Fig. 3.2(a). Fig. 3.2(a) shows that most of the data points representing L moment ratios of the selected streams are located closer to the curve constructed from the G distributions.

Fig. 3.2(b) shows the L moment diagram based on L-kurtosis and L-skewness for the selected Ontario streams. Again, for each stream the entire streamflow record was used. Polynomial approximations of the theoretical relationship between L-kurtosis and L-skewness developed by Stedinger et al (1993) were used to determine the L moment

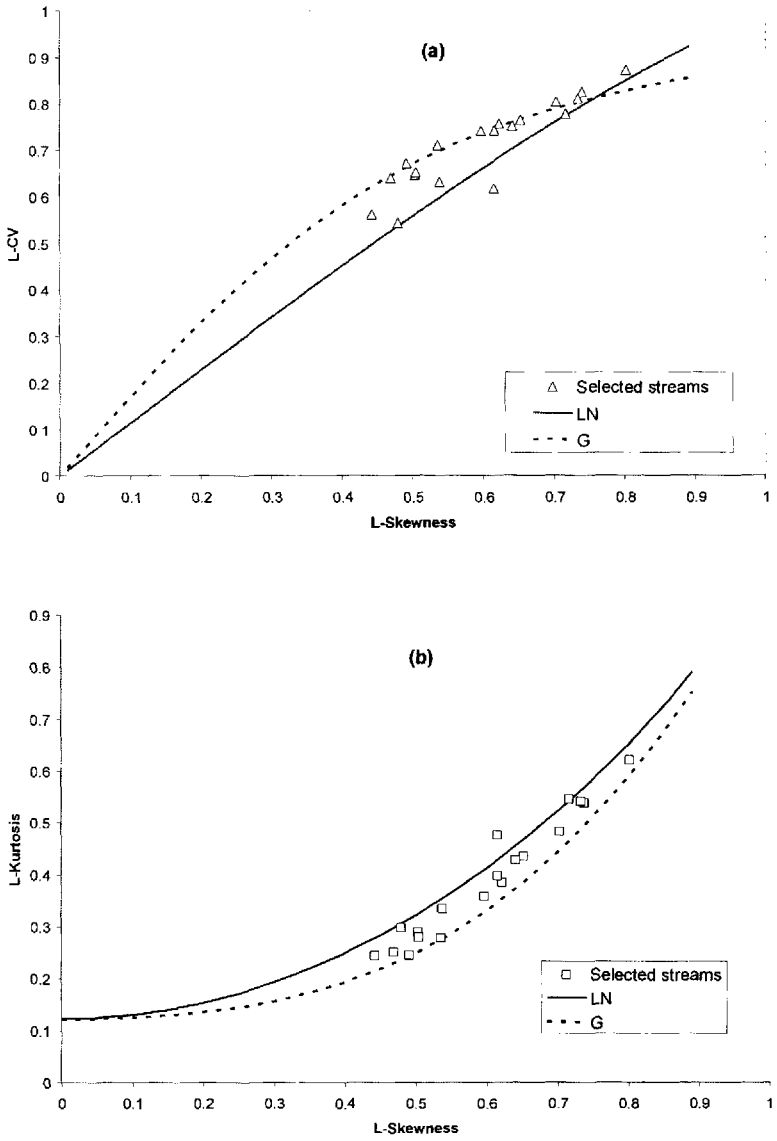


**Fig 3.2:** L-moment diagrams for the selected streams (a) L-coefficient of variation vs L-skewness; (b) L-kurtosis vs L-skewness

ratios for the G and LN distributions. In Fig. 3.2(b), the L moment ratios for the G and LN distributions are drawn as the dashed and solid lines, respectively. The data points representing the L moment ratios of the selected Ontario streams are located in between the two lines. This indicates again that frequency distributions of daily streamflows from small southern Ontario streams with zero flows cannot be well approximated by the conventional LN distributions. From Fig. 3.2(b) alone, the G distribution family cannot

be judged as representing better the frequency distribution of streamflows from small southern Ontario streams. Hence, other more complex distributions or modifications of the G and LN distributions may be necessary and may perform better for small streams.

## 3.4 Alternative Flow Distribution Models

### 3.4.1 Three-parameter Lognormal Distributions

Conventional two-parameter LN distributions may be modified to deal with zero flows. For example, LeBoutillier and Waylen (1993) and Stedinger (1980) proposed the following three-parameter LN distribution,

$$f_Q(q) = \frac{1}{(q-\varsigma)\sigma\sqrt{2\pi}} e^{\frac{-\{\ln(q-\varsigma)-\mu)\}^2}{2\sigma^2}} \tag{3.13}$$

where $\sigma$ and $\mu$ are the shape and scale parameters, respectively, which are both greater than zero; $\varsigma$ is the threshold parameter and $q > \varsigma$. In this study we are more interested in small streams that may have a percentage of zero flows. For those streams, a suitable flow threshold would be zero (i.e., $\varsigma = 0$) and the three-parameter LN distribution reduces to the conventional two-parameter LN distribution. Thus, three-parameter LN distribution models in the form of Eqn. (3.13) are not suitable for our study purposes.

Using the U.S. Geological Survey's (USGS) streamflow data from 1571 sites, Limbrunner et al. (2000) applied L moment diagrams and showed that daily streamflows are well approximated by both the conventional two- and three-parameter LN (i.e., Eqn. (3.13)) distributions. The USGS Hydro-climatic Data Network consists of 21 regions with 1659 sites, with widely varying drainage areas. For instance, Region 2 or the Mid-Atlantic region lists streams with drainage areas ranging from 3.8 to 61,696 $km^2$. Vogel and Fennessey (1993) showed that daily streamflow data from 23 sites in Massachusetts with drainage areas ranging from 4.4 to 384 $km^2$ were best approximated by the generalized Pareto distribution. The other distributions that were considered by Vogel and Fennessey (1993) included the normal, Gumbel, exponential, generalized extreme

value, three-parameter lognormal, Pearson type 3, and the lower bound of the five parameter Wakeby distribution.

For the purposes of our study, we are more interested in simple form pdfs so that closed-form analytical solutions of $Q_{1/2}$ and $Q_e$ can be obtained based on these pdfs. This is why we confined our earlier analysis to relatively simple pdf forms. The analysis in this study confirmed that for small southern Ontario streams with zero flows, the conventional LN distribution is not a good choice. Instead a distribution related to the G distribution that explicitly considers zero flows should perhaps be investigated.

### 3.4.2 Mixed Gamma Distributions

The following mixed gamma (MG) distribution that explicitly considers zero flows is proposed

$$f_q(Q) = \begin{cases} (1-\gamma)\delta(q), & q = 0 \\ \dfrac{\gamma q^{\alpha-1} e^{-q/\beta}}{\beta^{\alpha}\Gamma(\alpha)}, & q > 0 \end{cases} \tag{3.14}$$

where $\alpha$, $\beta$, and $\gamma$ are distribution parameters. The distribution presented in Eqn. (3.14) consists of two parts. The first part contains a dirac delta function and the parameter $\gamma$ representing the fraction of non-zero flows. The second part provides description of the G distribution of non-zero flows.

The mean $(\mu)$ and variance $(\sigma^2)$ of the proposed MG distribution were determined to be

$$\mu = \gamma\alpha\beta \tag{3.15}$$

$$\sigma^2 = \gamma\alpha\beta^2(\alpha + 1 - \gamma\alpha) \tag{3.16}$$

The values of $\alpha$ and $\beta$ are therefore related to the moments of the distribution through the following relationships

$$\alpha = \frac{1}{\gamma(1+CV^2)-1} \tag{3.17}$$

$$\beta = \frac{\mu\left[\gamma\left(1+CV^2\right)-1\right]}{\gamma} \tag{3.18}$$

In Eqns. (3.17) and (3.18), $\mu$ and CV are the mean and coefficient of variation of the entire streamflow series, including both zero and non-zero flows. To fit the MG distribution to streamflow data, first of all, the value of $\gamma$ is calculated as the fraction of non-zero flows; then applying the method of moment, the estimated values of $\alpha$ and $\beta$ are determined either using Eqns. (3.17) and (3.18) with the population moments replaced by sample moments calculated from all flows (first method) or by fitting a separate G distribution to the non-zero flows (second method). A third fitting procedure is to strictly apply the method of moment and use all the first three moments of distribution (third method). In this study, all three fitting procedures were applied to determine which fitting procedure results in the most accurate discharge indices determined from MG distribution.

### 3.4.3 Mixed Lognormal Distributions

Similarly, mixed lognormal (MLN) distributions that explicitly consider zero flows may be used. The same parameter $\gamma$ can be used to denote the fraction of non-zero flows, the MLN distribution form is similar to that of MG except that the G pdf in the part that describes the distribution of non-zero flows is replaced by the LN pdf. To fit the MLN distribution to streamflow data, first of all, the value of $\gamma$ is calculated as the fraction of non-zero flows; then applying the method of moment, the estimated values of $\mu_x$ and $\sigma_x$ are calculated with zero flows removed. The other two fitting methods as described for MG may also be applied for MLN. However, the analytical expressions involved are much more complex and experiment with the MG distributions showed that different fitting method resulted in only minor differences in the discharge indices values. Therefore, for MLN distributions, only one fitting method was used in this study. MLN is included here to see if the lack of fit of LN distributions for small streams can be reduced by considering zero flows separately.

### 3.4.4 Goodness-of-Fit of Alternative Distribution Models

Flow exceedence probabilities calculated based on the fitted MG and MLN distributions were determined and plotted along side those calculated from the fitted G and LN distributions in Fig. 3.1. For the stream of 02HM005, the value of $\gamma$ is 0.99, that is why in Fig. 3.1 the flow exceedence probabilities from the fitted G and MG distributions are almost identical. The same is true for LN and MLN. However, for the stream of 02GH013, the $\gamma$ value of 0.78 resulted in clearly distinguishable exceedence probability curves from the fitted G and MG distributions, and from the fitted LN and MLN distributions. Fig. 3.1 shows that visually, exceedence probability curves from the fitted MG distributions are just as good as the fitted G and better than the fitted LN and MLN distributions. Fig. 3.1 also shows that MLN does not improve the goodness-of-fit of the LN distribution substantially. The K-S test statistics shown in Table 3.2 also illustrate the aspect that MG does not obviously improve over G. However, MLN proved to be somewhat better than LN. But overall, G and MG are better than LN and MLN. Since our objective is to use the theoretical flow distribution models to generate estimates of effective and f-load discharges, comparison on the estimation accuracy for these discharge indices provided the ultimate test.

### 3.4.5 Analytical Solutions of Discharge Indices for the Proposed Distributions

Substitute the MG distribution (i.e., Eqn. (3.14)) into Eqn. (3.7), we have

$$\mu_L = \frac{a\gamma\beta^b\Gamma(\alpha+b)}{\Gamma(\alpha)} \tag{3.19}$$

and the conditional mean load given $Q < q$ can be calculated as

$$E[L|Q<q] = \frac{a\beta^b\gamma\Gamma(\alpha+b)}{\Gamma(\alpha)}F(q|\alpha+b,\beta) \tag{3.20}$$

where $F(q|\alpha+b,\beta)$ is the value of the CDF of a G distribution with parameters $(\alpha+b,\beta)$ evaluated at q.

Substitute Eqns. (3.19) and (3.20) into Eqn. (3.10), we have

$$F(q|\alpha+b,\beta)=1-f \tag{3.19}$$

Therefore, the f-load discharge for streams where the streamflow follows a MG distribution and sediment transport follows a power law relationship can be determined using the inverse of the CDF of a G distribution. Setting f to 0.5, the half discharge may also be determined using Eqn. (3.19).

Following the same derivation procedures, it can be shown that Eqn. (3.19) can be used to calculate the f-load discharges for G distributions as well. When streamflows follow the proposed MG distributions, it can also be shown that the effective discharge can be expressed by the same equation as that for the G distribution [i.e., Eqn. (3.4)]. The difference is that when MG is used, the estimated values of $\alpha$ and $\beta$ in Eqns. (3.4) and (3.19) can be determined by any one of the three fitting methods; while when G is used, the estimated values of $\alpha$ and $\beta$ in Eqns. (3.4) and (3.19) are determined based on all flows. Because zero flows transport zero sediment loads, the value of parameter $\gamma$ does not affect the relative distribution of sediment loads over different flow ranges and therefore does not appear in the expressions for effective and f-load discharges. Similarly, when streamflows follow the proposed MLN distributions, the effective discharge and half discharge can be expressed by the same equations as those for the LN distributions [i.e., Eqns. (3.3) and (3.9), respectively]. However, unlike when LN distribution is fitted to the streamflow series, in using Eqns. (3.3) and (3.9) with MLN distribution being fitted to the streamflows , $\mu_x$ and $\sigma_x$ are calculated with zero flows removed first.

## 3.5 Discharge Indices Calculated Using Different Flow Distribution Models

To compare and evaluate the accuracy in the analytical estimation of discharge indices provided by different theoretical flow distributions, the analytical solutions of

discharge indices based on different theoretical flow distributions for the 19 selected streams were compared with their corresponding empirical values. For each stream, the value of the exponent of the sediment rating curve b needs to be determined. Since no sediment transport data were available for any of the selected streams, assumptions were made about the b values for the selected streams. This does not negatively affect our study here because we are not interested in the actual values of the discharge indices and assumptions of varying b values may actually broaden the study scope. For similar study purposes, Nash (1994) reported that b values range from 1.23 to 3.02 for suspended sediment load. Goodwin (2004) reported that b values are 1.68 and 1.86 for the Red river and the Russian river, respectively. Vogel et al. (2003) reported a b value of 1.84 for the Susquehanna River at Harrisburg, Pennsylvania. Lenzi et al. (2006) reported an extremely high b value of 5.37 for a small stream in the Rio Cordon catchment located in the Eastern Italian Alps. These earlier findings about b values are used to guide the selection of representative b values. As a starting point, a b value of 2 was used to determine the different discharge indices for all of the 19 streams, later on, higher and lower b values were used for three of the selected 19 streams to explore the influence of b values.

### 3.5.1 Comparison between Mixed Gamma and Other Distributions

Using an assumed b value of 2, effective and half discharge values determined both empirically from the streamflow series themselves and analytically from fitted G, MG, LN, and MLN distributions were calculated for all of the 19 streams. Table 3.3 shows these discharge values. The empirically determined $Q_{1/2}$ and $Q_e$ values can be considered as the most accurate because they are based on the frequency distributions of actual streamflow series and does not use any fitted theoretical pdf. Of the three methods of fitting MG distributions, $\alpha$ and $\beta$ values determined using the second method resulted in the most accurate $Q_{1/2}$ values. Using the two other methods of fitting, $Q_{1/2}$ values are only marginally different from those resulting from the second method. The results

**Table 3.3:** Values of different discharge indices for the selected southern Ontario streams (b = 2)

| Stream ID | A ($km^2$) | Discharge indices | | | | | | | | | | $T_{Q_e}$ [5] (yr) |
|---|---|---|---|---|---|---|---|---|---|---|---|---|
| | | $Q_{1/2}$ [1] (Emp.) | $Q_{1/2}$ [2] (MG) | $Q_{1/2}$ [2] (G) | $Q_{1/2}$ [2] (LN) | $Q_{1/2}$ [2] (MLN) | $Q_e$ [3] (MG) | $Q_e$ [3] (G) | $Q_e$ [3] (LN) | $Q_e$ [3] (MLN) | $Q_e$ [4] (TEC) | |
| 05QD008 | 0.34 | 0.026 | 0.027 | 0.028 | 0.043 | 0.033 | 0.018 | 0.018 | 0.008 | 0.010 | 0.025 | 1.44 |
| 05PD019 | 0.54 | 0.055 | 0.047 | 0.050 | 0.076 | 0.061 | 0.032 | 0.032 | 0.013 | 0.016 | 0.027 | 1.08 |
| 05PD022 | 0.56 | 0.050 | 0.047 | 0.049 | 0.076 | 0.062 | 0.031 | 0.031 | 0.013 | 0.016 | 0.050 | 1.31 |
| 05QD015 | 0.97 | 0.043 | 0.045 | 0.047 | 0.059 | 0.051 | 0.032 | 0.032 | 0.017 | 0.020 | 0.027 | 1.1 |
| 05QD018 | 0.97 | 0.020 | 0.020 | 0.021 | 0.028 | 0.022 | 0.014 | 0.014 | 0.007 | 0.009 | 0.014 | 2 |
| 05PD028 | 1.25 | 0.096 | 0.123 | 0.126 | 0.222 | 0.188 | 0.079 | 0.079 | 0.028 | 0.033 | 0.105 | 1.44 |
| 05PD017 | 1.68 | 0.130 | 0.136 | 0.139 | 0.224 | 0.194 | 0.089 | 0.089 | 0.035 | 0.040 | 0.100 | 1.1 |
| 02GA032 | 2.51 | 0.890 | 0.456 | 0.456 | 0.870 | 0.870 | 0.284 | 0.280 | 0.093 | 0.093 | 0.300 | 1.14 |
| 05QD017 | 2.6 | 0.072 | 0.069 | 0.069 | 0.081 | 0.081 | 0.047 | 0.048 | 0.028 | 0.028 | 0.075 | 1.83 |
| 05PD023 | 3.9 | 0.120 | 0.115 | 0.115 | 0.129 | 0.129 | 0.082 | 0.083 | 0.052 | 0.052 | 0.070 | 1.4 |
| 02GH013 | 3.9 | 1.540 | 1.303 | 1.314 | 3.011 | 2.662 | 0.807 | 0.807 | 0.216 | 0.245 | 1.000 | <1.04 |
| 05PD015 | 7.25 | 0.259 | 0.240 | 0.240 | 0.268 | 0.268 | 0.172 | 0.173 | 0.110 | 0.110 | 0.180 | 1.53 |
| 02BF005 | 11.5 | 1.240 | 1.058 | 1.058 | 1.220 | 1.220 | 0.742 | 0.750 | 0.451 | 0.451 | 0.520 | <1.05 |
| 02HE001 | 13.9 | 1.130 | 0.991 | 0.991 | 1.293 | 1.293 | 0.660 | 0.666 | 0.337 | 0.337 | 0.450 | <1.04 |
| 02GH001 | 14.2 | 3.910 | 2.324 | 2.326 | 4.192 | 4.162 | 1.458 | 1.458 | 0.507 | 0.511 | 2.500 | 1.64 |
| 02GA036 | 17.9 | 3.710 | 3.873 | 3.873 | 7.075 | 7.075 | 2.424 | 1.860 | 0.830 | 0.830 | 5.400 | 1.42 |
| 02HA022 | 20 | 2.410 | 2.749 | 2.756 | 5.732 | 5.558 | 1.703 | 1.703 | 0.506 | 0.522 | 4.000 | 2.16 |
| 02HM005 | 155 | 12.15 | 12.746 | 12.768 | 15.986 | 15.888 | 8.633 | 8.633 | 4.662 | 4.691 | 6.700 | <1.03 |
| 02HA020 | 168 | 23.8 | 21.401 | 21.638 | 39.417 | 35.717 | 13.545 | 13.545 | 4.654 | 5.137 | 20.000 | 1.3 |

Notes:

1: Half discharge values determined empirically.

2: Half discharge values determined from theoretical distributions.

3: Effective discharge values determined from theoretical distributions.

4: Effective discharge values determined from the TEC approach.

5: Recurrence interval of $Q_e$ in years.

reported here are from the use of the second fitting method. The $Q_{1/2}$ values estimated using G, MG, LN, and MLN distributions are tabulated in Table 3.3. Table 3.3 shows that for the estimation of $Q_{1/2}$, G and MG performs equally good but G and MG perform much better than LN and MLN.

As a further proof of the accuracy of the analytical $Q_{1/2}$ values determined from G and MG distributions, regression analyses between the empirical and analytical values of $Q_{1/2}$ determined using LN, MLN, and MG were conducted. These analyses resulted in an $R^2$ (coefficient of determination) value of 0.99 and a slope of 0.91 between empirical $Q_{1/2}$ and the $Q_{1/2}$ determined based on MG distribution; an $R^2$ value of 0.98 and a slope of 1.58 between empirical $Q_{1/2}$ and the $Q_{1/2}$ determined based on LN distribution; and an $R^2$ value of 0.98 and a slope of 1.47 between empirical $Q_{1/2}$ and the $Q_{1/2}$ determined based on MLN distribution. Fig. 3.3 shows the data points and their respective regression lines. $R^2$ values closer to 1 suggest better one-to-one correlations; and the slope values closer to unity indicate better one-to-one matches. Therefore, the regression analysis results show that MG distributions provide the best estimate of half discharges.

In addition to the regression analysis, the relative percentage of error for the $Q_{1/2}$ values obtained from each type of distribution was also determined. In determining the relative percentage of error, the $Q_{1/2}$ values obtained empirically were considered as the true value. The relative percentage of error is calculated as $\left(=\frac{\text{Abs}[Q_{1/2}(\text{empirical}) - Q_{1/2}(\text{Analytical})]}{Q_{1/2}(\text{empirical})} \times 100\%\right)$. The results show that the average percentage of errors for $Q_{1/2}$ values determined from LN (48%) and MLN (35%) far exceeds that from MG (12.8%) and G (13.5%) distribution. Once again, these results indicate that half discharge values obtained from the MG distribution conforms to the

empirical $Q_{1/2}$ values better than those determined from the conventional LN and MLN distributions for small southern Ontario streams.

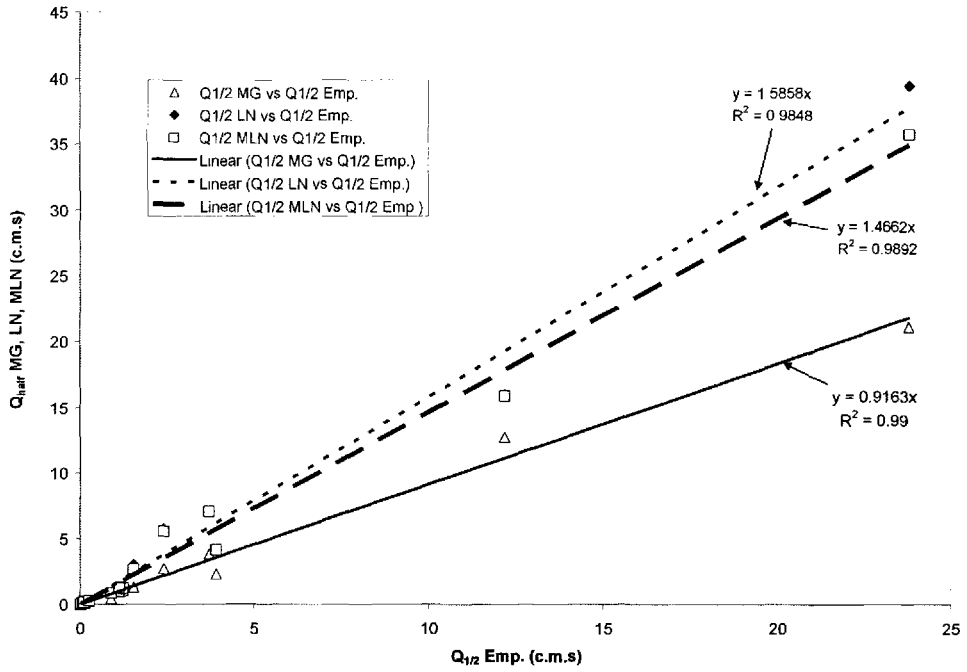


**Fig 3.3:** Comparison between $Q_{1/2}$ (empirical) vs $Q_{1/2}$ (MG); $Q_{1/2}$ (empirical) vs $Q_{1/2}$ (LN) and $Q_{1/2}$ (empirical) vs $Q_{1/2}$ (MLN)

Closer inspection of Table 3.3 also suggests that, in average, MG provides the best estimate in $Q_e$ as well. Table 3.3 lists the $Q_e$ values determined from the TEC approach and also from different theoretical distributions. In determining the relative percentage of error for these distributions, the $Q_e$ value obtained from the transport effectiveness curve approach was considered as the true value. A relative percentage of error of 27% was found for the $Q_e$ values determined from the MG distribution. Whereas, $Q_e$ values determined from G, LN and MLN distributions had relative percentage of errors of 28%, 58% and 54%, respectively.

The above conclusions are based on a typical b value of 2. To investigate the influence of b values, three streams were selected and for each of them b values ranging from 1 through 5 were assumed. The three selected streams are 02HM005 (155 $km^2$) with $\mu$ and $\sigma$ of 2.52 and 3.92 $m^3$/sec; 02HE001 (13.9 $km^2$) with $\mu$ and $\sigma$ of 0.17 and 0.29 $m^3$/sec; and 05QD008 (0.34 $km^2$) with $\mu$ and $\sigma$ of 0.003 and 0.007 $m^3$/sec. These $\mu$ and $\sigma$ were determined by including the zero flows. The wide ranges of drainage areas and b values were used to represent diverse watershed and stream reach characteristics.

Since the true value of $Q_{1/2}$ can be more accurately determined than that of $Q_e$ and the performance of different pdfs for the estimation $Q_{1/2}$ and $Q_e$ seem to follow the same trend, only $Q_{1/2}$ values were determined empirically and analytically for each of the selected three streams with different b values. The results are summarized in Table 3.4. The relative percentages of error were also included in Table 3.4.

**Table 3.4:** $Q_{1/2}$ values for different values of b and the resulting percentage of errors

| Stream ID | b | $Q_{1/2}$ | | | | | % of Error | | | |
|---|---|---|---|---|---|---|---|---|---|---|
| | | emp | LN | MLN | MG | G | LN | MLN | MG | G |
| 02HM005 | 1 | 4.930 | 4.674 | 4.665 | 6.711 | 6.702 | 5 | 5 | 36 | 36 |
| | 2 | 12.150 | 16.026 | 15.643 | 12.746 | 12.767 | 32 | 29 | 5 | 5 |
| | 3 | 19.660 | 54.943 | 52.457 | 18.812 | 18.864 | 179 | 167 | 4 | 4 |
| | 4 | 25.970 | 188.368 | 175.915 | 24.887 | 24.970 | 625 | 577 | 4 | 4 |
| | 5 | 32.300 | 645.807 | 589.928 | 30.965 | 31.079 | 1899 | 1726 | 4 | 4 |
| 05QD008 | 1 | 0.025 | 0.008 | 0.010 | 0.014 | 0.014 | 69 | 60 | 43 | 46 |
| | 2 | 0.026 | 0.043 | 0.033 | 0.027 | 0.028 | 67 | 27 | 3 | 9 |
| | 3 | 0.060 | 0.241 | 0.108 | 0.039 | 0.043 | 302 | 80 | 34 | 28 |
| | 4 | 0.102 | 1.342 | 0.354 | 0.052 | 0.058 | 1222 | 249 | 49 | 43 |
| | 5 | 0.110 | 7.467 | 1.162 | 0.065 | 0.073 | 6688 | 957 | 41 | 34 |
| 02HE001 | 1 | 0.340 | 0.338 | 0.335 | 0.507 | 0.507 | 1 | 2 | 49 | 49 |
| | 2 | 1.130 | 1.298 | 1.286 | 0.991 | 0.991 | 15 | 14 | 12 | 12 |
| | 3 | 2.270 | 4.987 | 4.937 | 1.477 | 1.477 | 120 | 117 | 35 | 35 |
| | 4 | 3.210 | 19.152 | 18.961 | 1.964 | 1.964 | 497 | 491 | 39 | 39 |
| | 5 | 3.830 | 73.553 | 72.821 | 2.452 | 2.452 | 1820 | 1801 | 36 | 36 |

It can be seen from Table 3.4 that, overall, MG and G distributions provide the most accurate estimation of $Q_{1/2}$ . It was also found that for each stream, the relative percentage of error for LN distributions increases as the b values increase. For instance,

for 02HE001, the relative percentage of error for LN distribution increased from 0.5% for $b=1$ to 1820% for $b=5$. Again, for 02HM005, the relative percentage of error increased from 5.2% for $b=1$ to 1899% for $b=5$. The same trend was also noticeable for the MLN distribution. There is no such trend for G and MG distributions. As shown in Table 4, the maximum relative percentage of error for MG distributions was 49% for $b=4$ in 05QD008 and there is no obvious relationship between b values and the relative percentage of error. This indicates that the variability of b does not contribute to a significant error in the half discharge values determined from G and MG distributions. Therefore in stream restoration projects involving small streams, in addition to better goodness-of-fit between flow frequency distributions and more accurate estimation in half discharges, when there is a high degree of uncertainty associated with b values, use of G or MG distributions is probably a better choice in the estimation of $Q_{1/2}$ values. As shown in Table 3.4, the analytical solutions of $Q_{1/2}$ determined from G and MG distributions are closer to the empirical $Q_{1/2}$ values for all the b values.

### 3.5.2 Relationship between Effective and f-load Discharges

As defined earlier, f-load discharge is the discharge above which f fraction of the total long-term sediment load is transported. For instance, $Q_{0.3}$ is the discharge level above which 30% and below which 70% of the total long-term sediment load is transported. For a specific river, $Q_e$ obviously equals to a specific $Q_f$, what is unknown is the value of f and what is worth investigating is whether the $Q_e$'s of all rivers that follow the same family of flow distributions equal to their respective $Q_f$'s with the same or similar f values.

In order to examine if there is a relationship between a specific f-load discharge and effective discharge for small southern Ontario streams, f-load discharges were determined using Eqn. (3.19) for the selected streams for f values of 0.2, 0.3, 0.5 (half discharge), 0.6, 0.75, and 0.9. The exponent of the sediment rating curve, b, was assumed to take on values of 1, 2, 3, and 5. For each b value, box plots are used to show

the range of the ratio between $Q_e$(TEC) and $Q_f$ values of the 19 streams. For example, in Fig. 3.4(a), each box provides information about the upper and lower quartiles, median (represented as a notch), and the minimum and maximum values of $Q_e / Q_f$ with a specific value of f for the 19 selected streams. All the boxes in Fig. 3.4(a) are based on $Q_e$ and $Q_f$ values determined for a b value of 1. The closer the notch is to 1 for a particular f value, the better would be the match between $Q_e$ and $Q_f$. Fig. 3.4(a) shows that the $Q_e/Q_f$ ratio is closest to 1 for an f value of 0.9. However, the upper and lower quartile values range from 1.6 to 0.25, which is a very broad range as compared to the other boxes for lower f values. Fig. 3.4(b) shows box plots of the $Q_e / Q_f$ ratios for a b value of 2. From Fig. 3.4(b), it can be seen that the $Q_e/Q_f$ ratio is closest to 1 for an f value of 0.6. Fig. 3.4(c) indicates that the $Q_e/Q_f$ ratio is closest to 1 for an f value of 0.5, and the $Q_e/Q_f$ ratio is also fairly close to 1 for an f value of 0.6 when the value of b is 3. Fig. 3.4(d) indicates that $Q_e/Q_f$ ratio is closest to 1 for an f value of 0.6 when the value of b is 5.

Collectively, Figs. 3.4(b), (c) and (d) seem to suggest that for b values of 2 and above, $Q_e$ and $Q_{0.6}$ are close to each other for many small southern Ontario streams. When b = 1, in spite of the fact that an f value of 0.9 provided the closest match between $Q_e$ and $Q_f$ as compared to other f values, the broad range of quartiles

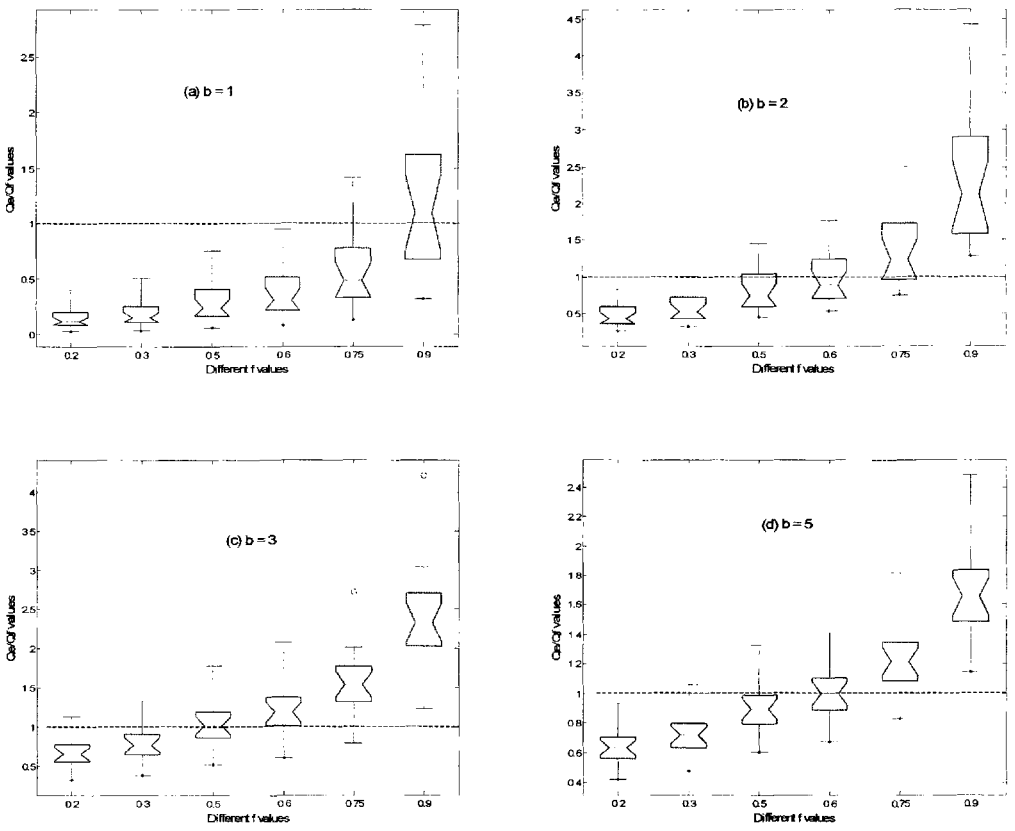


**Fig 3.4:** Box plots of $Q_e / Q_f$ for the selected streams with b values of (a) b = 1; (b) b = 2; (c) b = 3; and (d) b = 5

for the f value of 0.9 is of concern in suggesting that there does not exist a reliable relationship between $Q_e$ and $Q_f$ for low b values. On the other hand, $Q_e$ and $Q_f$ values for the cases of low b values were found to be very low and during the determination of $Q_e$, the size of the class intervals needed to be adjusted many times. Therefore, for such low b values, it is probably a better idea to determine and use f-load discharges. When $b \geq 2$, if it becomes difficult to determine $Q_e$ using the TEC approach, $Q_{0.6}$ can be used as an appropriate substitute.

## 3.6. Summary and Conclusions

The determination of the effective discharge $Q_e$ of a stream based on the transport effectiveness curve (TEC) approach is problematic for many small streams. Furthermore, the 'transport effectiveness' term defined by Wolman and Miller (1960) is only a measure of the effectiveness of individual flow rates and not a measure of the effectiveness of individual flood events (Vogel et al. 2003). Half discharge ($Q_{1/2}$) and other f-load discharges overcome some of the shortcomings of $Q_e$ as they are calculated based on the cumulative total mass of sediment transported by flows up to some specific levels. So far, however, the only analytical solution of $Q_{1/2}$ and other f-load discharges was derived assuming that flows follow lognormal (LN) distributions.

The accuracy of the analytical solutions of both $Q_e$ and $Q_{1/2}$ are dependent on the goodness-of-fit between the frequency distribution of the flow series and the theoretical pdf. Goodness-of-fit analyses of small southern Ontario streams with zero flows indicate that these streams are better approximated by gamma (G) and not the conventional lognormal (LN) distributions. Both K-S test statistics and L-moment diagrams support this finding. Therefore, in this study a mixed gamma distribution that explicitly considers zero flows is introduced to represent the frequency distribution of those small streams. In fitting the MG distribution the best results can be obtained by firstly determining the $\gamma$ values from the fraction of non-zero flows; then the remaining two parameters can be determined by separating the non-zero flows and fitting a G distribution to those flows. Mixed LN distributions (MLN) were also used as a comparison to see if the goodness-of-fit of LN distributions can be improved by considering zero flows separately. In terms of goodness-of-fit, MG does not improve over G. But MLN improves marginally over LN distribution.

Analytical solutions of $Q_e$ and $Q_f$ were determined from the G, MG and MLN distributions. For a typical value of 2 of the exponent of the sediment rating curve b, the

analytical solutions of $Q_e$ and $Q_{1/2}$ based on different theoretical pdfs were compared with their respective empirical values for the selected streams. The results indicate that for $Q_{1/2}$, MG provides the most accurate estimation for all the selected streams although the improvement over G is marginal. For $Q_e$, MG clearly provides the most accurate estimate as compared to the other three distributions. For different watershed sediment and channel reach characteristics, b values typically range from 1 to 5. In order to investigate the influence of the b value on the accuracy of analytical solutions of $Q_{1/2}$; $Q_{1/2}$ values from G, MG, LN and MLN distributions were determined for three streams for which the assumed b values changed from 1 to 5. As the value of b increased from 1 to 5, $Q_{1/2}$ determined from G and MG distributions provided consistently the most accurate solutions when compared with $Q_{1/2}$ (empirical). For $Q_{1/2}$ from LN and MLN, it was found that as the value of b increased, the relative percentage of error also increased. The change of b values did not change the accuracy of the analytical solutions of $Q_{1/2}$ (G) and $Q_{1/2}$ (MG). Thus for streams where there is a high degree of uncertainty associated with the value of b, the proposed analytical solution based on MG and G distributions is probably a better choice for determining effective and f-load discharges.

To determine the fractional sediment load that $Q_e$ transports, $Q_e$ values determined using the TEC approach were compared with $Q_f$ (MG) values for the selected streams with varying b values. The results indicate that for b values of 2 and above, $Q_e$ is approximately equal to $Q_{0.6}$ for small southern Ontario streams. Thus, if for a particular stream with $b \geq 2$, determination of $Q_e$ using the TEC approach becomes tedious or problematic; $Q_{0.6}$ can be determined instead and used as an appropriate substitute. For $b < 2$, no clear relationship between $Q_e$ and any specific $Q_f$ was observed.

The main objective of this study is to verify and broaden the application of the concept of f-load discharges, which was previously limited to LN distributions. At the same time, the results of the study provide more insight into the concept of effective

discharge. However, application of the results from this study to regions other than southern Ontario or streams with larger drainage areas should be made with caution.

# References


1. Andrews, E.D., (1980) "Effective and bankfull discharges of streams in the Yampa River basin, Colorado and Wyoming." *Journal of Hydrology,* 46, 311-330.
2. Barry, J. J., Buffington, J. M., King, J. G., (2004) "A general power equation for predicting bedload transport rates in gravel bed rivers." *Water Resources Research,* 40, doi: 10.1029/2004WR003190, 2004.
3. Biedenharn, D.S., and Copeland, R.R., (2000) *Effective discharge calculation,* ERDC/CHL HETN-II-4 US Army Corps of Engineers, Vicksburg, MS.
4. Daviau, J-L., Adamowski, K., Patry, G.G. (2000) "Regional flood frequency analysis using GIS, L-moment and Geostatistical methods." *Hydrological Processes,* 14, 2731-2753.
5. Emmett, W.W. and Wolman, M.G., (2001) "Effective discharge and gravel-bed rivers." *Earth Surface Processes and Landforms,* 26, 1369-1380.
6. Goodwin, P., (2004) "Analytical solutions for estimating effective discharge." *Journal of Hydraulic Engineering,* 130(8), 729-738.
7. Haan, C.T. (1977) *Statistical methods in hydrology,* Printed by the Iowa State University Press, Iowa.
8. Hosking, J. R. M., (1990) "L-moments: Analysis and estimation of distributions using linear combinations of order statistics." *Journal of Royal Statistical Society, Ser. B.,* 52(1), 105-124.
9. HYDAT, (2001) *Surface Water and Sediment Data,* Released by Environment Canada, National Archives and Data Management Branch, 4905 Dufferin St., Downsview, ON M3H 5T4, Canada.
10. Jingyi, Z. and Hall, M.J., (2004) "Regional flood frequency analysis for Gan-Ming river basin in China." *Journal of Hydrology,* 296, 98-117.

11. Kumar, R., and Chatterjee, C. (2005) "Regional flood frequency analysis using L-moments for North Brahmaputra region of India." *Journal of Hydrologic Engineering*, 10(1) doi: 10.1061/(ASCE) 1084-0699 (2005) 10:1(1).
12. Kumar, R., Chatterjee, C., Kumar, S., and Lohani, A.K. (2003) "Development of regional flood frequency relationships using L-moments for Middle Ganga Plains Subzone 1(f) of India." *Water Resources Management*, 17, 243-257.
13. LeBoutillier, D. W., and Waylen, P. R., (1993) "A stochastic model of flow duration curves." *Water Resources Research*, 29(10), 3535-3541.
14. Lenzi, M. A., Mao, L., Comiti, F., (2006) "Effective discharge for sediment transport in a mountain river: computational approaches and geomorphic effectiveness." *Journal of Hydrology*, 326, 257-276.
15. Limbrunner, J.F., Vogel, R.M., and Brown, L.C. (2000) "Estimation of harmonic mean of a lognormal variable." *Journal of Hydrologic Engineering*, 5(1), 59-66.
16. Nash, D.B., (1994) "Effective sediment-transporting discharge from Magnitude-Frequency analysis." *Journal of Geology,* 102, 79-95.
17. Quader, A., Guo, Y, and Stedinger, J. R., (2007) "Analytical estimation of effective discharge using mixed exponential distribution models." submitted to *Canadian Journal of Civil Engineering*, currently under review.
18. Sichingabula, H. M., (1999) "Magnitude-frequency characteristics of effective discharge for suspended sediment transport, Fraser River, British Columbia, Canada." *Hydrological Processes*, 13, 1361-1380.
19. Stedinger, J.R., (1980) "Fitting log normal distributions to hydrologic data." *Water Resources Research*, 16(3), 481-490.
20. Stedinger, J.R., Vogel, R.M., and Foufoula-Georgiou, E. (1993) "Frequency analysis of extreme events." *Handbook of Hydrology*, D.R. Maidment, ed., McGraw-Hill Book Co., Inc., New York, N.Y.
21. Vogel, R.M. and Fennessey, N.M. (1993) "L-Moment diagrams should replace product moment diagrams." *Water Resources Research*, 29(6), 1745-1752.
22. Vogel, R. M., Stedinger, J. R., Hooper, R. P., (2003) "Discharge indices for water quality loads." *Water Resources Research*, 39(10), doi: 10.1029/2002WR001872, 2003.

23. Vogel, R.M. and Wilson, I. (1996) "Probability distribution of annual maximum, mean, and minimum streamflows in the United States." *Journal of Hydrologic Engineering*, 1(2), 69-76.
24. Wolman, M.G., and Miller, J.P., (1960) Magnitude and frequency of forces in geomorphic processes, *Journal of Geology,* 68, 54-74.

# Chapter 4

## Hydrological and Sedimentological Parameters Affecting Effective Discharge of Small Urban Streams

Asif Quader and Yiping Guo

**Abstract:** Channel-forming discharge is an important design variable in stream restoration projects. Effective discharge ($Q_e$) is the only channel-forming discharge used in practice with magnitudes affected by both hydrological and sedimentological characteristics of the watershed and stream reach. This paper identifies the most critical hydrological and sedimentological characteristics associated with $Q_e$ and other related variables of interest. Continuous simulation of hypothetical catchments was conducted to generate hourly streamflow data. $Q_e$ and other relevant variables were determined from post-simulation analyses of the generated streamflow series. Global sensitivity analysis of the input parameters indicated that $Q_e$ is highly sensitive to, firstly, the exponent of the sediment rating curve ($\beta$); secondly, the watershed storage coefficient; and thirdly, the time of concentration of the watershed. Furthermore, this study shows that only when $\beta$ values are within a specific range, $Q_e$ and the discharge corresponding to a return period of 1.5 years are close to each other.

**Keywords:** Sensitivity analysis, urban watershed, stream restoration, continuous simulation

## 4.1 Introduction

The channel-forming discharge of a river reach is the constant discharge value that given enough time for it to last would produce width, depth, and slope of the river reach equivalent to those produced by the natural hydrograph (Shields et al. 2003). A channel-forming discharge is commonly used directly or indirectly as a design variable in many stream restoration projects (Skidmore et al. 2002). Detailed hydraulic and morphometric designs in stream restoration projects are so heavily dependent on the magnitude of the channel-forming discharge that inaccurate estimation of this parameter can cause more harm than good to the natural environment of the stream after restoration. This study was undertaken to identify the critical watershed hydrological and sedimentological parameters affecting the magnitude of the channel-forming discharge.

Bankfull discharge ($Q_b$), effective discharge ($Q_e$), and discharge with a particular return period ($Q_t$) are all considered as the possible channel-forming discharges (Shields et al. 2003). Of the three different types, $Q_b$ is the first accepted channel-forming discharge in practice (Doll et al. 2003; Keystone Stream Team 2002; Moody et al. 2003; Rosgen 1994). However, under many circumstances, $Q_b$ is estimated as the $Q_t$ with a return period of 1.5 or 2.5 years since $Q_b$ itself is more difficult to estimate. The mean discharge that transports the largest fraction of the sediment load over a long period is defined as the effective discharge $Q_e$ (Andrews 1980). $Q_e$ is the only channel-forming discharge that quantitatively incorporates sediment transport of the stream reach in its estimation. The high degree of uncertainty associated with the field estimation of $Q_b$ (Riley 1972; Woodyer 1968; Williams 1978) and the sometimes misleading values of $Q_b$ for deeply incised urban streams (Copeland et al. 2000) have resulted in increased use of $Q_e$. Hence, the focus of this paper is on $Q_e$ and $Q_t$ with a return period of 1.5 and 2.5 years.

The flow pattern at a stream reach is the product of precipitation and upstream catchment characteristics. The rate of sediment transport at a stream reach is related to supply rate as well as parameters such as critical shear stress, effective grain diameter,

diffusion coefficient, settling velocity, etc. Lack of observed data is one of the most challenging problems in stream restoration. Small urban streams usually do not have a long-term observed flow record. Scarcity of data is more obvious in relation to sediment transport. This scarcity forces design engineers to adopt $Q_b$ or $Q_t$ as the channel forming discharge (Doll et al. 2003; Keystone Stream Team 2002).

The available streamflow records are usually with time-steps of a day (i.e., mean daily flows). For small streams, flood events may last only a few hours, resulting in peak discharges much greater than the corresponding mean daily discharges. Therefore, for small streams, mean daily flow series can under-represent the occurrence of short-duration, high-magnitude flow events. To properly estimate the channel-forming discharges for small streams, the time-steps of the streamflow series should be 1 hour or shorter (Biedenharn and Copeland 2000). However, among the many earlier studies investigating channel-forming discharges, the vast majority used daily streamflow data, only Lenzi et al. (2006) used flows at a 5-min time-step for determining $Q_e$ at the Rio Cordon catchment in Italy (with a drainage area of 5 $km^2$).

For small streams where no streamflow data is available or only daily streamflow data are available, one way to generate streamflow data at shorter time-steps is through continuous simulation using a hydrologic model of the watershed. In this study, continuous simulation of hypothetical catchments ranging in size from 5 to 50 $km^2$ was conducted to generate small time-step streamflow series. The generated streamflow series were used for the purpose of determining $Q_e$, $Q_t$ and related variables of interest. The resulting $Q_e$, $Q_t$ and other output values for each hypothetical catchment and its downstream stream reach are used as samples from real catchments and stream reaches in subsequent sensitivity analysis to determine the most influential input parameters.

Sensitivity analysis involves quantification of the change in model output corresponding to the change in one or more of the model inputs (Mishra et al. 2003). Selection of the suitable sensitivity analysis method depends on the purpose of the study, the characteristics of the model, and the computational cost that the investigator can

afford. There are two groups of sensitivity analysis methods: local and global sensitivity analyses. Local sensitivity analysis methods only concentrate on the local impact of the factors (i.e., parameters) on the model output. Local sensitivity measures are usually based on derivatives of the output with respect to input factors and can be obtained by varying the input factors around their nominal values.

Global sensitivity analysis (GSA) apportions the output variability to the variability of the input factors (Saltelli et al. 2001). Global sensitivity measures can only be obtained by conducting modeling experiments covering the entire space over which the input factors may vary. In the case of non-linear models, local derivatives used for identifying the relative rank of importance of input factors in contributing to the variability of the output can be misleading. Therefore, instead of relying on local sensitivity measures, the entire input factor space (possibly generated from Monte Carlo simulation) should be investigated through GSA. Using GSA, the sensitivity measures are determined either from regression analysis covering the complete input factor space or from the ratios between the output variance contributed by each input and the total output variance. Thus GSA provides a means of determining model-free sensitivity measures. In the past, GSA was applied in 3D eutrophication models (Pastres et al. 1999), large scale hydrological models (Francos et al. 2003), flood inundation models (Hall et al. 2005), agronomic models (Penciolelli and Hue 2005), and analytic models representing the transport of radionuclide (Hedin 2002). GSAs were also conducted for better engineering of artificial genetic circuits (Feng et al. 2004), for identification of genetic parameters in plant breeding experiments (Markowski et al. 2005), and for environmental risk assessment (Mishra 2004). In our study, GSA sensitivity measures provide a quantitative way of ranking the relative importance of each input parameter in affecting the output of interest.

The physiographic characteristics of a watershed/catchment and its downstream stream reach could be extremely diverse in nature. For design engineers involved in stream restoration to use their time and resources more efficiently, it is necessary to understand the relative importance of each of the watershed and stream reach

characteristics in affecting the value of $Q_e$ and $Q_t$ that is used as the channel-forming discharge. In this study, samples of catchments and stream reaches were obtained from the entire hydrological and sedimentological input factor space using Monte Carlo sample generation. Continuous simulation of sample catchments was conducted to generate short time-step streamflow series. Simulated streamflows and the sediment rating curve representing the sediment transport characteristics of a sample stream reach were used to determine $Q_e$, $Q_t$ and other variables of interest. GSA was then conducted to determine quantitatively the critical input parameters. In response to Quader et al. (2006), Goodwin (2006) emphasized the need for identifying the critical parameters influencing the effective discharge through sensitivity analysis. This study was completed partly in response to that call of attention.

## 4.2 Estimation of Effective Discharge

The definition of effective discharge $Q_e$ is based on the magnitude-frequency concept proposed by Wolman and Miller (1960). According to the magnitude-frequency concept, the geomorphic impact of a particular magnitude of flood event is directly proportional to the product of the amount of sediment carried by that event and its frequency of occurrence. Transport effectiveness of individual flows is thus defined as the product of sediment load transported by the flow and its frequency of occurrence. For a particular stream, the curve relating the transport effectiveness to individual flows within the entire range of possible flows is known as the transport effectiveness curve. The peak of the transport effectiveness curve is determined as the $Q_e$ for the particular stream reach.

In using the transport effectiveness curve approach for the estimation of $Q_e$, identification of a single distinguishable peak is dependent on the size of the class interval used in the frequency analysis of the flow series. Therefore, the transport effectiveness curve approach has received its fair share of criticism (Sichingabula 1999; Vogel et al. 2003; Lenzi et al. 2006). To overcome some of the difficulties, Biedenharn

and Copeland (2000) suggested a set of guidelines for determining $Q_e$ using the transport effectiveness curve approach. In this study, those guidelines were strictly followed.

Most of the studies pertaining to effective discharge utilize the transport effectiveness curve approach for determining $Q_e$, only a few (e.g., Goodwin 2005; Nash 1994; Vogel et al. 2003) investigate the alternative analytical approach. Pioneered by Nash (1994), the analytical approach to the estimation of $Q_e$ fits a theoretical probability distribution function (pdf), f(Q), to the frequency distribution of the flow series and uses a sediment rating curve as shown in (1).

$$Q_s = \alpha Q^{\beta} \tag{4.1}$$

In (4.1), $\alpha$ and $\beta$ are the fitting parameters; $Q_s$ is the sediment transport rate (kg/sec); and Q is the flow rate ($m^3$/sec). The transport effectiveness (E) is the product of f(Q) and $Q_s$.

$$E = f(Q) \times Q_s \tag{4.2}$$

$Q_e$ as defined earlier can be determined by differentiating (4.2) with respect to Q and equating it to zero. The final analytical solution of $Q_e$ is a function of the parameters used in f(Q) and $\beta$ of the sediment rating curve. For example, if the streamflow follows a gamma pdf, the analytical solution of $Q_e$ is (Goodwin 2004),

$$Q_e = \beta_g[\beta + (\alpha_g - 1)] \tag{4.3}$$

where $\alpha_g$ and $\beta_g$ are the distribution parameters of a gamma pdf.

The analytical solution of $Q_e$ is dependent on the exponent ($\beta$) and independent of the coefficient ($\alpha$) of the sediment rating curve. Nash (1994) demonstrated that the value of $\beta$ provides information about the discharge threshold necessary to induce the movement of sediment. In the case of higher $\beta$ values, there exists an apparent threshold, below which the sediment transport rate is very small [Figure 4, Nash (1994)]. Emmett and Wolman (2001) illustrated that the value of $\beta$ is strongly correlated with bed materials of large sizes, which in turn is closely related to the flow threshold necessary to initiate sediment transport. Barry et al. (2004) pointed out that the value of $\beta$ reflects the

relative measure of supply-related channel armoring. This relative armoring term was found to be dependent on the shear stresses under the bankfull discharge and the shear stresses required for the mobilization of surface and subsurface materials. Lenzi et al. (2006) illustrated the importance of the high threshold discharge and high $\beta$ values in mountainous streams. For both bedload and suspended sediment load, the value of $\beta$ captures substantial amounts of information about the sediment transport characteristics of a stream reach.

Unlike $\alpha$, which varies widely for bedload and suspended sediment load transported at various stream reaches, the range of values that $\beta$ is observed to take is comparatively small. This is mainly due to $\beta$'s dependence on the relative measure of armoring, which is unlikely to vary widely with changing catchment physiography and channel morphology (Barry et al. 2004). $\beta$ values are reported to range from as low as less than 1 for dissolved sediment (Nash 1994) to as high as 5 for bedload in gravel bed streams (Emmett and Wolman 2001; Lenzi et al. 2006). Therefore a range of 0.5~5 for $\beta$ is used in the sensitivity analysis to cover all the possible types of stream reaches and indirectly all the possible sizes of sediment particles.

## 4.3 Continuous Simulation to Generate Sample Streamflow Series

Continuous hydrologic models accounting for the soil-moisture balance of the watershed over a long period are suitable for simulating streamflows at different temporal resolutions (Ponce 1989). Some of the available continuous simulation models with a wide range of applications are SWMM (Huber and Dickinson 1988), HMS-SMA (Fleming and Neary 2004), CASC2D (Senarath et al. 2000), SAC-SMA (Zhang et al. 2004), and HEC-HMS (Olivera 2001; Anderson et al. 2002). In this study, HEC-HMS developed by the Hydrologic Engineering Center (HEC) of the U.S. Army Corps of Engineers (USACE) was used.

### 4.3.1 Input Parameters Selected for Sensitivity Analysis

The size of hypothetical catchments representing samples of small urban watersheds was varied from 5 to 50 $km^2$. The 40-years (1960-1999) of hourly rainfall data from Pearson International Airport in Toronto, Ontario were used as the precipitation input to represent typical southern Ontario climate conditions. The watershed model requires input about the loss rate, the rainfall-runoff transformation processes, and the baseflow amounts and variations. Some of the input parameters have very limited impact on the output of interest and may be excluded from sensitivity analysis. Other input parameters definitely have some impact on the output of interest and must be included in the sensitivity analysis. For those input parameters, the values that they can possibly take must be established so that samples of watershed can be constructed randomly and evenly across these possible values through Monte Carlo generation.

The deficit/constant loss method of HEC-HMS was used in this study with an initial deficit of 2.54 mm and a maximum deficit of 25.4 mm. For different hypothetical catchments, the initial deficit values were kept constant. In other words, initial deficit was not selected as one input factor for which sensitivity analysis is conducted. This is appropriate because the value of initial deficit only affects the simulation results during the short starting period and will not affect significantly the statistical properties of the long-term simulation results. The selected large maximum deficit value reflects typical southern Ontario conditions of deep soil and low groundwater table. The pervious areas of urban catchments are mainly grass lands, the maximum deficit for different grass lands may only be slightly different from one another. To reduce the dimensionality of the input factor space, maximum deficit was therefore kept at the same value and not included as an input parameter for sensitivity analysis.

The value of the constant loss rate (i.e., the ultimate infiltration capacity $f_c$) depends on the soil type and varies from 0.36 mm/hr for clay to 11.4 mm/hr for deep sand, deep loess and aggregated silts (USACE 2000). $f_c$ of the soils of the watershed is selected as one of the input parameters for sensitivity analysis. The reported broad range

of values of $f_c$ was used to cover all the possible types of soils. The Penman's method was used to determine the potential evapotranspiration (PET) rate in mm/day for each month in Toronto, Ontario. These average monthly values were used as infiltration capacity recovery rates in between precipitation events in continuous simulation. The percent imperviousness (h) is also selected as one of the input parameters for sensitivity analysis with a range of variation from 10 to 85%.

The Clark unit hydrograph method was used in this study for overland flow routing. This routing technique recognizes that the discharge at any point in time is dependent on the translation and storage characteristics of the watershed. These two characteristics are represented respectively by the time of concentration ($t_c$) and the storage coefficient (K). Both $t_c$ and K are selected for sensitivity analysis. Even for urban catchments of the same small size, depending on the shape, slope and nature (e.g. sewered vs. unsewered, with or without detention ponds), the $t_c$ of the catchment can vary from a few minutes to a few hours and even a day. To include all the possible values, the range of variation for $t_c$ is set to be from 0.3 to 15 hours for catchments of 5 $km^2$, from 0.5 to 18 hours for catchments of 10 $km^2$, from 1 to 22 hours for catchments of 20 $km^2$, and from 1 to 25 hours for catchments of 50 $km^2$. The value of K can increase because of storage delay caused by detention ponds or natural depressional areas. Similar to $t_c$, even for catchments of the same size, depending on the nature of the catchment, its K value can vary significantly. Therefore, the same wide ranges of values for K were included in the sensitivity analysis to cover all the possible cases. Because different characteristics of a catchment control largely its $t_c$ and K values, $t_c$ and K for the same catchment are considered independent with each other.

HEC-HMS simulates baseflow of a flood hydrograph using three parameters: initial discharge, recession constant (RC) and the ratio of threshold to peak discharge ($Q_{th}/Q_p$). $Q_{th}$ is the discharge at the point of a falling limb of a hydrograph where recession begins and $Q_p$ is the peak discharge of the hydrograph. In a long term continuous simulation, the initial discharge does not have a significant effect on the statistics calculated from the simulated flow series. Thus, the initial discharge is not

selected as one of the input parameters for sensitivity analysis. Of the two remaining parameters, the recession constant (RC) represents the rate of exponential decay of the recession limb of the hydrograph and has values that typically range from 0.5 to 0.95. The values for $Q_{th}/Q_p$ typically range from 0.05 to 0.15 (USACE 2000). These two parameters were selected for sensitivity analysis and the reported ranges of values that they may take were used in the sensitivity analysis.

### 4.3.2 Hydrological Simulation and Output Variables of Interest

The ranges of values of selected hydrological input parameters (i.e. $f_c$, h, $t_c$, K, RC, and $Q_{th}/Q_p$) and the single sedimentological parameter $\beta$ in our sensitivity analysis are summarized in Table 4.1. These selected input parameters are treated as random variables uniformly distributed within their specified ranges. Uniform distributions are appropriate because our purpose is to use these distributions to generate random samples of input parameter values evenly spread over their possible ranges. The input parameters are considered to be statistically independent of one another because different watershed characteristics control their values.

**Table 4.1:** Input Factors and Distributions Used in Sensitivity Analysis

| Input Factor | Range of Values for Various Drainage Areas | | | | Distribution |
|---|---|---|---|---|---|
| | 5 ($km^2$) | 10 ($km^2$) | 20 ($km^2$) | 50 ($km^2$) | |
| $f_c$ (mm/hr) | 0.36-11.4 | 0.36-11.4 | 0.36-11.4 | 0.36-11.4 | Uniform |
| h (%) | 10-85 | 10-85 | 10-85 | 10-85 | Uniform |
| $t_c$ (hr) | 0.3-15 | 0.5-18 | 1-22 | 1-25 | Uniform |
| K (hr) | 0.3-15 | 0.5-18 | 1-22 | 1-25 | Uniform |
| $Q_{th}/Q_p$ | 0.05-0.15 | 0.05-0.15 | 0.05-0.15 | 0.05-0.15 | Uniform |
| RC | 0.5-0.95 | 0.5-0.95 | 0.5-0.95 | 0.5-0.95 | Uniform |
| $\beta$ | 0.5-5 | 0.5-5 | 0.5-5 | 0.5-5 | Uniform |

Hence, random samples were generated for each input parameter using Monte Carlo sample generation with the linear congruent method. A total of 105 samples were generated for each input parameter. For catchments of a specific size, 105 sets of input

parameter values representing 105 possible catchment conditions are then constructed by taking sequentially one value for each input parameter from their respective randomly generated value sequence. This sampling procedure ensures unbiased estimation of the mean and variance of the output variables. Hydrologic simulation for each of the constructed hypothetical catchments was then conducted to determine the corresponding output variable values.

In addition to the estimation of $Q_e$ for each hypothetical condition, discharges corresponding to return periods of 1.5 and 2.5 years (i.e. $Q_{1.5}$ and $Q_{2.5}$) were determined by analyzing the annual maximum flow series constructed from the simulated hourly streamflows. The return period for each of the values in the annual maximum flow series was determined using the Weibull plotting position formula. A smooth curve was then fitted to the individual return period and corresponding annual maximum flow points. $Q_{1.5}$ and $Q_{2.5}$ are determined from that fitted curve. The return period of $Q_e$ ($T_{Q_e}$) and the percentage of time $Q_e$ is exceeded (PTQEX) are two other output variables that are calculated along with $Q_e$. $T_{Q_e}$ was determined from the fitted flood frequency curve obtained using the annual maximum flow series and PTQEX values were determined from the flow duration curves constructed using the entire simulated hourly flow series. Table 4.2 lists the five output variables investigated in this study. Investigation of all these output variables can provide a better understanding of $Q_e$.

**Table 4.2:** Definition of Output Variables

| Output Variable | Definition |
|---|---|
| $Q_e$ ($m^3$/sec) | Effective discharge |
| $Q_{1.5}$ ($m^3$/sec) | Discharge with a return period of 1.5 yrs |
| $Q_{2.5}$ ($m^3$/sec) | Discharge with a return period of 2.5 yrs |
| $T_{Q_e}$ (yr) | Return period of effective discharge |
| PTQEX | Percentage of time the effective discharge is exceeded |

### 4.3.3 Validation of Hydrologic Models

Although hydrological models constructed in this study are not used to represent any real catchments and calibration of them against any measured streamflow data is not necessary, some form of validation is still necessary to ensure that the simulated diverse range of streamflows are within or in line with the ranges of values observed in nature. To this end, the statistical properties (i.e., the mean $\mu$ and the standard deviation SD) of streamflow series generated from hypothetical catchments and observed in real streams located in the same region are compared.

For each selected drainage basin size, 105 sets of continuous simulations were performed using randomly generated input parameter values. Therefore, for each selected drainage basin size, there are 105 $\mu$ and SD values. The maximum and minimum of these means and standard deviations are plotted in Fig. 4.1 and Fig. 4.2, respectively, against their corresponding drainage area.

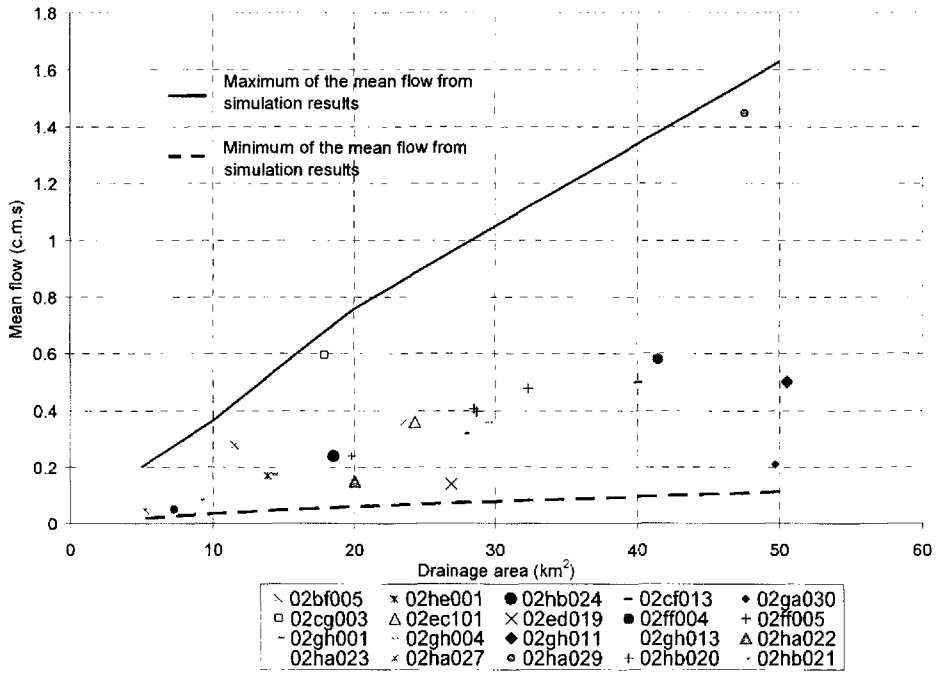


**Fig 4.1:** Mean flows of southern Ontario streams compared with the bounded region of simulation

The solid and dashed lines in Figs. 4.1 and 4.2 represent the maximum and minimum, respectively, of the mean and standard deviation of flows for different drainage areas. Following that, the μ and SD values of 20 streams (HYDAT 2001) with drainage areas within the range of 5-50 $km^2$ located in southern Ontario were also plotted in Figs. 4.1 and 4.2.

The mean flows of the real streams as shown in Fig. 4.1 are within the region bounded by the maximum and minimum as determined from this simulation study. The standard deviations of flows of the selected real streams as shown in Fig. 4.2 also lie largely within the bounded region determined from this simulation study. The SD of most of the streams lies close to the dashed line (i.e. the minimum SD values) of the bounded region.

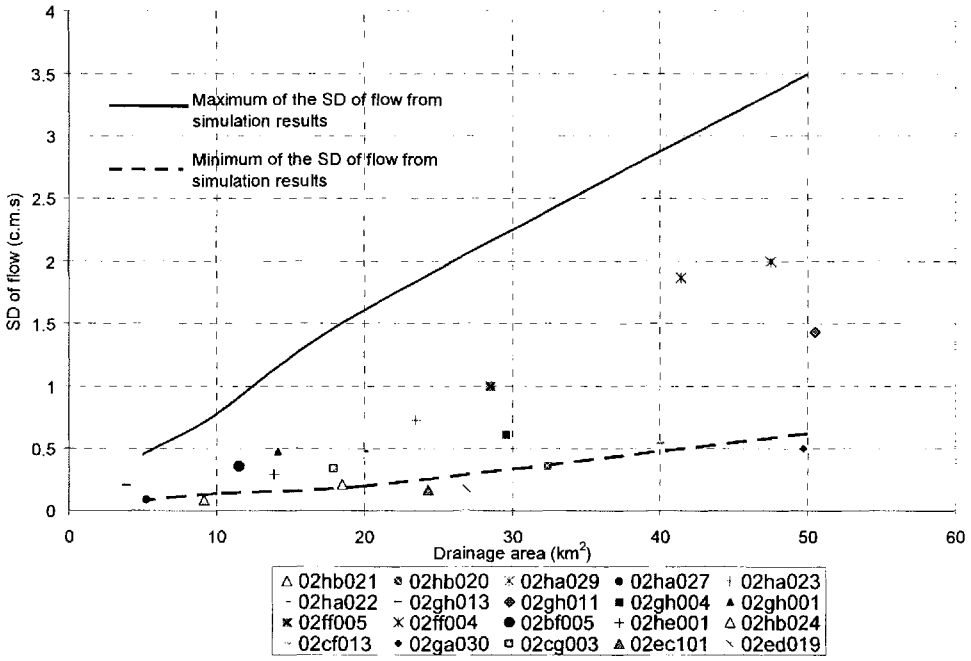


**Fig 4.2:** Standard deviation of flows of southern Ontario streams compared with the bounded region of simulation

The SD values of four real streams were found just outside of the dashed line. Compared to the simulated hypothetical watersheds, the hydrologic characteristics of the real watersheds from the same region may not vary significantly from each other. This may

be the reason that the SDs of flows from real rivers in the region do not cover as wide a region as that covered by simulated streamflows. The daily time-step of the observed flows also reduces their SDs. The hydrologic models used in this study are therefore validated by the fact that the $\mu$ and SD values of real streams are located within the bounded region covered by simulation results.

## 4.4 Global Sensitivity Analysis

The aim of our global sensitivity analysis (GSA) is to determine quantitatively the relative importance of a watershed's hydrological and sedimentological characteristics in affecting its $Q_e$ and related variables. Both variance-based and linear regression-based GSA techniques are available. The linear regression-based techniques explore the entire interval of the definition of each input factor and the effect of each factor represents an average over the possible values of other factors (Saltelli et al. 2004). Sensitivity measures obtained from linear regression-based techniques provide a qualitative comparison of the relative importance of each input factors. The main advantage of the linear regression-based techniques is that they require much smaller sample sizes and thus much less model runs. Comparatively, variance-based sensitivity measures (e.g., FAST, Sobol' etc.) obtained from variance-based GSA techniques are more quantitative representations of the relative importance of each input factor and require much larger sample sizes.

In this study, a stepwise GSA involving both the linear regression-based and variance-based approaches was applied to relieve some of the computational burdens. Firstly, the effects of all the input factors on the desired output variable for different catchment sizes were investigated using linear regression-based GSA. Based on the sensitivity measures obtained thereof, a preliminary screening was made and the insensitive factors were removed from further GSA. Secondly, the reduced number of input factors was included in another round of GSA to determine the sensitivity indices using the Sobol' method. Sobol' method is one of the variance-based GSA techniques that require moderate sample size and generate reliable sensitivity measures. This two-

step GSA reduces significantly the required number of model runs and makes GSA feasible for our specific problem. In the following, the Sobol' and the linear regression-based GSA techniques are briefly described.

### 4.4.1 Method of Sobol'

This method may be described by first defining the input factor space $\Omega^k$ as a k-dimensional unit cube, i.e.,

$$\Omega^k = \{X | 0 \le x_i \le 1; i = 1,2,...,k\}$$

The k input factors (i.e., $x_1$, $x_2$, ... $x_k$) may be denoted as a k-dimensional vector X. The main theme of the Sobol' method is to decompose the function y = f(X), representing the input-output transformation made inside a model, into summands of increasing dimensionality, i.e.,

$$f(x_1, x_2, ...., x_k) = f_0 + \sum_{i=1}^{k} f_i(x_i) + \sum_{1 \le i < j \le k} f_{ij}(x_i, x_j) + ... + f_{1,2,...k}(x_1, ..., x_k)$$

In the above equation, $f_0$ is a constant, which can be evaluated by

$$f_0 = \int_{\Omega^k} f(X) dX$$

Sobol' (Saltelli et al. 2001) showed that the decomposition is unique and that all the terms can be evaluated via multidimensional integrals:

$$f_i(x_i) = -f_0 + \int_0^1 ... \int_0^1 f(X) dX_{\sim i},$$

$$f_i(x_i) = -f_0 - f_i(x_i) - f_j(x_j) + \int_0^1 ... \int_0^1 f(X) dX_{\sim (ij)}$$

Where $dX_{\sim i}$ denotes integration over all variables except $x_i$ ; and $dX_{\sim (ij)}$ denotes integration over all variables except $x_i$ and $x_j$. Analogous formulas can be obtained for the higher-order terms. As a consequence all the summands are orthogonal to one another. The total variance is defined as (Saltelli et al. 2001)

$$D = \int_0^1 ... \int_0^1 f^2(X) dX - f_0^2$$

while partial variances $D_{i_1},...,D_{i_s}$, where $1 \le i_1 < ... < i_s \le k$ and $s = 1,...,k$ are computed from each of the terms in the decomposition equation as

$$D_{i_1,...,i_s} = \int_0^1 ... \int_0^1 f^2_{i_1,...,i_s}\left(x_{i_1},...,x_{i_s}\right) dx_{i_1},...,dx_{i_s}$$

Due to the orthogonality between the summands, we have

$$D = \sum_{i=1}^{k} D_i + \sum_{1 \le i < j \le k} D_{ij} + ... + D_{1,2,...,k}$$

Hence, the sensitivity indices are defined as,

$$S_{i_1,...,i_s} = \frac{D_{i_1,...,i_s}}{D} \tag{4.6}$$

Deducing from this general definition, the first-order sensitivity index $S_i$ for factor $x_i$ measures the main effect of $x_i$ on the output; while $S_{ij}$, for $i \neq j$, is the second-order sensitivity index which measures the interaction effect (the part of the variation in f(X) due to $x_i$ and $x_j$ that cannot be explained by the sum of the individual effects of $x_i$ and $x_j$), and so on. The sum of all the sensitivity indices is unity. For our purposes, the first-order indices can be used as a quantitative measure to compare the relative importance of the input parameters in affecting the output of interest. The total sensitivity index of a parameter is the sum of all the sensitivity indices involving that parameter. To use the method of Sobol', all the integrals are evaluated using Monte Carlo integrals. Details can be found in Hall et al. (2005).

## 4.2 Regression-based Methods

Regression-based methods are based on the assumption that the input and output factors are linearly (or at least monotonically) related as follows

$$y = \delta_0 + \sum_{i=1}^{k} \delta_i x_i \tag{4.7}$$

In (4.7) $\delta_0$ and $\delta_i$ are the regression coefficients; $i = 1, 2,..., k$ represents the number of input parameters. The goodness-of-fit of this regression model may be evaluated using the coefficient of determination $\left(R_y^2\right)$. The applicability of the regression-based sensitivity

analysis techniques is dependent on the magnitude of $R_y^2$. According to Saltelli et al. (2004), $R_y^2 \geq 0.7$ indicates that the regression model is able to represent a large part of the variation of y and sensitivity analysis may be conducted using the regression-based techniques. The coefficients $\delta_i$ and other aspects of the construction of the regression model can be used to indicate the importance of the individual $x_j$ on the variation of y. Many sensitivity measures are based on or partially on the regression model in (4.7). Provided below is a brief description of the regression-based sensitivity measures used in this study.

Pearson product moment correlation coefficient (PEAR) is a measure of the linear relationship between two random variables. An empirical measure of the relationship between y and $x_i$ is given by

$$\mathrm{PEAR}(y,x_i) = \frac{\sum_{l=1}^{c}(y_l - \bar{y})(x_{il} - \bar{x}_i)}{\sqrt{\sum_{l=1}^{c}(y_l - \bar{y})^2}\sqrt{\sum_{l=1}^{c}(x_{il} - \bar{x}_i)^2}}$$

where c is the sample size, $x_{il}$ is the l th sampled value of factor $x_i$, and $y_l$ is the corresponding output value. While the regression coefficient $\delta_i$ characterizes the effect that a unit change in $x_i$ has on y; PEAR can be viewed as characterizing the effect that changing $x_i$ by a fixed fraction of its standard deviation has on y, and this effect is measured relative to the standard deviation of y. Thus, PEAR is a measure of the sensitivity of y with respect to $x_i$.

When more than one input factor is under consideration, partial correlation coefficient (PCCs) can be used to provide a measure of the linear relationships between the output variable y and the individual input factors. PCCs differ from PEARs in that they measure the degree of linear relationships between y and $x_i$ with the linear effects of the other input factors removed. Details can be found in, e.g., Pastres et al. (1999).

The regression coefficients in (4.7) are influenced by the units in which the factors are measured; hence they themselves cannot be used as a sensitivity measure. However, by normalizing each input factor and then regress the output variable on the normalized input factors, we remove the impact of measurement units. The resulting regression coefficient is referred to as the standardized regression coefficient (SRC), and when the input factors are independent, the absolute values of SRCs can provide information on the degree of importance of the selected input variables. PEARs, PCCs, and SRCs provide related, but not identical, measures of input factor importance. It would be beneficial to have all of them calculated and compared since the required sample size is small and the associated computational burden is bearable.

Rank transformation is used to mitigate the problems associated with poor linear fits to nonlinear input-output relationships. Both input and output data are replaced with their corresponding ranks, and then the usual regression and correlation procedures are performed on these ranks. Specifically, the smallest value of each variable is assigned the rank 1, the next largest value is assigned rank 2, and so on up to the largest value. The analysis is then performed with these ranks being used as the values for the input and output variables. The use of rank-transformed data results in an analysis based on the strength of monotonic relationships rather than on the strength of linear relationships.

With the Pearson product moment correlation coefficient calculated on ranks, we obtain Spearman's rank correlation coefficients (SPEAR). Similarly, standardized rank regression coefficient (SRRCs) and partial rank-correlation coefficients (PRCCs) can be calculated using the rank-transformed data. In order to capture both the linear and non-linear aspects of input and output relations, all the six regression-based sensitivity measures are calculated in this study.

As shown in Table 4.1, in our study, we have 7 input factors for which sensitivity analysis is required. The determination of the $1^{st}$ order Sobol' indices requires 144 samples for a problem involving 7 input factors. To reduce the number of simulation runs, preliminary sensitivity analysis using regression-based method was conducted to identify

the less critical/insensitive input factors. It was found that 2 of the 7 input factors are insensitive and therefore excluded from the Sobol' sensitivity indices calculation. In using the regression-based techniques for catchments of a particular size, 105 samples were generated. For applying the Sobol' method with 5 input factors, 112 samples were generated.

## 4.5 Results and Discussions

### 4.5.1 Critical Parameters Affecting Effective Discharge and Other Output Variables

For a catchment of a specific size, samples of different input factor values were generated through Monte Carlo simulation. These samples were used as catchments with different hydrologic characteristics. Continuous simulation of these catchments generated samples of continuous streamflow series. Using these sample flow series and sample β values, the corresponding $Q_e$, $Q_{1.5}$, $Q_{2.5}$, $T_{Q_e}$, and PTQEX were determined. A total of 105 different samples were generated resulting in 105 $Q_e$, $Q_{1.5}$, $Q_{2.5}$, $T_{Q_e}$, and PTQEX values for catchments of a specific size. These output values together with their corresponding input factor values were used in sensitivity analysis to determine the 6 regression-based sensitivity measures.

Having catchments of 4 different sizes, and with each size, 5 output variables of interest affected by 7 input factors, we ended up with many values of sensitivity measures. What is presented and discussed below are some of the typical ones. The values of PEAR for a drainage basin of 5 $km^2$ affecting $Q_e$ were -0.36 for K, -0.24 for $t_c$, and 0.68 for β; the absolute PEAR values for the other 4 input factors are much lower. The $R_y^2$ value was found to be 0.65, indicating that the regression model is not quite able to represent a large enough part of the variation of $Q_e$. However, $R_y^2$ values were found to increase as the size of the drainage basin increases, with values reaching up to 0.7 for drainage basins of 50 $km^2$. The PEAR values affecting $Q_e$ for catchments of 50 $km^2$ were found to be -

0.33 for K, -0.23 for $t_c$, and 0.73 for β; the absolute PEAR values for the other 4 input factors are much lower. The PEAR values demonstrated the same trend for drainage areas of 10 and 20 $km^2$ for $Q_e$. The rest of the regression-based measures, i.e., SRC, PCC, PRCC, SPEA, and SRRC, also demonstrated very similar trends for $Q_e$. Fig. 4.3 shows the complete regression-based sensitivity analysis results for $Q_e$ for catchments of 50 $km^2$. As the size of the watershed increases or reduces, the values of the regression-based sensitivity measures for $Q_e$ do not change much.

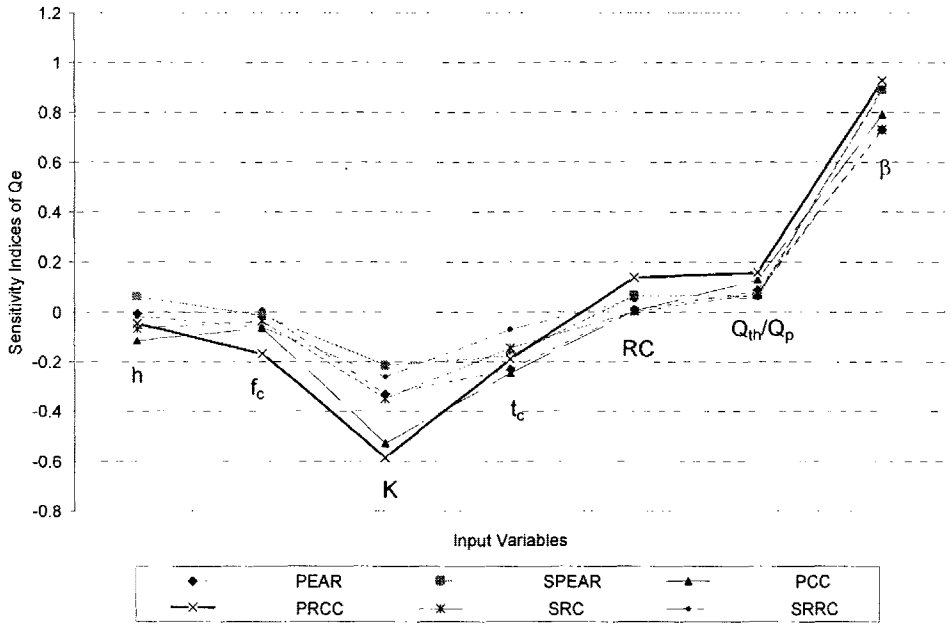


**Fig 4.3:** Regression-based sensitivity measures of $Q_e$ for catchments of 50 $km^2$

From Fig. 4.3 it can be seen that compared to β, K, and $t_c$, the other 4 input factors are much less critical in affecting $Q_e$. Since RC and $Q_{th}/Q_p$ only affect the baseflows of a stream and are not critical in affecting $Q_e$, during the second step of our sensitivity analysis, RC and $Q_{th}/Q_p$ are removed as input factors. For all the simulation runs, typical constant values of 0.65 and 0.062 were maintained for RC and $Q_{th}/Q_p$, respectively. For $Q_e$, the total Sobol' indices for input factors of β, K, $t_c$, h, and $f_c$ were determined to be 0.97, 0.33, 0.11, -0.03, and -0.12, respectively, for catchments of 20 $km^2$. The first order Sobol' indices for the input factors of β, K, $t_c$, h, and $f_c$ were determined to be 0.48, -

0.087, -0.077, -0.02, and -0.012, respectively. The Sobol' indices for some input factors were found to be negative. This is a numerical error caused by small sample size which occurs when the sensitivity indices are close to zero. Thus the negative values may be taken as zeros. The differences between the total and first order Sobol' indices, especially with respect to β, K and $t_c$, indicate that in addition to the influence of each individual input factor, the interactions between the factors themselves also play an important role in governing the effective discharge. Both the regression-based sensitivity measures and Sobol' indices suggest that β plays a predominant role in controlling the value of $Q_e$; h and $f_c$ have a negligible impact on $Q_e$; while $t_c$ and K have a small to moderate impact on $Q_e$. The negative values of regression-based sensitivity measures for K and $t_c$ means that the lower the $t_c$ or K, the higher the $Q_e$ (i.e., the channel form is controlled by high magnitude flow events).

Fig. 4.4 summarizes the regression-based sensitivity analysis results for $Q_{1.5}$ from catchments of 5 $km^2$. For catchments of other sizes, the results were very similar and are not presented. The $R_y^2$ was found to be 0.81 indicating that the regression model can explain the majority of the variation in $Q_{1.5}$. Fig. 4.4 shows that $Q_{1.5}$ is most sensitive to h, K and $t_c$, while RC and $Q_{th}/Q_p$ are much less sensitive input factors. When conducting the second stage variance-based sensitivity analysis, RC and $Q_{th}/Q_p$ were therefore excluded. For catchments of 20 $km^2$, the total Sobol' indices for $Q_{1.5}$ were found to be 0.52, 0.42, 0.33, and -0.047 for K, h, $t_c$, and $f_c$ respectively. The 1st order Sobol' indices for $Q_{1.5}$ were found to be 0.47, 0.21, 0.17, and 0.058 for h, K, $t_c$, and $f_c$, respectively. The Sobol' sensitivity indices values suggest that K, h, and $t_c$ are the three most important factors affecting the value of $Q_{1.5}$, the effect of $f_c$ is almost negligible. For $Q_{2.5}$, regression-based sensitivity analysis results are similar to those for $Q_{1.5}$. The total Sobol' indices for $Q_{2.5}$ were found to be 0.61, 0.41, and 0.28 for K, $t_c$, and h, respectively, illustrating that as the return period increases, the corresponding flood peaks become less sensitive to h.

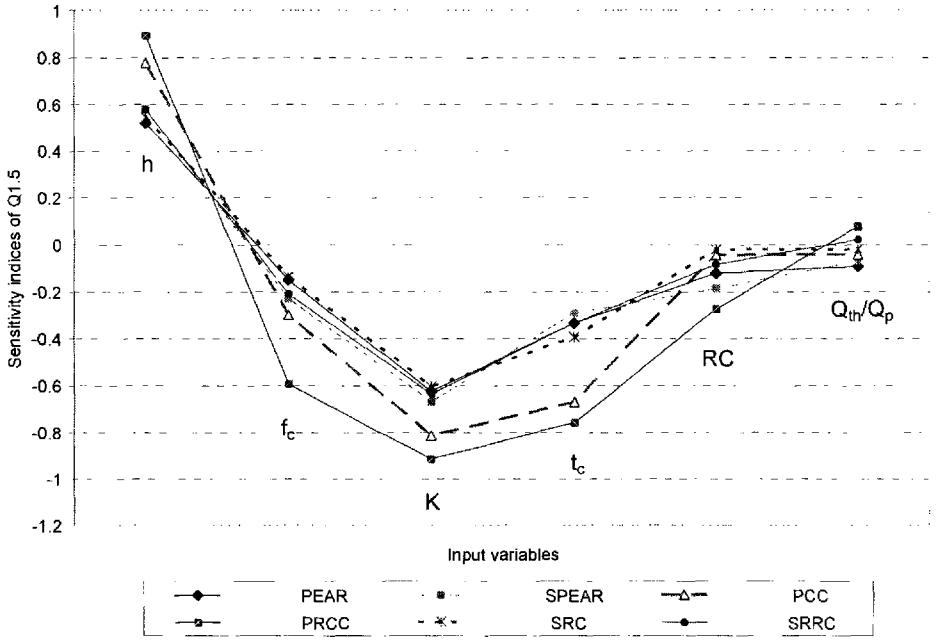


**Fig 4.4:** Regression-based sensitivity measures of $Q_{1.5}$ for catchments of 5 $km^2$

Figs. 4.5 and 4.6 graphically present the regression-based sensitivity indices of each input factors influencing $T_{Q_e}$ and PTQEX, respectively, for catchments of 50 $km^2$. The sensitivity indices of the input factors for drainage areas of 5, 10, and 20 were also determined but are not presented here due to space limitations. Averaged across the different regression-based sensitivity analysis methods and catchment sizes, the regression-based sensitivity indices for $T_{Q_e}$ and PTQEX were found to be 0.74 and -0.65, respectively, for β. The absolute values of the average regression-based sensitivity indices for all other input factors are much less. The average $R_y^2$ values for $T_{Q_e}$ and PTQEX were 0.56 and 0.58, respectively. The Sobol' sensitivity indices also showed that $T_{Q_e}$ and PTQEX are most heavily influenced by β.

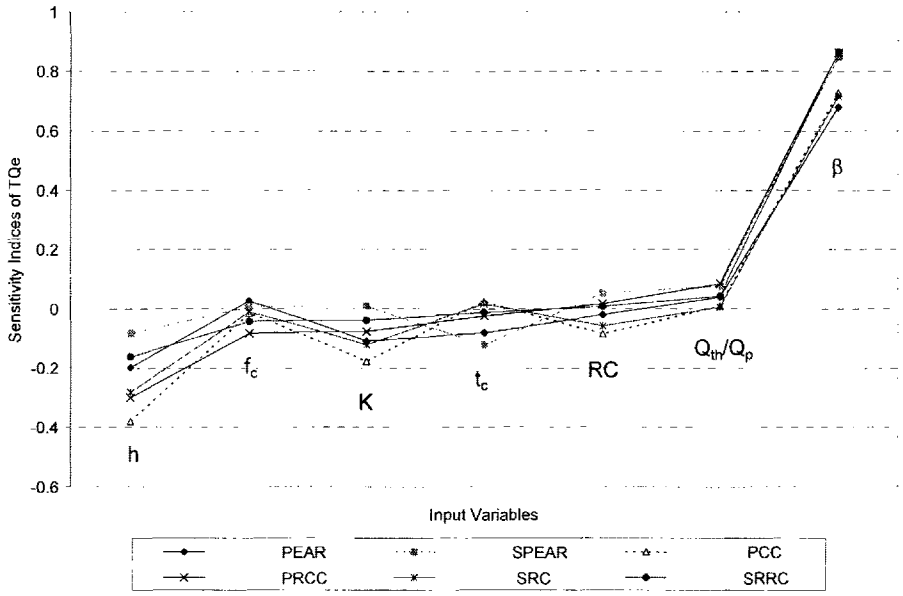


**Fig 4.5:** Regression-based sensitivity measures of $T_{Q_e}$ for catchments of 50 $km^2$

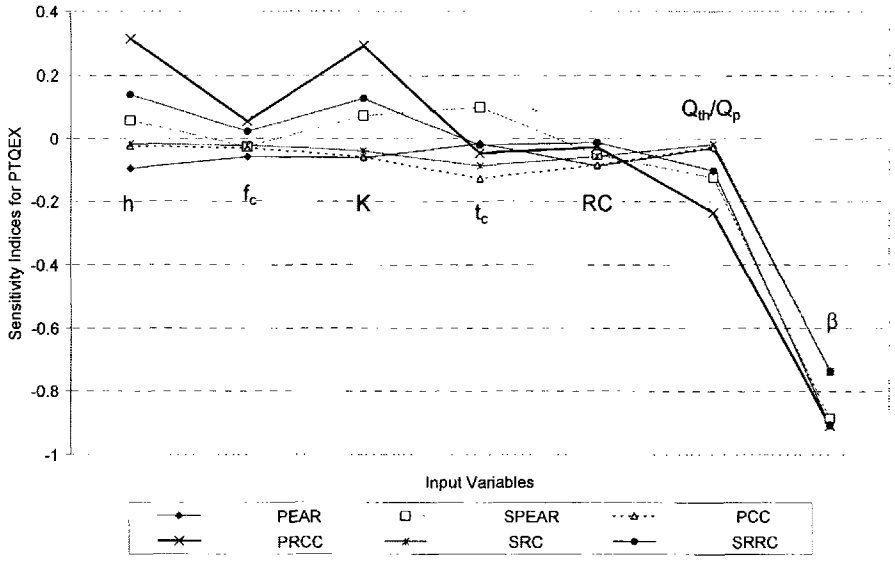


**Fig 4.6:** Regression-based sensitivity measures of PTQEX for catchments of 50 $km^2$

### 4.5.2 Relationship between Effective Discharge and Discharges of Specific Return Periods

The 105 pairs of $Q_e$ versus $Q_{1.5}$ and $Q_e$ versus $Q_{2.5}$ data obtained from the preceding analysis were used to explore the relationship between $Q_e$ and $Q_{1.5}$ (or $Q_{2.5}$). When data for different $\beta$ values are plotted together, $Q_e$ and $Q_{1.5}$ or $Q_{2.5}$ show no correlation for any of the four catchment sizes. However, a closer observation reveals that the value of $\beta$ may play an important role in the correlation. Thus, the range of $\beta$ values is divided into three intervals, i.e., $0.5 \le \beta < 2$, $2 \le \beta < 3.5$, and $3.5 \le \beta \le 5$. For each one of these intervals, the corresponding $T_{Q_e}$ values were examined separately. When $0.5 \le \beta < 2$, $T_{Q_e}$ for all of the four catchment sizes were found to be less than 1 year. When $2 \le \beta < 3.5$ and for catchments of 10 km$^2$, the mean of $T_{Q_e}$ was found to be 1.2 years, with a maximum of 3.2 years and a minimum of less than 1 year. Similar results were observed for catchments of 5, 20 and 50 km$^2$ when $2 \le \beta < 3.5$. The $T_{Q_e}$ values when $3.5 \le \beta \le 5$ range from 1.1 to 10 years with a mean of 3.4 years and a standard deviation of 2.2 years for catchments of 5 km$^2$. Similarly, higher return period $Q_e$ values were also found for catchments of 10, 20, and 50 km$^2$ when $3.5 \le \beta \le 5$. In summary, the above results show that as the value of $\beta$ increases, the corresponding return period of $Q_e$ in average increases as well, although the relationship between the two is not a simple linear one.

The ratios between $Q_e$ and $Q_{1.5}$ as well as between $Q_e$ and $Q_{2.5}$ were also determined. Box plots of these ratios show that for all catchment sizes, when $3.5 \le \beta \le 5$, the median value of the ratios is closest to 1 between $Q_e$ and $Q_{2.5}$. Ratio of 1 indicates a perfect match. Fig. 4.7(a) shows the box plots of $Q_e / Q_{2.5}$ for catchments of 5 km$^2$, where the median together with the upper and lower quartiles are shown as a notch, the minimum and maximum values are shown as whiskers. Similar results were obtained for catchments of 10, 20, and 50 km$^2$. The relationship between $Q_e$ and $Q_{1.5}$ (or $Q_{2.5}$) were

also assessed using $\log_{10}$-difference plots. The results again indicate that the $\log_{10}$-difference between $Q_e$ and $Q_{2.5}$ are closest to zero (i.e., no difference between the two log transformed values) for $3.5 \leq \beta \leq 5$. Fig. 4.7(b) presents the box plots of $\log_{10}$-difference between $Q_e$ and $Q_{2.5}$ for catchments of 20 $km^2$. Fig. 4.7(b) shows that the median of the box plot when $3.5 \leq \beta \leq 5$ is closest to zero. In Fig. 4.7(b), a dot placed at the bottom of each whisker indicates that there are no data outside the whisker. These results reveal that only when $3.5 \leq \beta \leq 5$ there exists a strong relationship between $Q_e$ and $Q_{2.5}$.

In the study conducted by Emmett and Wolman (2001), the return period of $Q_b$ was estimated to be approximately 1.5 yrs, and the values of $Q_e$ and $Q_b$ were reported to be almost equal to each other when the value of $\beta$ is 2.5. In our study, further analysis showed that $Q_e$ and $Q_{1.5}$ were almost equal when $\beta = 3.5$. This difference in findings led us to a detailed comparison between the two studies. The major difference between our study and that of Emmett and Wolman (2001) is that hourly streamflow is used in our study while daily streamflow is used in theirs. For the same river, the magnitude of $Q_{1.5}$ (and $Q_{2.5}$) obtained from hourly streamflow data is higher than that obtained from daily streamflow data, because daily streamflow series averages out peak hourly flows. Similarly the magnitude of $Q_e$ for a specific $\beta$ value obtained from hourly streamflow data is higher than that obtained from daily streamflow data using the transport effectiveness curve approach. This is the main reason that explains the difference between our finding and that of Emmett and Wolman (2001) about the relationship between $Q_e$ and $Q_{1.5}$. The other fact that may explain the difference is that the size of the drainage basins investigated by Emmett and Wolman (2001) are considerably larger than the ones investigated in this study.

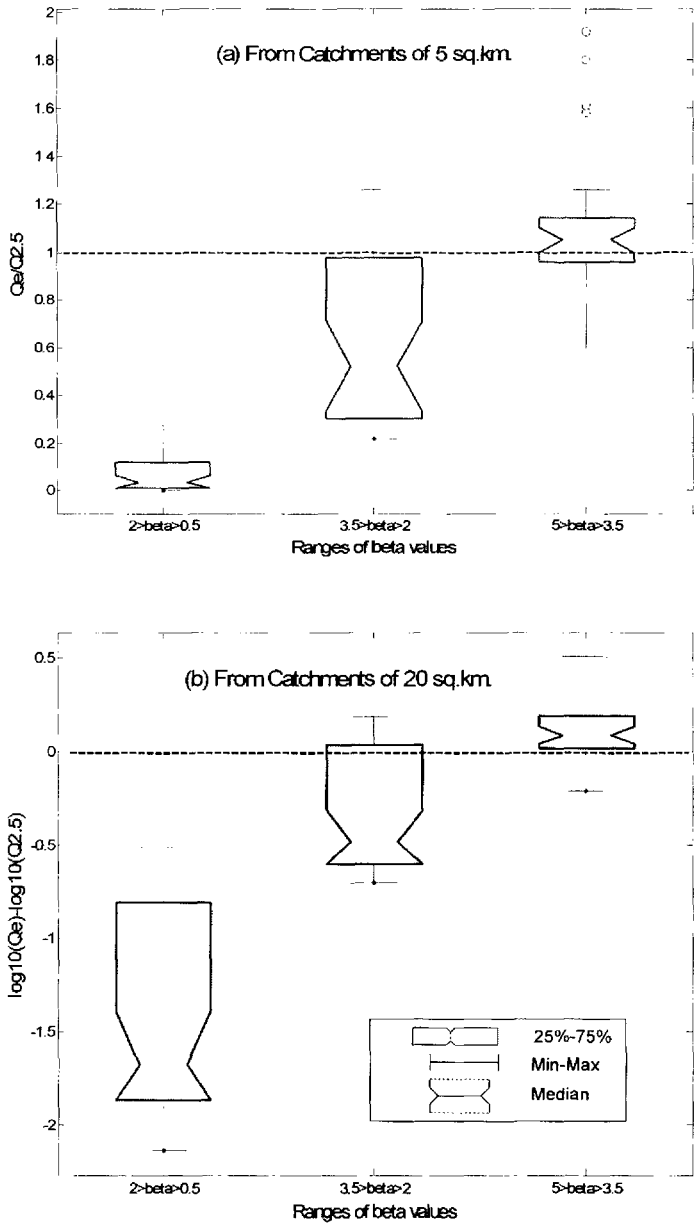


**Fig 4.7:** Comparative analysis between $Q_e$ and $Q_{2.5}$ for drainage areas of (a) 5 $km^2$; (b) 20 $km^2$

The finding that strong relationship between $Q_e$ and discharges with a specific return period only exists when $\beta \geq 3.5$ presents warning to jurisdictions where discharges

with a specific return period are adopted as the channel-forming discharge. Only for stream reaches where a high threshold discharge needs to be exceeded before any significant mobilization of sediment takes place (e.g., streambeds composed of clay or gravel bed streams with large particles), this adoption may be advisable because these reaches may meet the condition that $\beta \geq 3.5$. However, for reaches where $\beta < 3.5$, the return periods of $Q_e$ for the vast majority of these river reaches are less than 1.5 years and adoption of discharges with a specific return period as the channel-forming discharge may likely result in erroneous design.

## 4.6 Summary and Conclusions

This study utilizes global sensitivity analysis to determine the most critical watershed hydrological and sedimentological parameters influencing the values of effective discharge $Q_e$ and other related variables of interest. The results of this study indicate that the three most important parameters influencing $Q_e$ are the exponent of the sediment rating curve ( $\beta$ ), the watershed storage coefficient ( K ) and time of concentration ( $t_c$ ). Furthermore, the Sobol' total sensitivity indices show that $\beta$ accounts for the variability of $Q_e$ about 2 and 4 times more than K and $t_c$, respectively. The return period of $Q_e$ ( $T_{Q_e}$ ) and percentage of time $Q_e$ is exceeded (PTQEX) were also found to be most heavily influenced by $\beta$. Therefore, for a more accurate estimation of $Q_e$, more resources should be devoted to the estimation of the $\beta$ value. Watershed sediment and stream reach characterization is a starting point in determining the value of $\beta$. The catchment's storage and translation characteristics should also be better quantified.

A common practice in stream restoration is to use discharges corresponding to return periods of 1.5 or 2.5 years as the channel-forming discharge. If $Q_e$ is the closest to the true channel-forming discharge, the results of this study indicate that for urban drainage basins within the range of 5-50 $km^2$, this practice would provide a reasonable estimate only when $\beta \geq 3.5$. When $\beta < 3.5$, using $Q_e$ and $Q_{1.5}$ (or $Q_{2.5}$) analogously or

assuming that $Q_{1.5}$ (or $Q_{2.5}$) is the channel-forming discharge is not recommended because the return periods of $Q_e$ for the vast majority of these rivers are less than 1.5 years and no correlation seems to exist between $Q_e$ and $Q_{1.5}$ (or $Q_{2.5}$).

Completion of a stream restoration project without any knowledge of $\beta$ can seriously hamper and may ultimately lead to the failure of the project. Practicing engineers are often forced to work with limited amount of information under a fixed budget, findings from this study may guide engineers to optimize the use of resources and focus more on the critical hydrological and sedimentological parameters affecting effective discharge. In addition, the temporal resolution of streamflow series was found to be influential in affecting the values of $Q_e$ and $Q_{1.5}$ (or $Q_{2.5}$). For small urban streams, finer temporal resolution streamflow series (with time-steps less than or equal to 1 hour) should be used. Conclusions from earlier studies where the drainage area is much larger or where daily streamflow data were used should be applied with caution.

# References


1. Anderson, M.L., Chen Z-Q, Kavvas, M.L., Feldman, A., (2002) "Coupling HEC-HMS with atmospheric models for prediction of watershed runoff." *Journal of Hydrologic Engineering,* 7(4), 312-318.
2. Andrews, E.D., (1980) "Effective and bankfull discharges of streams in the Yampa River basin, Colorado and Wyoming." *Journal of Hydrology,* 46, 311-330.
3. Barry, J. J., Buffington, J. M., King, J. G., (2004) "A general power equation for predicting bedload transport rates in gravel bed rivers." *Water Resources Research*, 40, doi: 10.1029/2004WR003190, 2004.
4. Biedenharn, D.S., and Copeland, R.R., (2000) *Effective discharge calculation*, ERDC/CHL HETN-II-4 US Army Corps of Engineers, Vicksburg, MS.
5. Copeland, R. R., Biedenharn, D. S., Fischenich, J. C., (2000) *Channel-forming discharge*, US Army Corps of Engineers, ERDC/CHL CHETN-VIII-5.
6. Doll, B.A., Grabow, G.L., Hall, K.R., Halley, J., Harman, W.A., Jennings, G.D., Wise, D.E., (2003) *Stream restoration: a natural channel design handbook*,

Prepared by the North Carolina Stream Restoration Institute, NC State University. A copy of this handbook can be downloaded from www.bae.ncsu.edu.

7. Emmett, W.W. and Wolman, M.G., (2001) "Effective discharge and gravel-bed rivers." *Earth Surface Processes and Landforms,* 26, 1369-1380.
8. Feng, X-J., Hooshangi, S., Chen, D., Li, G., Weiss, R., Rabitz, H., (2004) "Optimizing genetic circuits by global sensitivity analysis." *Biophysical Journal,* 87, 2195-2202.
9. Fleming, M., and Neary, V., (2004), "Continuous hydrologic modeling study with the hydrologic modeling system." *Journal of Hydrologic Engineering,* 9(3), 175-183.
10. Francos, A., Elorza, F.J., Bouraoui, F., Bidoglio, G., Galbiati, L., (2003) "Sensitivity analysis of distributed environmental simulation models: Understanding the model behavior in hydrological studies at the catchment scale." *Reliability Engineering and System Safety,* 79, 205-218.
11. Goodwin, P., (2004) "Analytical solutions for estimating effective discharge." *Journal of Hydraulic Engineering,* 130(8), 729-738.
12. Goodwin, P., (2006) Closure to 'Analytical solutions for estimating effective discharge', *Journal of Hydraulic Engineering,* 132(1), 114-115.
13. Hall, J.W., Tarantola, S., Bates, P.D., Horritt, M.S (2005) "Distributed sensitivity analysis of flood inundation model calibration." *Journal of Hydraulic Engineering,* 131(2), 117-126.
14. Hedin, A., (2003) "Probabilistic dose calculations and sensitivity analyses using analytic models." *Reliability Engineering and System Safety,* 79, 195-204.
15. Huber, W.C., and Dickinson, R.E. (1988) *Stormwater management model, version 4: User's manual*, Environmental Research Laboratory, Office of Research and Development, U.S. Environmental Protection Agency, Athens, GA.
16. HYDAT, (2001) *Surface Water and Sediment Data*, Released by Environment Canada, National Archives and Data Management Branch, 4905 Dufferin St., Downsview, ON M3H 5T4, Canada.
17. Keystone Stream Team, (2002) *Guidelines for natural stream channel design for Pennsylvania waterways*, Prepared by the Alliance for the Chesapeake Bay.

Electronic copies of this document are available at www.canaanvi.org/nscdguidelines.

18. Lenzi, M. A., Mao, L., Comiti, F., (2006) "Effective discharge for sediment transport in a mountain river: computational approaches and geomorphic effectiveness." *Journal of Hydrology*, 326, 257-276.
19. Markowski, D., Naud, C., Manod, H., Jeuffroy, M-H., Barbotin, A., (2005) "Global sensitivity analysis for calculating the contribution of genetic parameters to the variance of crop model prediction." *Proceedings of 5th International Conference on Sensitivity Analyses of Model Outputs* (SAMO), Santa Fe, New Mexico, USA.
20. Mishra, S., Deeds, N.E., RamaRao, B.S., (2003), "Application of classification trees in the sensitivity analysis of probabilistic model results." *Reliability Engineering and System Safety*, 79. 123-129.
21. Mishra, S., (2004), "Sensitivity analysis with correlated inputs- An environmental risk assessment example." *Proceedings of the Crystal Ball User Conference*, Denver, Colorado.
22. Moody, T., Wirtanen, M., Yard, S.N., (2003) *Regional relationships for bankfull stage in natural channels of the arid southwest*, Natural Channel Design Inc., 3410 S. Cocopah Drive, Flagstaff, AZ 86001.
23. Nash, D.B., (1994) "Effective sediment-transporting discharge from Magnitude-Frequency analysis." *Journal of Geology,* 102, 79-95.
24. Olivera, F., (2001) "Extracting hydrologic information from spatial data for HMS modeling." *Journal of Hydrologic Engineering,* 6(6), 524-530.
25. Pastres, R., Chan, K., Solidoro, C., Dejak, C., (1999) "Global sensitivity analysis of a shallow-water 3D eutrophication model." *Computer Physics Communications,* 117, 62-74.
26. Penciolelli, A and Hue, C., (2005) "Global sensitivity analysis to improve models in agronomy." *Proc. of 1st Open International Conference on Model and Simulation (OICMS)* Blaise Pascal University, France.
27. Ponce, V.M., (1989) *Engineering Hydrology*, Prentice-Hall, Englewood Cliffs, NJ.

28. Quader, A., Guo, Y., and Bui, T., (2006) Discussion of 'Analytical Solutions for Estimating Effective Discharge' by Peter Goodwin, *Journal of Hydraulic Engineering,* 132(1), 112-114.
29. Riley, S.J., (1972) "A comparison of morphometric measures of bankfull." *Journal of Hydrology,* 17, 23-31.
30. Rosgen, D.L., (1994) "A classification of natural rivers." *Catena,* 22, 169-199
31. Saltelli, A., Chan, K., and Scott, E.M., (2001) *Sensitivity Analysis, 2nd Ed.*, John Wiley & Sons Ltd. West Sussex, England.
32. Saltelli, A., Tarantola, S., Campolongo, F., Ratto, M., (2004) *Sensitivity Analysis in Practice: A Guide to Assessing Scientific Models*, John Wiley & Sons Ltd. West Sussex, England.
33. Senarath, S.U.S, Ogden, F.L., Downer, C.W., Sharif, H.O., (2000) "On the calibration and verification of two-dimensional, distributed, Hortonian, continuous watershed models." *Water Resources Research,* 36(6), 1495-1510.
34. Shields Jr, F.D., Copeland, R.R, Klingeman, P.C., Doyle, M.W., Simon, A., (2003) "Design for stream restoration." *Journal of Hydraulic Engineering,* 129(8), 575-584.
35. Sichingabula, H. M., (1999) "Magnitude-frequency characteristics of effective discharge for suspended sediment transport, Fraser River, British Columbia, Canada." *Hydrological Processes*, 13, 1361-1380.
36. Skidmore, P. B., Shields, F. D., Doyle, M. W., Miller, D. E., (2002) "A categorization of approaches to natural channel design." *Proc. of ASCE River Restoration Conference*, Reno, Nevada.
37. U.S. Army Corps of Engineers (USACE), (2000) *HEC-HMS Technical Reference Manual*, CPD-74B. Published by the U.S. Army Corps of Engineers, Davis, Calif.
38. Vogel, R. M., Stedinger, J. R., Hooper, R. P., (2003) "Discharge indices for water quality loads." *Water Resources Research*, 39(10), doi: 10.1029/2002WR001872, 2003.
39. Williams, G.P., (1978) "Bank-full discharge of rivers." Water *Resources Research*, 14(6), 1141-1154.

40. Wolman, M.G., and Miller, J.P., (1960) Magnitude and frequency of forces in geomorphic processes, *Journal of Geology,* 68, 54-74.

41. Woodyer, K.D., (1968) Bankfull frequency in rivers, *Journal of Hydrology,* 6, 114-142.

42. Zhang, Z., Victor, K., Smith, M., Reed, S., Wang, D., (2004) Use of next generation weather radar data and basin disaggregation to improve continuous hydrograph simulations, *Journal of Hydrologic Engineering,* 9(2), 103-115.

# Chapter 5

## Peak Discharge Estimation for Urban Catchments Using Analytical Probabilistic and Design Storm Approaches

Asif Quader and Yiping Guo

**Abstract:** The recently developed analytical probabilistic approach was used for estimation of peak discharge rates in a practical design case. The results were compared with those from the commonly used design storm approach. Differences in meteorological data analysis and representation of rainfall input, subcatchment aggregation, and the treatment of the catchment time of concentration between the two approaches were identified as the three main causes contributing to the discrepancy in peak discharge estimates. In spite of the differences, peak discharge estimates from the two approaches are generally comparable for the actual design case. Furthermore, this study revealed that discrepancies caused by subcatchment aggregation and difference in meteorological data analysis are approximately the same. Treating the time of concentration as a constant across storms of various magnitudes was found not to contribute to a large discrepancy. However, it was shown that the closer the time of concentration values used in the two approaches, the closer the resultant peak discharge estimates.

**Keywords:** Peak flow, catchment, urban runoff, design storms, probabilistic models, stormwater management

## 5.1 Introduction

The estimation of peak flows associated with various return periods is necessary for the design of hydraulic structures. If measured flow data are available, flood frequency analysis can be applied. Unfortunately for many small catchments, flow data are usually not available. In these cases, in addition to continuous simulation, two other approaches may be applied for design purposes: regional flood frequency analysis and the design storm approach. The heterogeneity of small urban catchments precludes the use of the regional flood frequency analysis approach. Thus, only two viable approaches are left for the estimation of peak discharges of various return periods from small urban catchments: the design storm and the continuous simulation approaches.

Continuous simulation with the input of observed long-term precipitation series at or close to the site of interest and subsequent frequency analysis on the generated peak flow series provide the most accurate estimates of peak discharge rates with various return periods for small urban catchments where observed flow data do not exist. However, this is so time consuming that in most cases of planning and design, the design storm approach is used instead. In the design storm approach, a design storm associated with the desired return period is used as an input to a stormwater model for estimation of the resulting storm runoff hydrograph, from which, the volume of runoff and the peak discharge are determined. Some of the widely used design storms are AES (Atmospheric Environment Services, Environment Canada) design storms, Chicago design storms, ISWS (Illinois State Water Survey) design storms, SCS (Soil Conservation Service) design storms, Uniform distribution storms (Marsalek and Watt, 1984), 1-hr design storms (Watt et al., 1986), and 24-hr design storms (Loukas and Quick, 1995). SWMM, HEC-1, HEC-HMS, OTTHYMO, MIDUSS, etc., are just a few examples of the many existing stormwater models commonly applied together with design storms for engineering design purposes.

Compared to the continuous simulation approach, the design storm approach is simple and straightforward to use. That is why it is widely used in actual engineering

design. However, the design storm approach has its problems and limitations. A design storm, which is a hydrologic event, has a number of characteristics, e.g., duration, total depth, average intensity, etc. As a result, it is almost impossible to characterize it as a statistical event with a unique return period. The many characteristics of a design storm may have their own specific frequency of occurrence. However, the design storm approach is based on the basic assumption that the design storm event and the resulting runoff hydrograph and all their characteristics have the same unique frequency of occurrence assigned to the design storm. The problems and limitations of the design storm approach were discussed in more detail by Adams and Howard (1986).

In spite of the problems and limitations of the design storm approach, it continues to be one of the most widely used approach for practical design calculations. An alternative approach, the analytical probabilistic approach, was recently developed with a promise of overcoming and eliminating some of the limitations and problems of the design storm approach. The development of the analytical probabilistic approach is briefly summarized as follows. Following the rainfall event-based meteorological data analysis procedure and the resultant exponential distributions of rainfall event volume, duration and inter-event time (Adams et al., 1986), Guo and Adams (1998a & b) derived mathematical expressions for the probability distributions of runoff volume and peak discharge rate from urban catchments. These derived mathematical expressions are all in closed-form, requiring no numerical solution procedures. The validity of these closed-form analytical solutions was tested by performing comparisons with results from the continuous simulation approach for a number of hypothetical test catchments. Guo and Adams (1999) also derived the probability distribution function of peak outflow rate from a detention pond downstream of an urban catchment. So far, verification of all the above-referenced analytical development was based on comparison to results obtained from continuous simulation. Guo (2001) provided the first comparison between the analytical probabilistic, design storm, and continuous simulation approaches for a hypothetical urban test catchment focusing, however, more on the design of flood control detention ponds.

Encouraged partly by the comparison results between the analytical probabilistic and the design storm approaches reported in Guo (2001), in this paper, for the first time, the analytical probabilistic approach was applied to a practical design case and the results were compared directly with those from the design storm approach only. Although continuous simulation is a more accurate approach of estimating peak discharge rates of various return periods, in the routine design of small scale stormwater management facilities, continuous simulation is rarely used. That is why in this comparison study, continuous simulation was no longer conducted. Instead, results from the design storm approach were used more or less as the standard or benchmark because of its wide acceptance in engineering design. Comparison of results from the analytical probabilistic and design storm approaches would not reveal which is better or correct as both approaches have their limitations, rather comparisons would provide us with a preliminary understanding of how results differ from each other. As the analytical probabilistic approach is a new approach and is fundamentally different from the design storm approach, such understanding will assist in its improvement and further development.

## 5.2 The Analytical Probabilistic Approach

The analytical probabilistic approach is based on the meteorological data analysis technique pioneered by Eagleson (1972) and discussed specifically for drainage system design by Adams et al (1986). For convenience, this technique is referred to as the rainfall event-based or simply event-based meteorological data analysis technique. According to this event-based technique, a continuous rainfall series observed at a point is divided into a series of discrete events. Consecutive events are separated by a dry period equal to or longer than a minimum time period without any rainfall. This minimum time period without any rainfall is termed the inter-event time definition (IETD). The characteristics of the separated individual rainfall events that would affect the drainage system and stormwater management system design and functioning the most are event volume ($v$), duration ($t$) and interevent time ($b$). Here interevent time $b$ is the actual length of time without rainfall between two consecutive rainfall events.

Probability distribution functions (PDF) are fitted to the histograms obtained from the frequency analysis for each of these event characteristics. Exponential PDFs were found to fit well the histograms of all three characteristics. These exponential PDFs are as follows:

$$f_V(v) = \zeta \exp(-\zeta v)$$

$$f_T(t) = \lambda \exp(-\lambda t)$$

$$f_B(b) = \psi \exp(-b\psi)$$

where $\zeta$, $\lambda$, and $\psi$ are distribution parameters, their values for a geographical location may be determined using historical rainfall data and a distribution parameter estimation method (e.g., method of moment). More details and the values of $\zeta$, $\lambda$, and $\psi$ used in this study may be found in Guo and Adams (1998a).

The PDFs of the rainfall event characteristics were used together with a functional relationship describing the rainfall-runoff transformation process to determine the probability distribution of the resulting runoff event characteristics. The derived probability distribution theory was used in the mathematical derivations. The basis of the derived probability distribution theory is that the probability distribution of a dependent (output) random variable is related to and may be derived from the probability distributions of the independent (input) random variables. By using the derived probability distribution theory and a rainfall-runoff transformation model similar to those used in stormwater models, Guo and Adams (1998a & b) derived the probability distribution functions for runoff event volume and peak discharge rate. The probability of exceedence for runoff event volume ($v_r$) is expressed analytically by Eqn. (5.1).

$$G_{V_R}(v_r) = \begin{cases} \exp(-\zeta S_{di}) & , \quad v_r = 0 \\ \exp(-\zeta S_{di} - \dfrac{\zeta}{h} v_r) & , \quad 0 < v_r \le hS_{dd} \\ \dfrac{\lambda}{\lambda + \zeta f_c - \zeta f_c h} \exp(-\zeta S_d - \zeta v_r) & \\ + \dfrac{\zeta f_c (1-h)}{\lambda + \zeta f_c - \zeta f_c h} \exp\left[ -\zeta S_{di} + \dfrac{\lambda}{f_c} S_{dd} - \dfrac{1}{h}(\zeta + \dfrac{\lambda}{f_c}) v_r \right] & , \quad v_r > hS_{dd} \end{cases} \tag{5.1}$$

In Eqn. (5.1), $S_{di}$ is the depression storage of the impervious area of the catchment in mm, $h$ is the fraction of imperviousness of the catchment, $f_c$ is the infiltration capacity of the soil (mm/hr), and $S_d = hS_{di} + (1 - h)S_{il}$, is the area-weighted depression storage of the impervious areas and the initial losses of the pervious areas of the urban catchment. In the term $S_d$, $S_{il}$ is the summation of the depression storage in the pervious area ($S_{dp}$) and the initial soil wetting infiltration volume ($S_{iw}$). Guo and Adams (1998a) provides a method of estimating $S_{iw}$ based on the values of more regularly used soil infiltration parameters. In Eqn. (5.1), the term $S_{dd}$ is the difference between the initial losses in the pervious area and depression storage in the impervious area (i.e., $S_{il}$ - $S_{di}$). These short-hand notations are introduced so that the analytical expressions can be simpler in form. In actual application of the analytical probabilistic approach, the required input parameters of the catchment are almost the same as those required for the application of the design storm approach.

The relationship between return period ($T_R$) and the probability of exceedence, $G_{V_R}(v_r)$, can be expressed as:

$$T_R = \frac{1}{\theta G_{V_R}(v_r)} \tag{5.2}$$

In Eqn. (5.2), $T_R$ is the return period in years; $\theta$ is the average number of rainfall events per year and $G_{V_R}(v_r)$ is the exceedence probability of runoff event volume ($v_r$) per rainfall event. From the exceedence probability $G_{V_R}(v_r)$, for a particular $T_R$, the corresponding runoff event volume ($v_r$) can be analytically determined by using Eqn. (5.1).

Guo and Adams (1998b) used a triangular hydrograph to correlate the peak discharge rate ($Q_p$) to the corresponding runoff event volume ($v_r$):

$$Q_p = \frac{2v_r}{t + t_c} \tag{5.3}$$

where $t$ is the duration of the input rainfall event and $t_c$ is the catchment time of concentration. Catchment time of concentration is assumed to be constant. The sum of $t$ and $t_c$ is thus the time base of the resulting runoff hydrograph. Using Eqn. (5.3) and applying the derived probability distribution theory, the exceedence probability of the peak discharge rate was also analytically determined (Guo and Adams, 1998b). Only the final results are reproduced here for ease of reference.

The analytical solutions are presented for two types of catchments. Catchments where $f_c < S_{dd}/t_c$ were identified as type I catchments. For type I catchments the peak discharge exceedence probability can be determined by using Eqn. (5.4).

$$P[Q_p > q_p] = \begin{cases} \dfrac{2h\lambda}{2h\lambda + \zeta q_p} \exp\left(-\zeta S_{dh} - \dfrac{\zeta t_c}{2h} q_p\right) & , \; q_p < 2f_c h \\ \dfrac{2\lambda\zeta(1-h)(q_p - 2f_c h)}{(2h\lambda + \zeta q_p)(2\lambda + \zeta q_p + 2f_c\zeta - 2hf_c\zeta)} \exp\left[-\dfrac{(\zeta S_{il} - \lambda t_c - f_c\zeta t_c)q_p - 2f_c\zeta h S_{dh} + 2\lambda h S_{dd}}{q_p - 2f_c h}\right] & \\ \quad + \dfrac{2h\lambda}{2h\lambda + \zeta q_p} \exp\left(-\zeta S_{dh} - \dfrac{\zeta t_c}{2h} q_p\right) & , \; 2f_c h \le q_p < \dfrac{2hS_{dd}}{t_c} \\ \dfrac{\lambda}{\lambda + \zeta\left(\dfrac{q_p}{2} + f_c - f_c h\right)} \exp\left(-\zeta S_d - \dfrac{\zeta t_c}{2} q_p\right) & , \; q_p \ge \dfrac{2hS_{dd}}{t_c} \end{cases} \tag{5.4}$$

Catchments where $f_c \ge S_{dd}/t_c$ were identified as type II catchments. For type II catchments the peak discharge exceedence probability can be determined by using Eqn. (5.5).

$$P[Q_p > q_p] = \begin{cases} \dfrac{2h\lambda}{2h\lambda + \zeta q_p} \exp\left(-\zeta S_{dh} - \dfrac{\zeta t_c}{2h} q_p\right) & , q_p < \dfrac{2hS_{dd}}{t_c} \\ \dfrac{2\lambda\zeta(1-h)(2f_c h - q_p)}{(2h\lambda + \zeta q_p)(2\lambda + \zeta q_p + 2f_c\zeta - 2hf_c\zeta)} \exp\left[-\dfrac{(\zeta S_{il} - \lambda t_c - f_c\zeta t_c)q_p - 2f_c\zeta h S_{dh} + 2\lambda h S_{dd}}{q_p - 2f_c h}\right] & \\ + \dfrac{2\lambda}{2\lambda + \zeta(q_p + 2f_c - 2f_c h)} \exp\left(-\zeta S_d - \dfrac{\zeta t_c}{2} q_p\right) & , \dfrac{2hS_{dd}}{t_c} \le q_p < 2f_c h \\ \dfrac{\lambda}{\lambda + \zeta\left(\dfrac{q_p}{2} + f_c - f_c h\right)} \exp\left(-\zeta S_d - \dfrac{\zeta t_c}{2} q_p\right) & , q_p \ge 2f_c h \end{cases} \tag{5.5}$$

In Eqn.s (5.4) and (5.5), $q_p$ is a given specific peak discharge value. Similar to the exceedence probability of runoff event volume, the exceedence probability for peak discharge is related to $T_R$ by Eqn. (5.2). To estimate the return period of a specific peak discharge value $q_p$, a catchment must be classified as either type I or type II first. Following this classification, the return period of a given peak discharge can be obtained by solving either Eqn. (5.4) or (5.5) directly. In a design situation, using this analytical probabilistic approach, the runoff volume or the peak discharge for a specific return period can be obtained by a simple trial and error procedure using Eqn.s (5.1), (5.2), (5.4), and (5.5). The analytical probabilistic approach and specifically Eqn.s (5.1) through (5.5) related to peak discharge rates are hereinafter referred to as the Analytical Probabilistic Stormwater Model (APSWM).

From the above description it can be seen that procedures followed by APSWM and the design storm approach for meteorological data analysis and subsequent representation of rainfall input for the transformation from rainfall to runoff are fundamentally different. APSWM follows the rainfall event-based procedure detailed in Adams et al. (1986) and uses exponential PDFs to represent the stochastic characteristics of rainfall. While the design storm approach follows the traditional procedure (i.e., construction and analysis of annual maximum or partial duration series for a set of pre-selected storm durations) of statistically analyzing historical rainfall data and represents the stochastic characteristics of rainfall using a set of design storms. This fundamental difference is expected to cause discrepancies in peak discharge estimates. One of the objectives of this study is to quantify the magnitude of the discrepancy of peak discharge

estimates caused by this fundamental difference between the two approaches. For ease of reference, this fundamental difference between the two approaches is hereinafter referred to as difference in meteorological data analysis.

## 5.3 Subcatchment Aggregation

For modeling and design purposes with the design storm approach, a catchment may be divided into a large number of subcatchments. Properties like soil infiltration capacity, depression storage for impervious and pervious areas, average slope, etc., may vary from one subcatchment to the next. For a developed urban area, these subcatchments may also be connected by pipes or channels of different sizes. These pipes and channels may be explicitly modeled or just considered implicitly and lumped into a subcatchment using the design storm approach.

To apply APSWM to determine the peak discharge rate of any return period for a location of interest within the same catchment, however, the entire area upstream of that location needs to be treated as one lumped catchment. This can be seen from the way Eqn.s (5.1), (5.4) and (5.5) are structured. Most of the characteristics for this lumped catchment can be obtained using an appropriate area-weighting technique. For example, if in using the design storm approach the entire area upstream of a location of interest is modeled as subcatchments 1, 2, ...$x$, the area-weighting calculation for these catchment characteristics can be simply performed as follows:

$$M = \frac{A_1 M_1 + A_2 M_2 ..... + A_x M_x}{A_1 + A_2 ..... + A_x} \tag{5.6}$$

In Eqn. (5.6), $M$ represents the value of the area-weighted lumped catchment characteristic; $M_1$, $M_2$, ... $M_x$ are the values of the catchment characteristic for subcatchments 1, 2 ...$x$, respectively; while $A_1$, $A_2$, ... $A_x$ are the areas of subcatchments 1, 2, ...$x$, respectively. This area-weighting technique can be applied to catchment characteristics such as $h$, $f_c$, $S_{di}$, $S_{dp}$, $S_{il}$, $S_{iw}$, $S_{dd}$, and $S_d$, but it cannot be applied to

determine the $t_c$ of the lumped catchment. To determine the $t_c$ of the lumped catchment, the flow paths across the entire area must be considered.

The subcatchment aggregation required for the application of APSWM obviously may contribute to discrepancies between results from APSWM and the design storm approach. The magnitude of this discrepancy has not been investigated by previous research related to the development of the analytical probabilistic approach. One of the purposes of this study is to gain a better understanding of the magnitude of the discrepancies that may be caused by the required subcatchment aggregation for the application of APSWM as compared to results obtained from the design storm approach.

## 5.4 Time of Concentration

Whether inputted externally by the user or calculated internally by a stormwater model, time of concentration plays a significant role in the estimation of peak discharge rate. A great deal of research has been devoted to the concept and estimation of time of concentration (Hotchkiss and McCallum, 1995). Time of concentration has been defined as the time required for a particle of water to flow hydraulically from the most distant point of the watershed or catchment to the outlet, design point or the point of interest (McCuen, 1989).

According to the above or similar $t_c$ definitions, a large number of $t_c$ estimation formulas were developed. These formulas may be divided into two types. Type 1 formulas express $t_c$ as a function of catchment characteristics only; while type 2 formulas express $t_c$ as a function of both catchment characteristics and the input rainfall intensity. Among the type 2 formulas, the kinematic wave formula (Singh, 1996) is one of the most widely used $t_c$ formula for hydrologic modeling and is used in this study.

In urban areas, subcatchments are usually connected by drainage pipes or channels. In some detailed modeling/design studies, both overland flow and pipe flow are considered for the estimation of the time of concentration. In these circumstances, to

measure the total travel time or $t_c$, a mixed velocity approach may be undertaken. The time of concentration is estimated by adding the different travel times along the principal flowpath as follows:

$$t_c = \sum_{m=1}^{p} t_{scf} + \sum_{n=1}^{q} t_{pipe} = \sum_{m=1}^{p} t_{scf} + \sum_{n=1}^{q} \frac{L_n}{V_n} \tag{5.7}$$

In Eqn. (5.7), $m$ indicates the number of subcatchments ranging from 1 to $p$, $n$ indicates the number of pipes ranging from 1 to $q$ in the principal flowpath or the longest flowpath from the most remote point of the catchment to the outlet or design point, $t_{scf}$ and $t_{pipe}$ are the travel times over subcatchments and along pipes, $L_n$ and $V_n$ are the length and the velocity of pipe flow. In Eqn. (5.7), $t_{scf}$ can be estimated by using the kinematic wave approach. For the determination of $t_{pipe}$, $V_n$ can be estimated by using the Manning's equation. Eqn. (5.7) is used in this study to estimate a catchment $t_c$.

In the design storm approach, the intensity of input rainfall varies with return period. The average intensity within a design storm can often be expressed as (Smith, 2000),

$$i = \frac{a_i}{(t_d + b_i)^{c_i}} \tag{5.8}$$

In Eqn. (5.8), $i$ is the average rainfall intensity within a design storm in mm/hr or in/hr; $t_d$ is the design storm duration in minutes; and $a_i$, $b_i$, and $c_i$ are constants dependent on the system of units used and the return period of the design storm. Some stormwater models use Eqn. (5.8) together with one Type 2 formula to estimate $t_c$, resulting in $t_c$ values to vary from design storm to design storm. Some other stormwater models even use the actual rainfall intensity or excess rainfall intensity at each modeling time step together with one Type 2 formula to estimate $t_c$, resulting in $t_c$ values to vary from modeling time step to time step.

Guo and Adams (1998b), in their original development of the analytical probabilistic approach, assumed and used a constant $t_c$ value for peak discharge estimation, in spite of the fact that the kinematic wave theory was used to estimate overland flow time. The constant overland flow time was obtained by using the kinematic wave formula together with a long-term average effective rainfall intensity characteristic of the location and the catchment. This was justified because it was believed that $t_c$ variations from storm to storm are small as compared to $t_c$ variations attributable to other causes (e.g., catchment length, slope, shape, and soil type, etc.). Comparison of the analytical probabilistic approach results with continuous simulation results did show that as long as a constant and representative $t_c$ value is used for a catchment, continuous simulation results are fairly close to those generated from the analytical probabilistic approach (Guo and Adams, 1998b).

In this study, the impact of $t_c$ on peak discharge rates estimated by APSWM was investigated further. Variable $t_c$ values were used experimentally for the first time in APSWM's development with the understanding that the initial development of APSWM actually assumed a constant $t_c$. The different $t_c$ values were obtained from corresponding design storm modeling runs of various return periods. The results were then compared to those where a constant $t_c$ value was used.

## 5.3 Comparison Study with an Actual Design Case

### 5.3.1 The Actual Design Case

The Cataraqui North Neighborhood (CNN), in the City of Kingston, Ontario, Canada was selected for the case study. In this study area, as a part of its stormwater management plan, three stormwater detention ponds B2E, B2W and B2S were planned to be constructed. In this study the total outflow discharging into pond B2E was analyzed by MIDUSS using the design storm approach for comparison with APSWM.

MIDUSS stands for Micro Interactive Design of Urban Stormwater System (MIDUSS) (Smith, 2000). It is a stormwater modeling software used for the detailed design of a range of devices for centralized or on site stormwater controls. It contains a versatile rainfall-runoff simulators and a number of built-in functions: five storm types; three infiltration models, and four overland flow methods. The design storm types included in MIDUSS are the Chicago hyetographs, the Huff quartile design storms, mass rainfall distribution curves, AES storms, and any other user defined storms. In the calculation of the runoff hydrograph for a particular catchment, the pervious and impervious areas are calculated separately and then added together. MIDUSS is chosen in this case study because it is widely used and accepted in Ontario, Canada for stormwater management planning and design.

Pond B2E of the case study area will provide treatment for runoff from a drainage area of 60.78 ha. Under the existing conditions, the area has 0% imperviousness. For ultimate conditions (i.e. fully developed with storm sewers in place) the drainage area is divided into 65 sub-areas or subcatchments. These 65 subcatchments are connected by pipes of various lengths and sizes. Fig. 5.1 shows the connections between the subcatchments and the pipes for the entire network up to the inlet at Pond B2E.

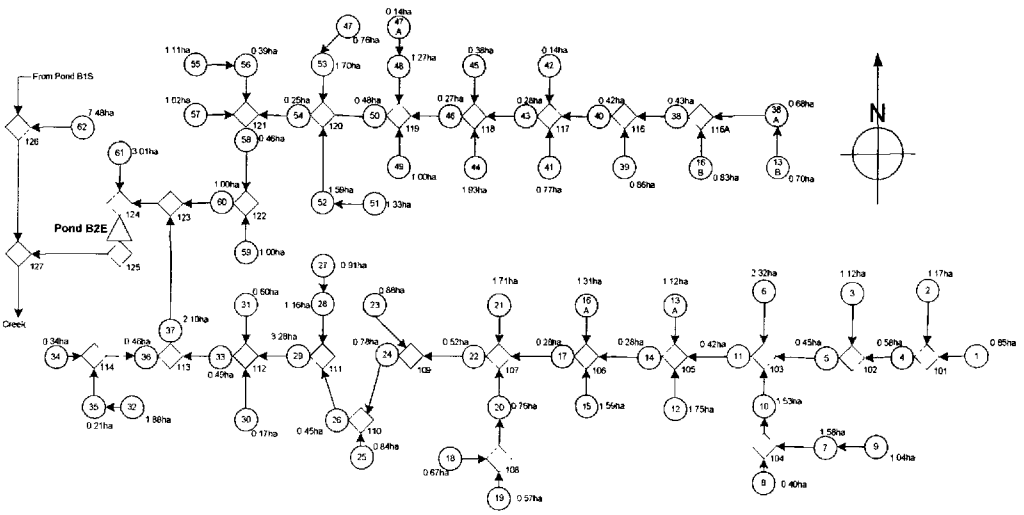


**Fig 5.1:** Subcatchment Configuration in the CNN Study Area (CNN Report I, 2001) (with permission)

The characteristics of the subcatchments and the sewer pipes underneath these subcatchments were obtained from Weslake Inc. (2002), the consultant of this design project. The average degree of imperviousness for the entire drainage area under fully developed conditions was estimated to be 31.5% using the area-weighting approach. This actual case with so many subcatchments was chosen so that the effect of the greatest extent of subcatchment aggregation may be examined. Both the design storm and the analytical approach have been applied for the fully developed conditions.

The soil information from CNN Report I (Weslake Inc., 2002) indicated that the subsurface of the undeveloped portion of the study area mainly consists of silt and clay, with clayey silt overlying inferred limestone bedrock. The top soil consists of very soft, molted, black organic clayey silt with a depth ranging from 0.6 to 1.0 m. The silt and clay depth varies from 1 to 2 m and includes a trace of sand immediately below the top soil layer. Based on the soil information, $f_c$ and $S_{hv}$ was estimated to be 3.6 mm/h and 13.2 mm respectively.

For the purposes of subcatchment aggregation, to determine a distinct overland flow length representative of a lumped catchment for the estimation of $t_c$, the area of the lumped catchment draining to the inlet of pond B2E was carefully considered. Fig. 5.1 indicates that the catchment area draining to the inlet of pond B2E consists of two main drainage networks, connecting at confluence 123. Beyond confluence 123, there is a pipe connection of 120 m, followed by an inlet to pond B2E. The contours and drainage networks indicate a symmetrical catchment. Therefore, the overland flow length ($L$) can be estimated as:

$$L = \frac{A}{2 \times W} \tag{5.9}$$

In Eqn. (5.9), $L$ is the overland flow length, $A$ is the catchment area, and $W$ is the channel length. $L$ is commonly defined as the average overland flow length from the edge of the

catchment to the design or outlet point (Smith, 2000). Based on that, $L$ was estimated to be 135 m.

### 5.3.2 Subcatchment Aggregation and Meteorological Data Analysis

For the selected actual case, a series of comparison studies were performed using APSWM and MIDUSS to quantify the discrepancies caused by subcatchment aggregation and difference in meteorological data analysis. The different features of each model setup used in these comparison studies together with their respective short-hand notations are described first:

**APSWM with Variable $t_c$:** As required, the study area was considered as a lumped catchment. Kinematic wave formula was used to estimate overland flow time for different input design storms used with MIDUSS runs. The average rainfall intensity for each design storm is obtained from Eqn. (5.8). In the lumping process, a single $t_c$ value for a specific $T_R$ value for the entire study area was determined by aggregating the $t_c$ values for all the subcatchments and travel times through the pipes connecting the subcatchments along the principal flow path. Thus five different $t_c$ values were obtained for five return periods (2, 5, 10, 50 and 100 years). Each of the five $t_c$ values were used as input to APSWM to estimate the peak discharge rate for the corresponding return period.

**MIDUSS with Discretized Catchment:** Peak discharge rates were estimated by using the design storm approach with the MIDUSS software. In this case, the whole study area is divided into 65 subcatchments interconnected by a series of pipes, as is typically done in actual stormwater management planning and design.

**MIDUSS with Lumped Catchment:** The 65 subcatchments of the study area are lumped together to form a single lumped catchment. The design storm approach is applied to this single lumped catchment for estimation of peak discharge rate for different return periods. Lumping was carried out according to the methodology outlined

previously ensuring that the lumped catchment is hydrologically equivalent to the discretized catchment.

Using the above-described model setups, both APSWM and MIDUSS were run for different return periods. The results are all plotted in Fig. 5.2. A series of comparisons were then performed using these modeling results. By using variable $t_c$ in the APSWM runs, $t_c$ is treated and estimated almost the same way in both approaches. To determine the effects of subcatchment aggregation and the difference in meteorological data analysis between the two approaches as well as their combined effect on the estimation of peak discharge rates, three comparisons were performed using the peak discharge results presented in Fig. 5.2. These comparisons and findings are presented as follows:

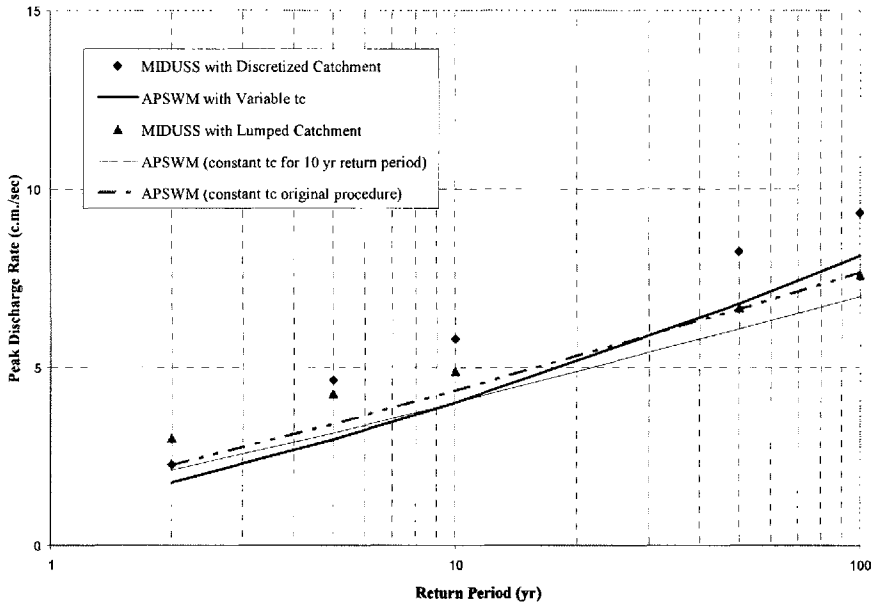


**Fig 5.2:** Peak Discharge Rates for Different Return Periods for Pond B2E

**First Comparison, MIDUSS with Discretized Catchment vs. APSWM with Variable $t_c$:** The two main differences, meteorological data analysis and subcatchment aggregation are both present in this set of comparison. From results presented in Fig. 5.2, it can be shown that the relative discrepancies for different return periods between the two

approaches range from 44% to 13%. Here, relative discrepancy is calculated as the ratio between the absolute difference and the average of the peak discharge values predicted by the two approaches for the same return period. Averaged throughout the return periods that are commonly of interest in stormwater management planning and design (i.e., 2-, 5-, 10-, 50-, 100-years), the average relative discrepancy is 27.7%. This 27.7% average relative discrepancy can be attributed to the combined effect of differences in meteorological data analysis and subcatchment aggregation. This comparison was done first because the two main differences are inevitable in the application of APSWM due to the fundamental differences between the two approaches.

**Second Comparison, MIDUSS with Discretized Catchment vs. MIDUSS with Lumped Catchment:** This comparison was conducted to examine the sole effect of subcatchment aggregation in applying the design storm approach. Following the same method of calculating relative discrepancies and average relative discrepancy, an average relative discrepancy was determined to be 19.2% between the two sets of MIDUSS runs. This 19.2% discrepancy results solely from the process of subcatchment aggregation in applying MIDUSS with the design storm approach.

The above finding generally agrees with results reported earlier by Zaghloul (1981). In Zaghloul's earlier study, the SWMM model was used to simulate runoff and peak flow resulting from actual storms from two urban catchments. For one of the catchment, the discretization levels ranged from 12 to 51 subcatchments, for the other catchment, the discretization levels ranged from 41 to 3 and 41 to 1 subcatchments. The relative discrepancies on the simulated peak flows between highly discretized catchment SWMM runs and highly aggregated catchment SWMM runs were found to be from 10% to 30%. The author concluded that the surface runoff hydrographs generated from both detailed subcatchments and aggregated equivalent catchment are similar. The second comparison in this study was conducted to partly confirm the earlier finding but using design storms instead of actual storms as input.

**Third Comparison, MIDUSS with Lumped Catchment vs. APSWM with Variable $t_c$:** In this comparison, both approaches model the same lumped catchment. The only difference is in meteorological data analysis. The average relative discrepancy across all return periods was found to be about 23.3%. This is rather surprising, because we initially expected a much larger discrepancy attributable to the difference in meteorological data analysis, given the fact that meteorological data analysis used in two approaches and the subsequent ways of representing rainfall input are totally different.

In addition to Fig. 5.2, the relative discrepancies for different return periods calculated from the above comparison studies were plotted in Fig. 5.3 against return periods. Examination of Fig. 5.3 suggests that there is no obvious correlation between relative discrepancy and return period. Thus, we can just use the average relative discrepancy to examine the effect of differences between the two approaches.

Judging from the second and third comparisons, it seems to suggest that discrepancies contributed by subcatchment aggregation in applying MIDUSS only are about the same (~20%) as those contributed by the difference in meteorological data analysis alone if APSWM and MIDUSS are both applied to model the same lumped catchment. However, results from the first comparison seem to suggest that the effects attributable to the differences in meteorological data analysis and subcatchment aggregation cancel each other out and resulting in an overall discrepancy lower than the sum of discrepancies caused by them individually, as long as the catchment $t_c$ is treated and estimated the same way in both approaches.

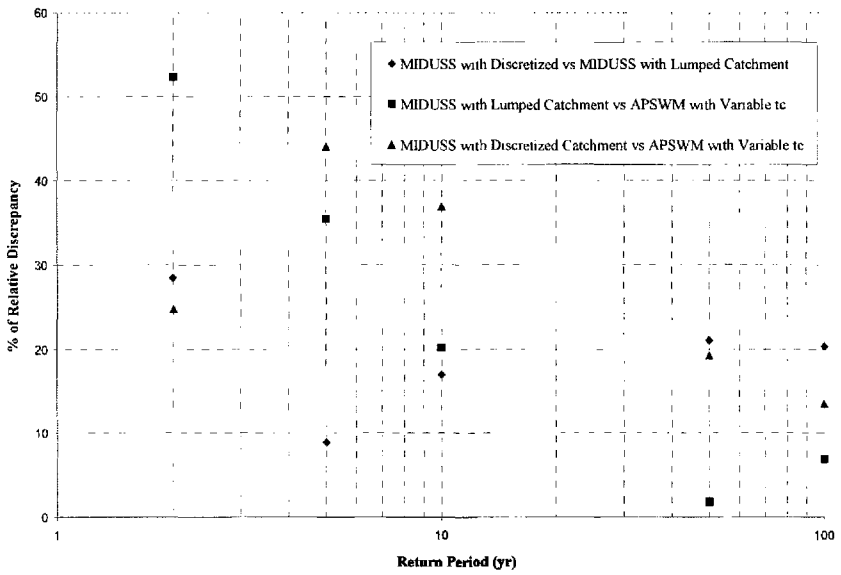


**Fig 5.3:** Relationship of the Percentage of Relative Discrepancy to $T_R$ Values

Overall, it can be seen that peak discharge results from the two approaches are generally comparable.

**The Use of Constant $t_c$ in APSWM**

Encouraged by the above findings, a better way of treating and estimating $t_c$ within APSWM is sought. Before this study, a constant $t_c$ was estimated for a catchment and used in APSWM. Although variable $t_c$ values may be used in the application of APSWM, one of the basic assumptions in the derivation of the analytical equations forming the basis of APSWM is that the catchment $t_c$ remains unchanged throughout time and throughout storms of different magnitudes. To be consistent with this basic assumption, in applying APSWM, it is preferable to use a constant $t_c$ value for each catchment.

In order to gain an appreciation of the discrepancies that might be caused by using one single constant $t_c$ in APSWM, two more comparisons were performed using the following two additional model setups:

**APSWM with Constant $t_c$ Obtained from MIDUSS Runs:** Instead of using five different $t_c$ values as in the **APSWM with Variable $t_c$** setup, the $t_c$ value corresponding to a return period of 10 years obtained from MIDUSS runs was used as input to APSWM for estimating peak discharge rates for any return periods of interest. For the actual case study, this constant $t_c$ was found to be 1.94 hours.

**APSWM with Constant $t_c$ Calculated Following Original Procedure:** The constant $t_c$ used in this APSWM setup was obtained following the original procedure proposed in Guo and Adams (1998b). In that procedure, pipe and open channel flow times are estimated following the same conventional way. For the estimation of overland flow time, kinematic wave equation is used together with a representative average effective rainfall intensity. This representative average effective rainfall intensity is calculated as the long-term average effective rainfall intensity considering the climate and the soils of the catchment. This long-term average effective rainfall intensity would normally be lower than the average intensities of design storms. As a result, the $t_c$ values estimated this way is more representative of catchment response under average storms and is longer than those estimated using the intensities of heavier design storms. A long-term average effective rainfall intensity of 4.25 mm/hr was determined for silty soils of the catchment according to this original procedure. By using this long-term average effective rainfall intensity and the kinematic wave equation for overland flow, a constant $t_c$ for the lumped catchment was determined to be 1.74 hours.

Using the above-described two more APSWM setups, additional APSWM runs were conducted. The resulting peak discharge rates are also plotted in Fig. 5.2. Using these additional results, two more comparisons were performed. These additional comparisons and findings are described as follows:

**Fourth Comparison, APSWM with Constant $t_c$ Obtained from MIDUSS Runs vs. APSWM with Variable $t_c$:** As expected and can be seen in Fig. 2, peak discharges for return periods lower than 10 years are higher and those for return periods higher than 10 years are now lower in comparison with the peak discharges estimated by variable $t_c$

values. The average relative discrepancy is about 9.8%. While comparing the peak discharge rates estimated by this run of APSWM with constant $t_c$ and those from the **MIDUSS with Discretized Catchment** runs, the average relative discrepancy is 28.3%, only slightly higher than the average of 27.7% between the **APSWM with Variable $t_c$** runs and the **MIDUSS with Discretized Catchment** runs. This seems to suggest that constant $t_c$ can be used in APSWM without causing significant discrepancy as compared to the design storm approach, as long as the constant $t_c$ used is representative of catchment response under heavy storm or design storm conditions.

**Fifth Comparison, APSWM with Constant $t_c$ Calculated following Original Procedure vs. MIDUSS with Discretized Catchment:** APSWM is nevertheless an independent peak discharge estimation approach by itself. APSWM's own constant $t_c$ estimation methodology needs to be tested and further improved. That is why at this point this last comparison was performed to gain an understanding on how large the discrepancy would be if APSWM and MIDUSS were both used in their intended ways for the actual design case. An average relative discrepancy was determined to be 20.2% from this last comparison. This 20.2% discrepancy is caused by all the differences between the analytical probabilistic and design storm approaches. The decrease in average relative discrepancy as compared to that of the first comparison is a direct result of the small increase in the catchment $t_c$ under heavier design storm conditions and average storm conditions (from 1.74 hours to about 1.94 hours).

It should be pointed out that the small decrease in $t_c$ values between the two additional APSWM setups described previously may be attributable to the fact that pipe flows constitute the majority of the flow time while overland flow time constitutes only a small portion of the total flow time over this test catchment. Thus, comparison results reported here can only be extrapolated to similar catchments where pipe flow or open channel flow predominates. Overall, Fig. 5.2 also show that for lower return periods, the methodology of determining $t_c$ does not have much influence on the estimated peak discharge rates. For higher return periods, however, variations in $t_c$ cause higher degrees of variation in peak discharge rates.

## 5.4 Summary and Conclusions

The design storm approach is so widely accepted now that it has almost become the industrial standard. The motivation of this study was to compare APSWM results directly with those from the design storm approach, and if possible, modify or improve APSWM so that it would generate results closer to those from the design storm approach. The three main differences between APSWM and the design storm approach are: (1) meteorological data analysis and subsequent representation of rainfall input for the transformation from rainfall to runoff; (2) APSWM's requirement of lumped catchments for its application versus the design storm approach's allowance of subcatchment divisions; and (3) APSWM's treatment of catchment $t_c$ as a constant across storms of various magnitudes versus some design storm approach's treatment of catchment $t_c$ as a quantity varying from storm to storm or even from modeling time-step to time-step.

Despite these differences, this case study demonstrates that peak discharges estimated by APSWM were generally in good agreement with those from the design storm approach. The average relative discrepancy between the two peak discharge estimation approaches was found to be about 25% for the different set of comparisons. Given the inaccuracies that are often inevitable in the estimation of $t_c$ (Hotchkiss and McCallum, 1995), this level of discrepancy is tolerable for engineering planning and design. This 25% level of overall discrepancy, the new and surprising finding that discrepancies caused by subcatchment aggregation and the difference in meteorological data analysis are of the same order of magnitude, together with those earlier findings reported in Guo (2001) seem to suggest that APSWM may be an alternative to the widely used design storm approach for peak discharge estimation.

This study also shows that a constant time of concentration may still be used in APSWM to better conform to the original assumption invoked in the derivation of equations forming the backbone of the analytical probabilistic approach. The reduction in discrepancy resulting from the use of variable time of concentration in APSWM is

insignificant. Instead, excess rainfall intensities more representative of heavy storm events can be used for $t_c$ estimation in APSWM so that APSWM may generate peak discharge estimates closer to those generated from the use of the design storm approach.

Nevertheless, comparison results presented in this paper only apply to the specific case and cannot be generalized. Before recommending APSWM for actual engineering use, more extensive tests and comparisons must be conducted. These additional tests and comparisons may be conducted on hypothetical or real catchments with a wide range of characteristics.

## References:


1. Adams, B.J., Fraser, H.G., Howard, C.D.D., Hanafy, M.S., 1986. "Meteorological Data Analysis for Drainage System Design", *Journal of Environmental Engineering*, Vol. 112, No.5: 827-847.
2. Adams, B.J., and Howard, C.D.D., 1986. "Design Storm Pathology", *Canadian Water Resources Journal*, Vol. 11, No.3: 49-55.
3. Eagleson, P.S., 1972. "Dynamics of Flood Frequency", *Water Resources Research*, Vol.8, No.4, pp: 878-897.
4. Guo, Y., 2001. "Hydrologic Design of Urban Flood Control Detention Pond", *Journal of Hydrologic Engineering*, Vol. 6, No. 6: 472-479.
5. Guo, Y. and Adams. B.J., 1999. "An Analytical Probabilistic Approach to Sizing Flood Control Detention Facilities", *Water Resources Research*, Vol. 35, No. 8. pp: 2457-2468.
6. Guo, Y. and Adams. B.J., 1998a. "Hydrologic Analysis of Urban Catchments with Event-based Probabilistic Models 1. Runoff Volume", *Water Resources Research*, Vol. 34, No. 12. pp: 3421-3431.
7. Guo, Y. and Adams. B.J., 1998b. "Hydrologic Analysis of Urban Catchments with Event-based Probabilistic Models 2. Peak Discharge Rate", *Water Resources Research,* Vol. 34, No. 12, pp: 3433-3443.
8. Hotchkiss, R.H. and McCallum, B.E., 1995. "Peak Discharge for Small Agricultural Watersheds", *Journal of Hydraulic Engineering*, Vol. 121, No.5: 36-48.

9. Loukas, A. and Quick, M.C., 1995. "24-H Design Storm for Coastal British Columbia", *Journal of Hydraulics Engineering*, Vol. 121, No. 12, pp: 889-899.
10. Marsalek, J. and Watt, W.E., 1984. "Design Storms for Urban Drainage Design", *Canadian Journal of Civil Engineering*, Vol. 11, No. 4, pp: 574-584.
11. McCuen, R.H., 1989. "Hydrologic Analysis and Design", Prentice-Hall Inc. Printed in the USA.
12. Singh, V.P., 1996. "Kinematic Wave Modeling in Water Resources: Surface-Water Hydrology", John Wiley & Sons, Inc. Printed in the USA.
13. Smith, A.A., 2000. "MIDUSS 98 User Manual and Help System Version 1.3", Published by Alan A. Smith Inc. Dundas, Ontario, Canada, L9H 3L4.
14. Watt, W.E., Chow, K.C.A., Hogg, W.D. and Lathem, K.W., 1986, "A 1-h Urban Design Storm for Canada", *Canadian Journal of Civil Engineering*, Vol. 13, pp: 293-300.
15. Weslake Inc., 2002. "Class Environmental Assessment for Master Drainage Plan for the Outlet B Tributary Area of the Cataraqui North Neighborhood City of Kingston", Abbreviated as *CNN Report I.* Available from Weslake Inc., 10-120 Lancing Drive, Hamilton, Ontario, Canada L8W 3A1.
16. Zaghloul, N. A., 1981. "SWMM Model and Level of Discretization", ASCE, *Journal of the Hydraulics Division*, Vol. 107, No. HY11, pp. 1535-1545.

# NOTATIONS

The following symbols are used in this paper:

A = area of a subcatchment

$a_i$, $b_i$, $c_i$ = constants dependent on the frequency of the storm in the Chicago method as used in Eqn. 8.

b = interevent time (hr)

$f_c$ = infiltration capacity of the soil (mm/hr)

$G_{V_R}(v_r)$ = probability of exceedence per rainfall event

h = degree of imperviousness of the catchment (expressed as a fraction or percentage)

i = intensity of rainfall (in/hr or mm/hr)

L = overland flow length

$L_n$ = length of pipe

M = subcatchment characteristic

m = number of subcatchments

n = the number of pipes

p = the maximum number of subcatchments

$Q_p$ = peak discharge rate (mm/hr)

q = the maximum number of pipes

$q_p$= peak discharge rate (mm/hr)

S = average slope of watershed

$S_d$ = area-weighted depression storage of the impervious and the initial losses of the pervious areas (mm)

$S_{dd}$ = difference between the initial losses in the pervious area and depression storage in the impervious area ($S_{il}$-$S_{di}$) (mm)

$S_{di}$ = depression storage in the impervious area (mm)

$S_{dp}$ = deprssion storage in the pervious area (mm)

$S_{il}$ = initial losses of the pervious area (mm)

$S_{iw}$ = initial soil wetting infiltration volume (mm)

$T_R$ = return period of the storm (yr)

t = duration of the storm (hr)

$t_c$ = time of concentration (hr)

$t_{ci}$ = time of concentration with a constant average intensity of rainfall (hr)

$t_d$ = storm duration (min)

$t_{pipe}$ = travel time through the pipe

$t_{scf}$ = travel time over the subcatchments

$V_n$ = velocity of pipe flow

v = volume of rainfall (mm)

$v_r$ = total runoff event volume (mm)

x = the total number of subcatchment

W = channel length

$\zeta$, $\lambda$, $\psi$ = fitting parameters of the probability distribution functions

$\theta$ = the average number of rainfall events per year

# Chapter 6

## Analytical Flow-Duration Relationships Derived from Watershed and Climate Characteristics

Yiping Guo and Asif Quader

**Abstract:** Using exponential probability density functions to describe the rainfall event characteristics of a locality and an event-based rainfall-runoff transformation function, closed-form analytical expressions were derived for the determination of the probability of exceedence of streamflow rates. This probability of exceedence as defined in this paper is equivalent to the percentage of time that a specific streamflow rate is exceeded. Therefore, flow-duration curves can be conveniently constructed using the derived analytical expressions. The main advantage of these analytical expressions is that they relate the flow-duration characteristics of a stream reach directly to its upstream watershed's and local rainfall characteristics. Comparison with flow-duration curves developed using continuous simulation results demonstrated that simplifying assumptions invoked in the derivation process are generally acceptable for small urban streams. With further testing and verification for more locations, the analytical expressions may be used in restoration studies for small streams with no or little streamflow data.

**Keywords:** Flow duration, probabilistic models, regional analysis, urban watershed, stream restoration, continuous simulation

## 6.1 Introduction

A flow duration curve (FDC) is a cumulative frequency curve which provides information about the percentage of time a specific discharge is equaled or exceeded in a given period (Searcy 1959). Along with hydrographs and mass curves, flow duration curves are capable of providing detailed information about the entire flow regime. The applications of FDCs range from hydropower development (Singh et al. 2001; Quimpo et al. 1983); low flow estimation for water resources management (Chalise et al. 2003; Smakhtin 2001; Zaidman et al. 2003); flow prediction at ungauged sites (Singh 1971; Fennessey and Vogel 1990; Yu et al. 2002; Yu and Yang 1996; Mimikou and Kaemaki 1985; Smakhtin 1999; Smakhtin and Masse 2000) and water quality management, including computation of total sediment yield (Male and Ogawa 1984; Cordova and Gonzalez 1997). FDCs have also been used to determine ecologically acceptable flow regime to support trout population in groundwater-dominated (Petts et al. 1999) and local (Strevens 1999) streams throughout the United Kingdom. Vogel and Fennessey (1995) provide a detailed description of the various uses of FDCs in the different fields of water resources engineering.

In addition to the conventional method of constructing FDCs with measured flow values, Cigizoglu and Bayazit (2000) also utilized the convolution theorem for obtaining FDC, considering both the stochastic and periodic components of streamflows. Application of this approach to small scale design problems is rather limited. Yu et al. (2002) identified homogeneous regions for FDC development based on discrimination and cluster analysis. Regional low flow models were then established for each homogeneous region using multivariate and fuzzy regression analysis. Furthermore, regional FDCs may be developed to transfer the entire flow duration curve information at gauged sites to ungauged sites by extrapolation or interpolation; provided that the ungauged site is located at a hydrologically homogeneous region. Quimpo et al. (1983) used exponential and power form models; while Mimikou and Kaemaki (1985) used polynomial models to analytically represent FDCs. In all these models, the parameters were related to the morphological characteristics of the upstream catchment. The

principle objective for the development and use of these regional FDC models is to characterize the flow pattern and magnitude at ungauged sites. Although some characteristics of the upstream catchment are utilized in the estimation of the parameter values, the previous regional FDC models do not explicitly consider the rainfall-runoff transformation and routing occurring on the upstream catchment. The local climatic characteristics are not directly incorporated into the models either.

Proper restoration of degraded stream channels requires accurate FDCs. However, scarcity of flow data is a serious problem that hinders many stream restoration projects in urban watersheds. With drainage areas $\leq 100\,km^2$ (Scholz and Booth 2001; Ness and Joy 2002) and impervious covers $\geq 15\%$ (Brown 2000), measured streamflow data are usually not available. For ungauged channels draining these small urban catchments, FDCs may be developed using regionalized FDC models. In the application of regression analysis for the purpose of regionalization, traditionally, the drainage area of the catchment, basin relief, length of the main river course, and a factor indirectly related to the climatic regime are considered as independent variables. In the resulting regional FDC model, either one or more of these factors are included. However, with increasing urbanization and changes in land use patterns, factors such as drainage area, basin relief and channel length alone are insufficient to characterize an urban catchment. Other characteristics, e.g., degree of imperviousness and infiltration characteristics of the soils need also to be included in the analysis. The increased number of independent variables (or parameters in the resulting FDC model) makes the regionalization approach infeasible for small urban catchments. The other remaining option for the development of FDCs for ungauged small urban catchments is to generate streamflows with continuous simulation using a hydrologic model of the catchment. Although the resulting FDCs can be accurate and include the effect of many of the catchment characteristics, the computational tasks involved are prohibitive for routine engineering design applications.

In this paper, an analytical flow-duration relationship is derived that takes into consideration both the detailed catchment characteristics and local climate conditions. For the description of local climate conditions, a continuous rainfall record is divided into

individual rainfall events based on a minimum time period without precipitation, known as the interevent time definition (IETD). These individual rainfall events possess both external (volume, duration, interevent time) and internal characteristics. Histograms obtained from the frequency analysis of the external characteristics of rainfall events are found to be best fitted by exponential probability density functions (pdfs) (Adams and Papa 2000). The probability distribution functions of rainfall event characteristics are therefore used to represent local climate conditions. Using rainfall events as the stochastic input to an urban catchment, the flow-duration relationship for that catchment is derived according to the derived probability distribution theory (Benjamin and Cornell 1972). Similar derived probability distribution approaches have been used in previous studies, e.g., Guo and Adams (1998a and b); Guo and Adams (1999a and b); Chen and Adams (2005); Behera et al. (2006) for different urban stormwater management problems. However, our recent literature review indicates that this probabilistic approach has not been used for the development of analytical flow-duration relationships. The objective of this study is to use the derived probability distribution theory to develop an analytical flow-duration relationship for small urban catchments that may be used later in stream restoration studies.

## 6.2 Derivation of flow-duration Relationships

### 6.2.1 Probabilistic Models of Rainfall Event Characteristics

Rainfall data analysis is the first step in our probabilistic approach. Continuous point rainfall records are divided into discrete rainfall events based on a pre-selected IETD. IETDs from 6 to 12 hours and usually longer than the catchment's time of concentration are considered appropriate. Individual rainfall events and the dry periods that immediately follow each rainfall event are characterized by their rainfall volume (v), rainfall duration (t), and interevent time (b). These individual external characteristics can be subjected to frequency analysis. Among the theoretical probability density functions (pdfs) fitted to the histograms during frequency analyses, the exponential pdfs were

found to fit satisfactorily (Howard 1976; Eagleson 1972; Adams et al. 1986). These exponential pdfs of rainfall event characteristics can be expressed as follows:

$$f_V(v) = \zeta \exp(-\zeta v)$$

$$f_T(t) = \lambda \exp(-\lambda t)$$

$$f_B(b) = \psi \exp(-b\psi)$$

Where $\zeta$, $\lambda$, and $\psi$ are the distribution parameters, their values may be estimated as equal to the inverse of the average rainfall volume, duration, and interevent time, respectively. The three random variables may be treated as mutually independent (Adams and Papa 2000; Guo and Adams 1998a). For different locations, values of the distribution parameters may be different. The resulting three pdfs partly characterize some of the climate conditions of a location.

### 6.2.2 Rainfall-Streamflow relationships

The rainfall-runoff transformation proposed by Guo and Adams (1998a) as shown in Eqn. (6.1) is also used in this study.

$$v_r = \begin{cases} 0 & , \quad v \le S_{di} \\ h(v - S_{di}) & , \quad S_{di} < v \le S_{il} + f_c t \\ v - S_d - f_c(1-h)t & , \quad v > S_{il} + f_c t \end{cases} \tag{6.1}$$

For each rainfall event, Eqn. (6.1) relates the volume of runoff $v_r$ to catchment characteristics including the degree of imperviousness h, depression storages for the pervious $(S_{dp})$ and impervious areas ($S_{di}$), and the ultimate infiltration capacity of the soil $f_c$. In Eqn. (6.1), $S_{il}$ is the initial loss in pervious areas, i.e., $S_{il} = S_{dp} + S_{iw}$, where $S_{iw}$ is the initial soil wetting infiltration volume, and $S_d = hS_{di} + (1-h)S_{il}$. Derivation details are provided in Guo and Adams (1998a).

The runoff hydrographs resulting from individual rainfall events can be approximated by a rectangle with durations of $t + t_c$, where t is the causal rainfall event duration and $t_c$ is the catchment time of concentration. Fig. 6.1 shows schematically this

approximation. Thus, the flow rate (Q) during the time interval of $(t + t_c)$ resulting from a rainfall event with duration t and volume v can be expressed as,

$$Q = \begin{cases} q_b & , \quad v \le S_{di} \\ q_b + \dfrac{h(v - S_{di})}{t + t_c} & , \quad S_{di} < v \le S_{il} + f_c t \\ q_b + \dfrac{[v - S_d - f_c(1-h)t]}{t + t_c} & , \quad v > S_{il} + f_c t \end{cases} \tag{6.2}$$

In Eqn. (6.2), $q_b$ is the constant baseflow rate. A runoff event will occur when $v > S_{di}$, and $v > S_{di}$ can lead to two different types of conditions, i.e., runoff generated only from impervious area and from both pervious and impervious areas. Following the runoff event, the dry period lasts for a period of $(b - t_c)$. The average length of a runoff event/interevent dry period cycle (simply referred to as a runoff event/interevent cycle or a cycle hereafter) can be found as follows,

$$E(t + b) = \int_0^\infty \int_0^\infty \lambda\psi \exp(-\lambda t - \psi b) = \frac{1}{\lambda} + \frac{1}{\psi}$$

where $E(t + b)$ denotes the expectation operation.

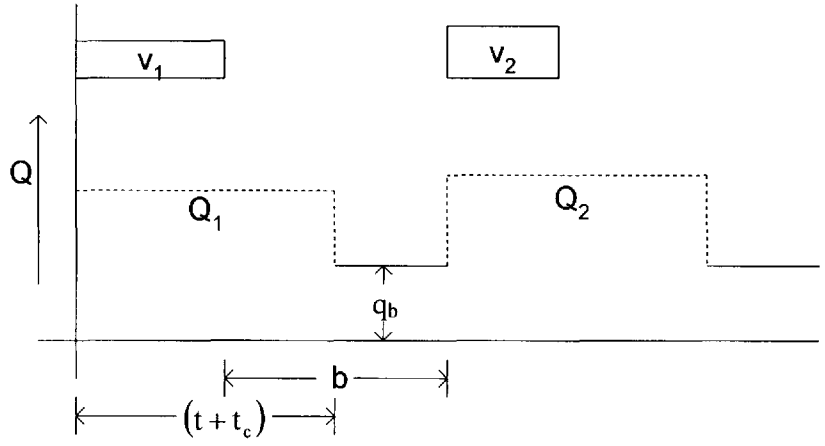


**Fig 6.1:** Constant baseflow ($q_b$) between two runoff events generated by two consecutive rainfall events

The key of our probabilistic approach is that the instantaneous flow rate Q is treated as a random variable with its own distribution. Eqn. (6.2) establishes the functional relationship between Q and independent random variables v and t as well as catchment characteristics. Let $P_e[Q > q]$ be the probability that Q exceeds a specific value q per runoff event/interevent cycle, based on Eqn. (6.2), it can be seen that the probability $P_e[Q > q]$, given $q > q_b$, is the sum of two components. Firstly, $P_{e_1}[Q > q]$, under the condition that $S_{di} < v \le S_{il} + f_c t$, and secondly, $P_{e_2}[Q > q]$, under the condition that $v > S_{il} + f_c t$. These two components are mutually exclusive. In Eqn. (6.2), q is in the units of mm/hr, i.e., mm of water over the catchment area per hour. Based on Eqn. (6.2), the probability distributions of v and t, and the derived probability distribution theory, $P_{e_1}[Q > q]$ and $P_{e_2}[Q > q]$ may be analytically determined.

### 6.2.3 Determination of Integration Regions and Basis of Derivation

According to the derived probability distribution theory, the values of $P_{e_1}$ and $P_{e_2}$ can be determined by integrating the joint pdf of v and t over appropriate regions. These regions of integration can be determined from the inequalities in the v-t plane that are used to define $P_{e_1}$ and $P_{e_2}$. Region 1 for determining $P_{e_1}[Q > q]$ is,

$$\begin{cases} q_b + \dfrac{h(v - S_{di})}{t + t_c} > q \\ S_{di} < v \le S_{il} + f_c t \end{cases}, \text{ or, } \begin{cases} v > \dfrac{q_{abf}}{h} t + \dfrac{q_{abf} t_c}{h} + S_{di} \\ S_{di} < v \le f_c t + S_{il} \end{cases}$$

where $q_{abf} = q - q_b$. Similarly, region 2 for determining $P_{e_2}[Q > q]$ is,

$$\begin{cases} q_b + \dfrac{[v - S_d - f_c(1-h)t]}{t + t_c} > q \\ v > S_{il} + f_c t \end{cases}, \text{ or, } \begin{cases} v > [q_{abf} + f_c(1-h)]t + q_{abf} t_c + S_d \\ v > f_c t + S_{il} \end{cases}$$

This shows that the region of integration in the v-t plane are governed by three straight lines:

$$\text{Line 1:} \quad v = f_c t + S_{il}$$
$$\text{Line 2:} \quad v = \frac{q_{abf}}{h} t + \frac{q_{abf} t_c}{h} + S_{di}$$
$$\text{Line 3:} \quad v = [q_{abf} + f_c(1-h)]t + q_{abf} t_c + S_d$$

The location and orientation of the three lines are controlled by their slopes and intercepts. Region 1 for determining $P_{e_1}$ is located above line 2 but below line 1, whereas region 2 for determining $P_{e_2}$ is located above both lines 1 and 3.

The slopes and intercepts of the three lines are dependent on $f_c$, $S_{il}$, $q_{abf}$, h, $t_c$ and $S_d$, indicating that changes in the flow magnitude $q_{abf}$ or catchment characteristics can cause the regions of integration to change, resulting in changes in the values of $P_{e_1}$ and $P_{e_2}$. The relationship of the slopes of the three lines is dependent on the relationship between $q_{abf}$ and $f_c h$. If $q_{abf} < f_c h$, the slopes of both lines 2 and 3 are less than that of line 1. Whereas $q_{abf} \geq f_c h$ results in the slope of line 2 to be greater than those of lines 3 and 1. The difference in slopes between lines 2 and 3 is,

$$\frac{q_{abf}}{h} - q_{abf} - f_c(1-h) = (1-h)\left(\frac{q_{abf}}{h} - f_c\right)$$

If $q_{abf} < f_c h$, this difference becomes negative, causing the slope of line 3 to be greater than that of line 2. Therefore when $q_{abf} < f_c h$, the relationship between slopes is line 1>line 3>line 2. Similarly when $q_{abf} \geq f_c h$, the difference between the slopes of line 1 and 3 is, $f_c - q_{abf} - f_c(1-h) = f_c h - q_{abf}$, which becomes negative, causing the slope of line 3 to be greater than line 1. Therefore, the relative magnitudes of the slopes are: line 2>line 3>line 1.

Similar to the slopes, the relative magnitude of the intercepts of the three lines can be determined in the same manner. The difference between the intercepts of line 1 and 2 is $S_{il} - \frac{q_{abf} t_c}{h} - S_{di} = S_{dd} - \frac{q_{abf} t_c}{h}$, where $S_{dd} = (S_{il} - S_{di})$. This indicates that the relative magnitude for the intercepts of the three lines depends on the relationship between $q_{abf}$

and $\frac{hS_{dd}}{t_c}$. The relative magnitude of the intercepts are dependent on whether $q_{abf} < \frac{hS_{dd}}{t_c}$ or $q_{abf} \geq \frac{hS_{dd}}{t_c}$. When $q_{abf} < \frac{hS_{dd}}{t_c}$, the intercept of line 1 is greater than line 2. Whereas the opposite is true when $q_{abf} \geq \frac{hS_{dd}}{t_c}$. The difference between the intercepts of line 1 and 3 is $S_{il} - q_{abf}t_c - S_d = hS_{dd} - q_{abf}t_c$. Therefore, $q_{abf} < \frac{hS_{dd}}{t_c}$ causes the intercept of line 1 to be greater than line 3 and $q_{abf} \geq \frac{hS_{dd}}{t_c}$ causes the opposite to become true.

The difference between the intercepts of lines 3 and 2 is $q_{abf}t_c + S_d - \frac{q_{abf}t_c}{h} - S_{di} = (1-h)S_{dd} - \frac{q_{abf}t_c}{h}(1-h)$. Therefore, if $q_{abf} \geq \frac{hS_{dd}}{t_c}$, the intercept of line 2 will be greater than line 3. Whereas the opposite will be true for $q_{abf} < \frac{hS_{dd}}{t_c}$. As a result, for the three lines, $q_{abf} < \frac{hS_{dd}}{t_c}$ causes the intercept of line 1>line 3>line 2. On the other hand, for the three lines $q_{abf} \geq \frac{hS_{dd}}{t_c}$ causes the intercept of line 2>line 3>line 1.

In summary, the magnitude of the slopes and the intercepts are controlled by the relationship of $q_{abf}$ to $f_ch$ and $\frac{hS_{dd}}{t_c}$, respectively. Therefore, the relationship between $f_c$ and $\frac{S_{dd}}{t_c}$ may cause two different conditions to arise. When $f_c < \frac{S_{dd}}{t_c}$, the three possible ranges of $q_{abf}$ that exist include: $q_{abf} < f_ch$, $f_ch \leq q_{abf} < \frac{hS_{dd}}{t_c}$, and $q_{abf} \geq \frac{hS_{dd}}{t_c}$. On the other hand, $f_c \geq \frac{S_{dd}}{t_c}$ results in three possible ranges of $q_{abf}$, namely, $q_{abf} < \frac{hS_{dd}}{t_c}$,

$\frac{hS_{dd}}{t_c} \le q_{abf} < f_c h$, and $q_{abf} \ge f_c h$. $f_c$, $S_{dd}$ and $t_c$ are three characteristics of an urban catchment. For the following analysis, catchments where $f_c < S_{dd}/t_c$ are defined as type I urban catchments; catchments with an $f_c$ value higher than $S_{dd}/t_c$ are referred to as type II urban catchments. For each of these two types of urban catchments and the possible ranges of $q_{abf}$ values, the relative magnitudes of the slopes and intercepts of the three lines are tabulated in Table 6.1. These relative magnitudes help define the appropriate regions of integration for the determination of $P_{e_1}$ and $P_{e_2}$, they will be used in the following derivations.

**Table 6.1:** Relative magnitudes of slopes and intercepts for the two types of urban catchments

| Catchment type | Range of $q_{abf}$ | Relative magnitude of slopes and intercepts[1] |
|---|---|---|
| Type I urban catchment: $f_c < \frac{S_{dd}}{t_c}$ | $q_{abf} < f_c h$ | S1>S3>S2<br>I1>I3>I2 |
| | $f_c h \le q_{abf} < \frac{hS_{dd}}{t_c}$ | S2>S3>S1<br>I1>I3>I2 |
| | $q_{abf} \ge \frac{hS_{dd}}{t_c}$ | S2>S3>S1<br>I2>I3>I1 |
| Type II urban catchment: $f_c \ge \frac{S_{dd}}{t_c}$ | $q_{abf} < \frac{hS_{dd}}{t_c}$ | S1>S3>S2<br>I1>I3>I2 |
| | $\frac{hS_{dd}}{t_c} \le q_{abf} < f_c h$ | S1>S3>S2<br>I2>I3>I1 |
| | $q_{abf} \ge f_c h$ | S2>S3>S1<br>I2>I3>I1 |

[1]S1, S2, and S3 represent the slope of line 1, line 2 and line 3, respectively;
I1, I2, and I3 represent the intercept of line 1, line 2 and line 3, respectively.

Let $\theta$ be the average total number of runoff event/interevent cycles of the period of interest (e.g., non-winter period) within each calendar or hydrologic year, $\theta\left(\frac{1}{\lambda}+\frac{1}{\psi}\right)$ is then the average length of that period per year. As defined earlier, $P_e[Q > q]$ is the

probability that Q exceeds a specific flow q per runoff event/interevent cycle. Since the duration of the runoff event within the cycle is $(t + t_c)$, the expected value of the duration when $Q > q$ per runoff event/interevent cycle can be determined from

$$D[Q > q] = \iint_R (t + t_c)\lambda\zeta \exp(-\lambda t - \zeta v)dvdt$$

where $D[Q > q]$ represents the expected value of the duration when $Q > q$ per runoff event/interevent cycle; R denotes the appropriate region of integration for random variables v and t such that $Q > q$; and $\lambda\zeta \exp(-\lambda t - \zeta v)$ is the joint pdf of v and t. The result that $Q > q$ is ensured by using the appropriate integration limits that form the regions of integration. As illustrated previously, these limits of integration are determined from the functional relationship expressed in Eqn. (6.2) and used to define $P_{e_1}$ and $P_{e_2}$. As the average total number of cycles per year is θ, the total duration per year when $Q > q$ is $\theta \cdot D[Q > q]$. Let $P[Q > q]$ be the probability that the instantaneous flow rate Q exceeds a specific value q during the period of interest per year, this probability can be determined as $\theta \cdot D[Q > q]$ divided by the average length of the period of interest per year, i.e.

$$P[Q > q] = \frac{\theta \cdot \iint_R (t + t_c)\lambda\zeta \exp(-\lambda t - \zeta v)dvdt}{\theta\left(\frac{1}{\lambda} + \frac{1}{\zeta}\right)} = \frac{1}{\left(\frac{1}{\lambda} + \frac{1}{\zeta}\right)} \iint_R (t + t_c)\lambda\zeta \exp(-\lambda t - \zeta v)dvdt \tag{6.3}$$

The above expression forms the basis in deriving $P[Q > q]$ for both types of urban catchments. In the context of flow-duration relationships or FDCs, $P[Q > q]$ can also be interpreted as the fraction (or percentage) of time a particular flow q is exceeded.

### 6.2.4 Flow-Duration Relationship for Type I Urban Catchments

In the case of type I urban catchments, $f_c < S_{dd} / t_c$ results in three possible ranges of $q_{abf}$ values as shown in Table 1. When $q_{abf} < f_c h$, the relationship between the slopes and the intercepts of the three lines in the v-t plane are: the slope of line 1>line 3> line 2

and the intercepts of line 1> line 3> line 2, respectively. Based on these relationships, the three lines are shown in Fig. 6.2. $P_e[Q > q]$ can be evaluated as the summation of integration of the joint pdf of v and t over two regions, i.e., region 1 for the determination of $P_{e_1}$ and region 2 for the determination of $P_{e_2}$. The same regions of integration (represented previously by R) are then used to determine $P[Q > q]$ in accordance with Eqn. (6.3).

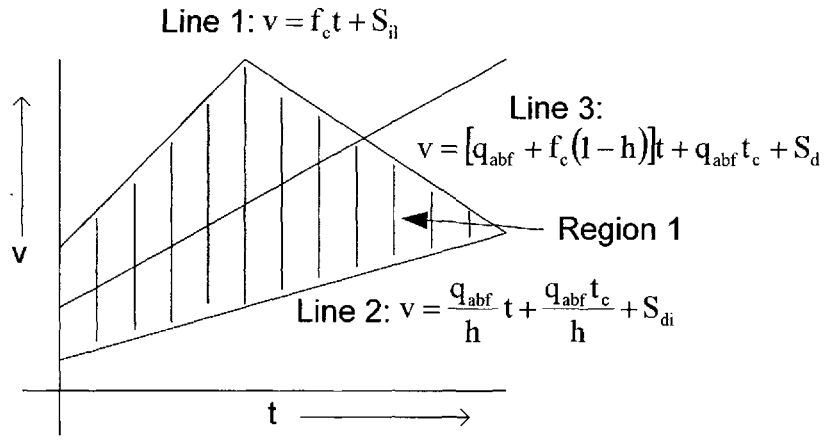


**Fig 6.2:** Region of integration for $P[Q > q]$ in type I urban catchments for $q_{abf} < f_c h$

As shown by the dashed lines in Fig. 6.2, region 1 lies above line 2 but below line 1; region 2 lies above both lines 1 and 3. Therefore, the limits of integration for v ranges from $\frac{q_{abf} t}{h} + \frac{q_{abf} t_c}{h} + S_{di}$ to $\infty$. The limits of integration for t ranges from 0 to $\infty$. $P[Q > q]$ when $q_{abf} \le f_c h$ can therefore be derived as,

$$P[Q > q] = \frac{1}{(1/\lambda + 1/\psi)} \int_0^{\infty} \int_{\frac{q_{abf}}{h} t + \frac{q_{abf} t_c}{h} + S_{di}}^{\infty} (t + t_c)\lambda\zeta \exp(-\lambda t - \zeta v) dv dt$$

$$= \frac{\lambda^2 \psi}{(\lambda + \psi)} \exp\left[-\zeta\left(\frac{q_{abf} t_c}{h} + S_{di}\right)\right]\left[\frac{1}{\left(\lambda + \frac{\zeta q_{abf}}{h}\right)^2} + \frac{t_c}{\left(\lambda + \frac{\zeta q_{abf}}{h}\right)}\right]$$

To simplify the expression of the above and following integration results, let

$$A_1 = \lambda + \frac{\zeta q_{abf}}{h}$$

$$A_2 = \lambda + \zeta\{q_{abf} + f_c(1-h)\}$$

$$A_3 = t_* = \frac{q_{abf}t_c - hS_{dd}}{f_c h - q_{abf}}$$

$$A_4 = \frac{q_{abf}t_c}{h} + S_{di}$$

$$A_5 = \frac{\lambda^2\psi}{(\lambda+\psi)}$$

$$A_6 = q_{abf}t_c + S_d$$

The above integration results can be written as

$$P[Q > q] = A_5 \exp(-\zeta A_4)\left[\frac{1}{A_1^2} + \frac{t_c}{A_1}\right] \tag{6.4}$$

When $f_c h \le q_{abf} < \frac{hS_{dd}}{t_c}$, the relative magnitude of the slopes and the intercepts of the three lines are: the slopes of line 2>line 3>line 1 and the intercepts of line 1>line 3>line 2. The location and orientation of the three lines are shown in Fig. 6.3. It can be demonstrated that the three lines in Fig. 6.3 intersect at one common point. The coordinate of the point of intersection of the three lines is denoted as $(v_*, t_*)$. The value of $t_*$ can be determined as,

$$t_* = \frac{q_{abf}t_c - hS_{dd}}{hf_c - q_{abf}}$$

In order to determine the probability of exceedence, the regions of integration (regions 1 and 2) in the v-t plane need to be identified.

From Fig. 6.3 it can be seen that region 1 is located below line 1 but above line 2. Fig. 6.3 also indicates that up to the coordinate $(v_*, t_*)$, region 1 exists and is shown by the shaded area. But beyond the point of intersection of the three lines, region 1 is non-existent. On the other hand, region 2 is located above lines 1 and 3. Therefore, if regions 1 and 2 are combined together, up to the point $(v_*, t_*)$, the limits of integration for v is from $\frac{q_{abf}t}{h} + \frac{q_{abf}t_c}{h} + S_{di}$ to $\infty$ and those for t is from 0 to $t_*$. Beyond the point of

intersection, the independent variables v and t ranges from $t[q_{abf} + f_c(1-h)] + q_{abf}t_c + S_d$ to $\infty$ and from $t_*$ to $\infty$, respectively.

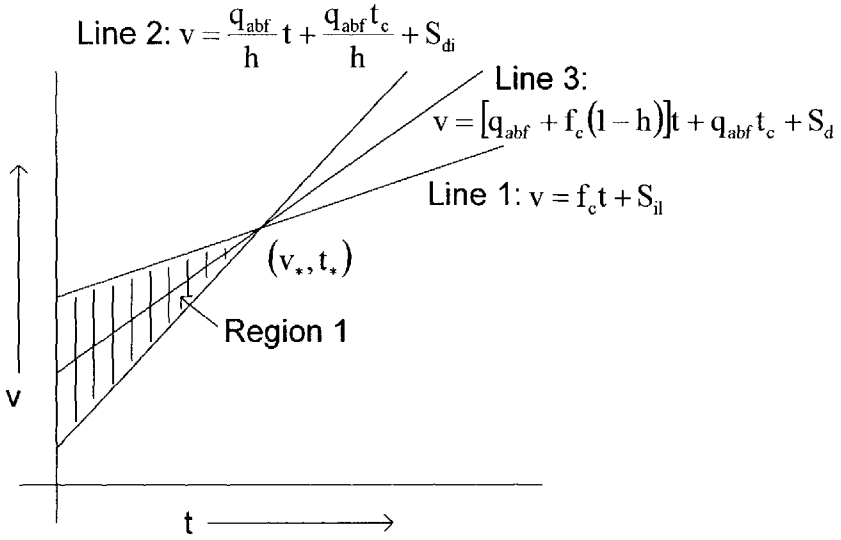


**Fig 6.3:** Region of integration for $P[Q > q]$ in type I urban catchments for

$$f_c h \le q_{abf} < \frac{hS_{dd}}{t_c}$$

Thus $P[Q > q]$ for $f_c h \le q_{abf} < \frac{hS_{dd}}{t_c}$ can be determined by using these limits.

$$\begin{aligned} P[Q>q] &= \frac{1}{\left(\frac{1}{\lambda}+\frac{1}{\psi}\right)}\left[\int_0^{t_*}\int_{\frac{q_{abf}}{h}t+\frac{q_{abf}t_c}{h}+S_{di}}^{\infty}(t+t_c)\lambda\zeta\exp(-\lambda t-\zeta v)dvdt\right. \\ &+ \left.\int_{t_*}^{\infty}\int_{[q_{abf}+f_c(1-h)]t+q_{abf}t_c+S_d}^{\infty}(t+t_c)\lambda\zeta\exp(-\lambda t-\zeta v)dvdt\right] \\ &= A_5 e^{-\zeta A_4}\left[\frac{1}{A_1^2}\left\{1-e^{-A_1A_3}(1+A_1A_3)\right\}+\frac{t_c}{A_1}\left\{1-e^{-A_1A_3}\right\}\right]+\frac{A_5 e^{-(\zeta A_6+A_2A_3)}}{A_2}\left[\frac{(1+A_2A_3)}{A_2}+t_c\right] \end{aligned} \tag{6.5}$$

Finally, for the range of $q_{abf} \ge \frac{hS_{dd}}{t_c}$, both the slopes and the intercepts of line 2>line 3>line 1, as shown in Table 6.1. Based on the magnitudes of the slopes and the intercepts, the positions of the three lines are shown in Fig. 6.4.

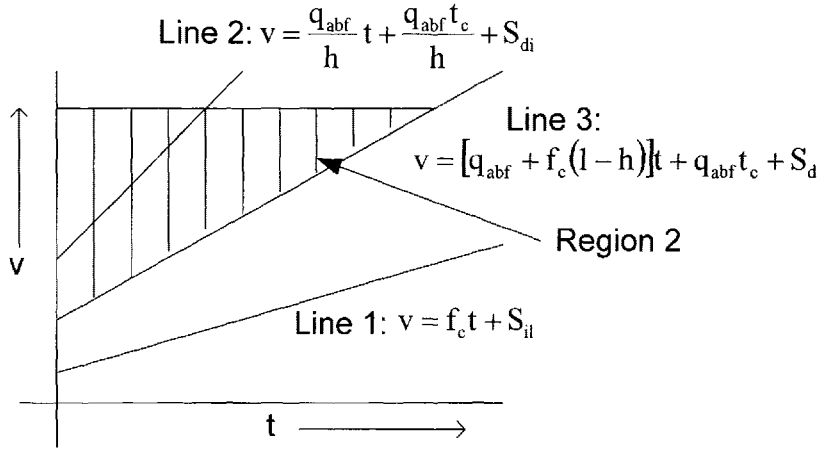


**Fig 6.4:** Region of integration for $P[Q > q]$ in type I urban catchments for $q_{abf} \geq \frac{hS_{dd}}{t_c}$

From Fig. 6.4 it can be seen that the area of integration for region 1 does not exist. However, region 2 lays above both lines 1 and 3. This indicates that in the integration, the lower limit for v should be set at $t[q_{abf} + f_c(1-h)] + q_{abf} t_c + S_d$, as it fulfills both conditions for region 2. Using these appropriate limits, $P[Q > q]$ can be derived as

$$\begin{aligned} P[Q > q] &= \frac{1}{\left(\frac{1}{\lambda} + \frac{1}{\psi}\right)} \int_0^{\infty} \int_{(q_{abf} + f_c - f_c h)t + q_{abf} t_c + S_d}^{\infty} (t + t_c)\lambda\zeta \exp(-\lambda t - \zeta v) dv dt \\ &= A_5 \exp(-\zeta A_6)\left[\frac{1}{A_2^2} + \frac{t_c}{A_2}\right] \end{aligned} \tag{6.6}$$

Using Eqn.s (6.4), (6.5) and (6.6), $P[Q > q]$ can be determined for a type I urban catchment.

## 2.5 Flow-Duration Relationship for Type II Urban Catchments

In the case of type II urban catchments where $f_c \geq \frac{S_{dd}}{t_c}$, there exists three ranges of $q_{abf}$ values, namely, $q_{abf} < \frac{hS_{dd}}{t_c}$, $\frac{hS_{dd}}{t_c} \leq q_{abf} < f_c h$, and $q_{abf} \geq f_c h$. For the first range, the relationship between the slopes and the intercepts of the three lines are the same as those

for the first range of $q_{abf}$ for type I urban catchments. As a result, the region of integration in the v-t plane is also the same. Therefore, the expression of $P[Q > q]$ for the first range (i.e., when $q_{abf} < \frac{hS_{dd}}{t_c}$) is the same as Eqn. (6.4).

In the second range, i.e., $\frac{hS_{dd}}{t_c} \le q_{abf} < f_c h$, the relative magnitude of the slopes and the intercepts causes the slopes of line 1>line 3>line 2 and the intercepts of line 2>line 3>line 1. The resulting positions of the three lines are shown in Fig. 6.5. Again $P[Q > q]$ can be evaluated as the summation of integration over two regions, i.e., region 1 for the determination of $P_{e_1}$ and region 2 for the determination of $P_{e_2}$. As shown in Fig. 6.5, the three lines also intersect at one common point. The coordinate of the point of intersection of the three lines is also denoted as $(v_*, t_*)$. Fig. 6.5 indicates that up to the point $(v_*, t_*)$, region 1, where $v < S_{il} + f_c t$ and $v > \frac{q_{abf} t}{h} + \frac{q_{abf} t_c}{h} + S_{di}$, does not exist. However, beyond $(v_*, t_*)$, region 1 is shown by a shaded area in Fig. 6.5. On the other hand, region 2 is above both lines 1 and 3. Therefore, by combining these two regions, up to the point $(v_*, t_*)$, the limits of integration for v should be from $t[q_{abf} + f_c(1-h)] + q_{abf} t_c + S_d$ to $\infty$, which ensures that the region of integration is above both lines 1 and 3. Up to the point $(v_*, t_*)$, the limits of integration of t should be from 0 to $t_*$. Beyond the point of intersection v should be integrated from $\frac{q_{abf} t}{h} + \frac{q_{abf} t_c}{h} + S_{di}$ to $\infty$ and t should be integrated from $t_*$ to $\infty$. Using these limits of integration, $P[Q > q]$ can be derived as:

$$P[Q>q] = \frac{1}{\left(\frac{1}{\lambda}+\frac{1}{\psi}\right)}\left[\int_0^{t_*}\int_{[q_{abf}+f_c(1-h)]t+q_{abf}t_c+S_d}^{\infty}(t+t_c)\lambda\zeta\exp(-\lambda t-\zeta v)dvdt + \int_{t_*}^{\infty}\int_{\frac{q_{abf}}{h}t+\frac{q_{abf}t_c}{h}+S_{dh}}^{\infty}(t+t_c)\lambda\zeta\exp(-\lambda t-\zeta v)dvdt\right]$$

$$= A_5 e^{-\zeta A_6}\left[\frac{1}{A_2^2}\left\{1-e^{-A_2A_3}(1+A_2A_3)\right\}+\frac{t_c}{A_2}\left\{1-e^{-A_2A_3}\right\}\right]+\frac{A_5 e^{-(\zeta A_4+A_1A_3)}}{A_1}\left[\frac{(1+A_1A_3)}{A_1}+t_c\right] \quad (6.7)$$

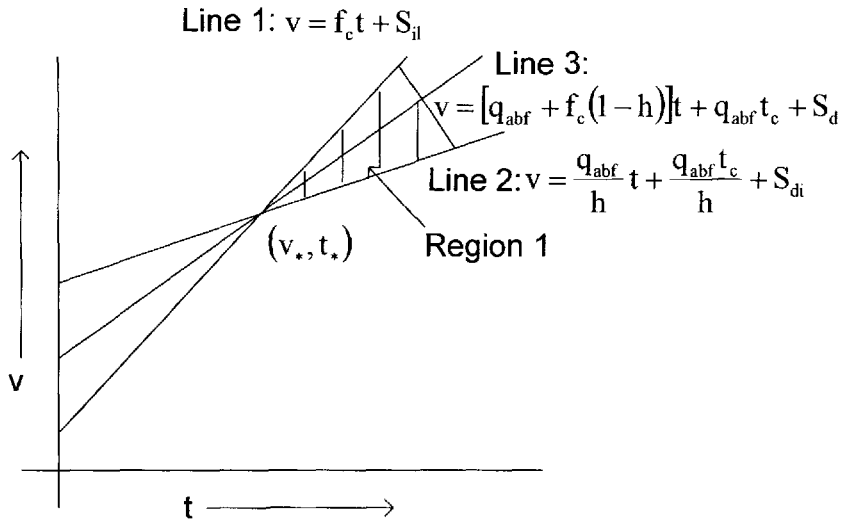


**Fig 6.5:** Region of integration for $P[Q > q]$ in type II urban catchments for $\frac{hS_{dd}}{t_c} \le q_{abf} < f_c h$

For the third range, or when $q_{abf} \ge f_c h$, the relative magnitude of the slopes and the intercepts are exactly the same as those for the third range of $q_{abf}$ of type I urban catchments. Therefore, the region of integration in the v-t plane is also the same. This results in a final expression of $P[Q > q]$ which is the same as Eqn. (6.6). Therefore, by using Eqn.s (6.4), (6.7) and (6.6), the probability of exceedence or the flow duration curve can be determined for type II urban catchments, provided that the local rainfall event statistics and the catchment characteristics are known.

The final forms of $P[Q > q]$ for the two types of urban catchments are summarized below.

**For Type I urban catchments:**

When $q_{abf} \le f_c h$, $P[Q > q] = A_5 \exp(-\zeta A_4)\left[\frac{1}{A_1^2} + \frac{t_c}{A_1}\right]$;

When $f_c h \le q_{abf} < \frac{hS_{dd}}{t_c}$,

$$P[Q > q] = A_5 e^{-\zeta A_4}\left[\frac{1}{A_1^2}\left\{1 - e^{-A_1 A_3}(1 + A_1 A_3)\right\} + \frac{t_c}{A_1}\left\{1 - e^{-A_1 A_3}\right\}\right] + \frac{A_5 e^{-(\zeta A_6 + A_2 A_3)}}{A_2}\left[\frac{(1 + A_2 A_3)}{A_2} + t_c\right];$$

When $q_{abf} \ge \frac{hS_{dd}}{t_c}$, $P[Q > q] = A_5 \exp(-\zeta A_6)\left[\frac{1}{A_2^2} + \frac{t_c}{A_2}\right]$.

**For Type II urban catchments:**

When $q_{abf} < \frac{hS_{dd}}{t_c}$, $P[Q > q] = A_5 \exp(-\zeta A_4)\left[\frac{1}{A_1^2} + \frac{t_c}{A_1}\right]$;

When $\frac{hS_{dd}}{t_c} \le q_{abf} < f_c h$,

$$P[Q > q] = A_5 e^{-\zeta A_6}\left[\frac{1}{A_2^2}\left\{1 - e^{-A_2 A_3}(1 + A_2 A_3)\right\} + \frac{t_c}{A_2}\left\{1 - e^{-A_2 A_3}\right\}\right] + \frac{A_5 e^{-(\zeta A_4 + A_1 A_3)}}{A_1}\left[\frac{(1 + A_1 A_3)}{A_1} + t_c\right];$$

When $q_{abf} \ge f_c h$, $P[Q > q] = A_5 \exp(-\zeta A_6)\left[\frac{1}{A_2^2} + \frac{t_c}{A_2}\right]$.

It is noted that when $q \le q_b$, or equivalently when $q_{abf} \le 0$, $P[Q > q] = 1$ for both types of catchments.

## 6.3 Validation of the Analytical Flow-Duration Relationships

Four hypothetical test catchments were set up to verify the newly derived analytical flow-duration relationships. To generate long term flow series from these test catchments, a 40-year historical rainfall record (1960-1999, non-winter period only for

each year) from the Toronto Pearson International Airport in Ontario, Canada was used. Driven by this input rainfall, continuous simulation of the catchment rainfall-streamflow process was performed using HEC-HMS (USACE 2000).

Instead of using the continuous rainfall record directly, the analytical probabilistic approach requires the statistics of the external characteristics of rainfall events. An IETD of 12 hours was chosen and the required rainfall event statistics are obtained from Adams and Papa (2000) for the Toronto Pearson International Airport ($\lambda$=0.108 $hr^{-1}$; $\zeta$=0.119 $mm^{-1}$; and $\psi$=0.0107 $hr^{-1}$).

HEC-HMS requires the following catchment characteristics: initial deficit, maximum deficit, degree of imperviousness, ultimate infiltration capacity of soils, time of concentration, storage coefficient, and baseflow rate. These catchment characteristics for each of the test catchments are tabulated in Table 6.2. To use the analytical flow-duration relationships, the following catchment characteristics are required: depression storage of the impervious area ($S_{di}$), depression storage of the pervious area ($S_{dp}$), initial soil wetting infiltration of pervious area ($S_{iw}$), ultimate infiltration capacity of the soil ($f_c$), time of concentration ($t_c$), and degree of imperviousness (h%) values. To ensure equivalence, catchment parameter values must be the same (if the definition of the parameters are the same) or properly related (if the definitions are different) between HEC-HMS and the analytical probabilistic approach. Since the definitions of degree of imperviousness and ultimate infiltration capacity of the soil are the same, the values of the two parameters are the same in HEC-HMS models and the analytical expressions.

**Table 6.2:** Catchment characteristics of test catchments

| Catchment Parameters | Test Catchment 1 | Test Catchment 2 | Test Catchment 3 | Test Catchment 4 (variable baseflow)[2] |
|---|---|---|---|---|
| Drainage area (A) (sq.km.) | 5 | 10 | 50 | 20 |
| $f_c$ (mm/hr) | 0.24 | 10 | 36 | 21 |
| h (%) | 80 | 70 | 20 | 50 |
| $S_{dp}$ (mm) | 4.5 | 4.5 | 4.5 | 4.5 |
| $S_{di}$ (mm) | 0 | 0 | 0 | 0 |
| $S_{iw}$ (mm) | 4 | 12.7 | 17.3 | 20.1 |
| $t_c$ (hr) | 1.5 | 1 | 3 | 2.5 |
| K (hr) | 3 | 1.5 | 1 | 2 |
| $t_{ca}$ (hr)[1] | 4.5 | 2.5 | 4 | 4.5 |
| $q_b$ in (c.m.s) | 0.5 | 0.6 | 1 | 0.7 |
| $q_b$ in (mm/hr) | 0.36 | 0.22 | 0.072 | 0.13 |

[1]Indicates the $t_{ca}$ (i.e., $K+t_c$) value used in the analytical flow-duration relationship

[2]Monthly baseflows are: 0.65, 0.65, 0.82, 1.03, 0.81, 0.66, 0.55, 0.55, 0.61, 0.7, 0.8, and 0.73 c.m.s.

For pervious areas of a catchment, the maximum deficit as used in HEC-HMS is defined as the maximum precipitation depth that can fall on the watershed without generating any runoff. Rainfall depth exceeding this deficit will infiltrate the soil mass at a constant rate of $f_c$ (USACE 2000). This definition of maximum deficit is equivalent to $(S_{dp} + S_{iw})$ as used in the analytical probabilistic approach. The sum of $S_{dp}$ and $S_{iw}$ is referred to as the initial losses of the pervious area (Guo and Adams 1998a) and denoted as $S_{il}$. The initial deficit as used in HEC-HMS specifies the initial condition to start the simulation. A value lower than the maximum deficit was used. This value only affects a few initial flow values generated. In constructing FDCs using the generated long-term flow series, these few initial flow values were removed. There is no related parameter in the analytical flow-duration relationship.

For impervious areas of a catchment, HEC-HMS does not account for any depression storage. Thus 100% of the rainfall falling on the impervious area is converted into runoff. In using the analytical probabilistic flow-duration relationship for each hypothetical catchment, $S_{di}$ was specified as 0, to ensure equivalence.

In HEC-HMS, excess rainfall is transformed to direct runoff using the Clark unit hydrograph (UH) method. Two parameters are required in using Clark UH, i.e., time of concentration $(t_c)$ and the storage coefficient (K). The analytical probabilistic FDC model requires a single $t_c$ value representing both the translation and storage effects of a catchment. In HEC-HMS, the storage effect of the catchment is modeled by a linear reservoir with storage coefficient K. For a linear reservoir, K is found to be equal to the average detention time or average time of travel through the reservoir (Guo and Adams 1999b). Therefore, the two Clark UH parameters were added $(\text{i.e.}, t_c + K)$ to determine an equivalent time of concentration $t_{ca}$ to be used in the analytical flow-duration relationship to represent both the translation and storage effect of the catchment.

Average monthly evapotranspiration rates are used in HEC-HMS. The soil moisture volume reduces at these rates during dry periods or interevent times. In this study, the average monthly values inputted to HEC-HMS models were determined from southern Ontario climatological data and range from 1.65 mm/day (December) to 6.33 mm/day (July). In the analytical probabilistic approach, the evapotranspiration mechanism is represented by the usage of a decay coefficient associated with the infiltration capacity recovery curve for the estimation of $S_{iw}$. The detailed derivation of this procedure can be found in Guo and Adams (1998a). To ensure equivalence between HEC-HMS models and the analytical probabilistic approach, this decay coefficient was determined based on southern Ontario conditions as well.

The drainage areas of the four test catchments vary from 5 to 50 $km^2$ to represent a wide range of small urban watersheds. The other characteristics of the catchments are also allowed to vary significantly between the four catchments to cover wider

possibilities. Constant baseflows are assumed for three of the four test catchments. Upon completion of continuous simulation, continuous hourly streamflow data were generated for each of the hypothetical test catchments. FDCs were then constructed from these continuous streamflows. FDCs constructed with the generated streamflows are compared with those obtained directly from the analytical flow-duration relationships. As shown in Figs. 6.6(a) and 6.6(b), for the first two test catchments, the two FDCs are in good agreement. For the third test catchment, as shown in Fig. 6.6(c), the two FDCs are in good agreement for exceedence probabilities that are 0.1% and above. For exceedence probabilities below 0.1%, the two FDCs start to deviate from each other. This is probably due to the rectangular hydrograph assumption made in the derivation process and the fact that the catchment is much larger than the first two test catchments. Since streamflow hydrographs resulting from some rainfall events may be better represented by triangles or trapezoids, the occurrence of extremely high flows may not be represented that well when streamflow hydrographs resulting from all rainfall events are assumed to be approximately rectangular. Larger catchment areas may magnify the resulting discrepancies.

In some climatic regions or catchments, baseflow may vary seasonally throughout the year. One way of accounting for the seasonal variation of baseflow in the proposed analytical probabilistic approach is to use the average baseflow rates. To test how well or poorly the analytical flow-duration relationship compares with that generated from continuous simulation results for catchments with fluctuating baseflows, the fourth hypothetical test catchment has variable baseflow rates in its HEC-HMS model. The drainage area of that catchment is 20 $km^2$ and the catchment characteristics are tabulated in Table 6.2.

(a)

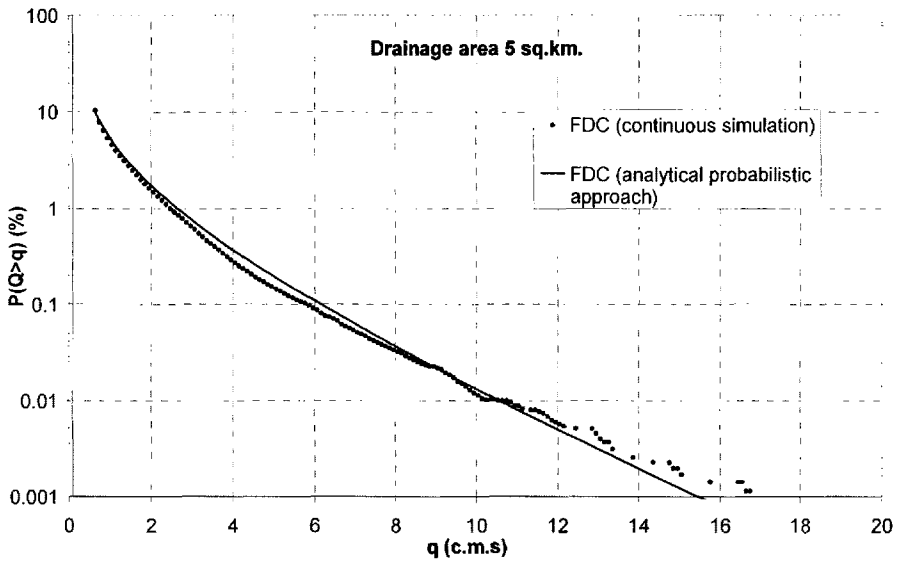
Drainage area 5 sq.km.
FDC (continuous simulation)
FDC (analytical probabilistic approach)
P(Q>q) (%)
q (c.m.s)
100
10
1
0.1
0.01
0.001
0
2
4
6
8
10
12
14
16
18
20

(b)

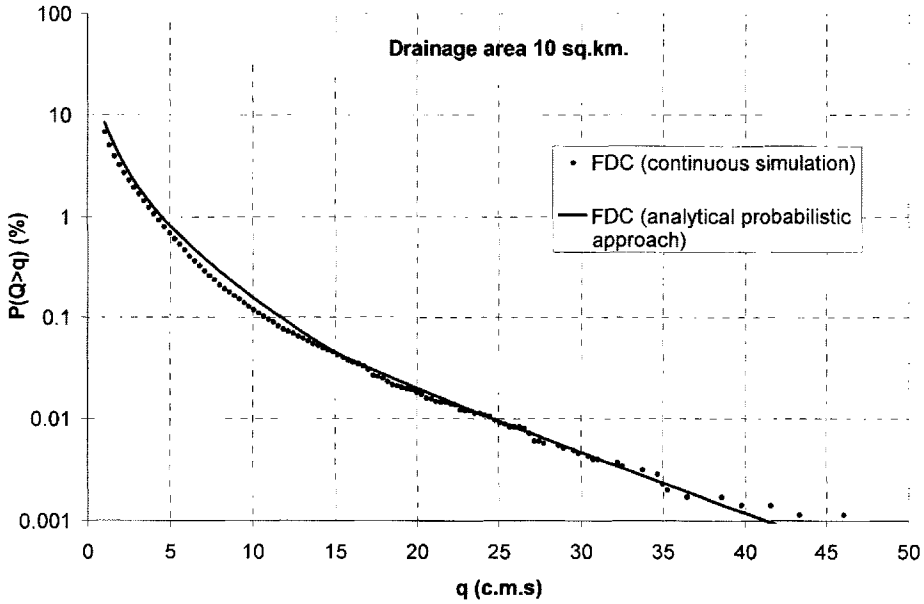
Drainage area 10 sq.km.
FDC (continuous simulation)
FDC (analytical probabilistic approach)
P(Q>q) (%)
q (c.m.s)
100
10
1
0.1
0.01
0.001
0
5
10
15
20
25
30
35
40
45
50

(c)

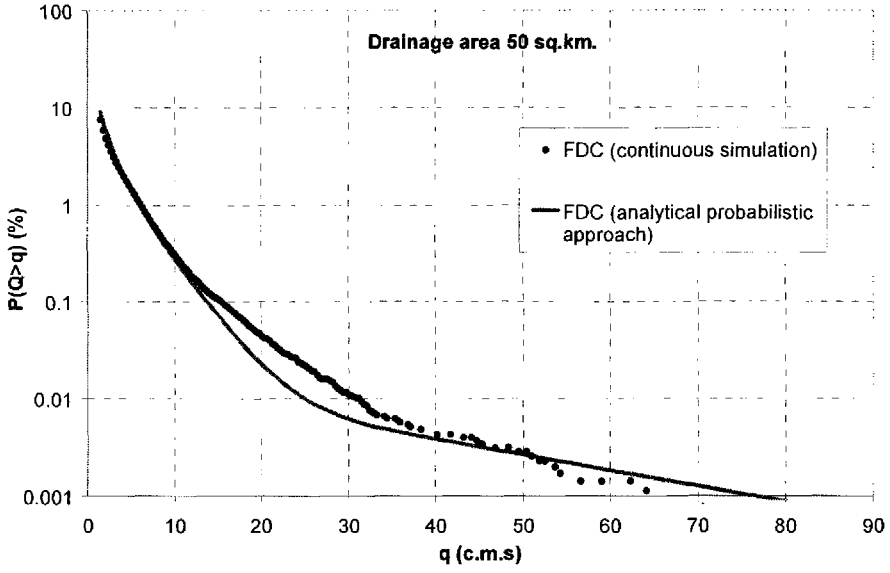


(d)

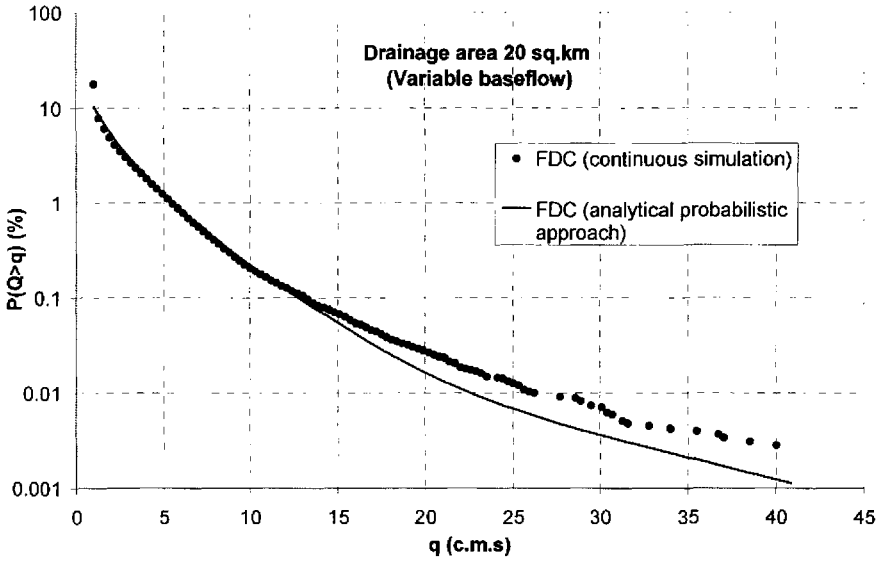


**Fig 6.6:** Comparison of two types of FDCs for different drainage areas [(a) 5 sq.km. (b) 10 sq.km. (c) 50 sq.km. (d) 20 sq.km. with variable baseflow]

Constant per unit catchment area monthly baseflow values determined from the Ganaraska river near Osaca, Ontario, Canada was used as a guide to specify baseflow

fluctuations in HEC-HMS. A single value, i.e., the average of the constant monthly values was used as the baseflow input to the analytical flow-duration relationships. Similar to the other three test catchments, the resulting two FDCs are compared in Fig. 6.6 (d). Fig. 6.6(d) shows that the two FDCs agree well with each other for exceedence probabilities of 0.1% and above. For exceedence probabilities below 0.1%, the general trend of the FDC constructed from continuous simulation results is well captured by the analytical curve, only minor differences exist. This may suggest that, at least for small streams located in Southern Ontario, the degree of variation in baseflows is insignificant and an average constant value may be used with the analytical flow-duration relationships to generate reasonably accurate FDCs.

## 6.4 Summary and Conclusions

In this study, analytical expressions for the determination of the probability that a specific streamflow is exceeded were derived. These closed-form analytical expressions may be used directly to construct flow-duration curves based on upstream catchment and local rainfall characteristics. In deriving these analytical expressions, the pdfs of the external characteristics of rainfall events and an event-based rainfall-runoff transformation function are used. It is assumed that the runoff hydrograph generated from an individual rainfall event is approximately rectangular and the baseflow rate is constant. To verify the reasonableness of these simplifying assumptions, FDCs constructed using the analytical flow-duration relationships were compared to those obtained using streamflow series generated from continuous simulation. The HEC-HMS continuous simulation models do not make the same simplifying assumptions. In the absence of long-term observed streamflow data, FDCs constructed using continuous simulation results can be regarded as accurate.

The main purpose for the construction of FDCs is usually to quantify the relative frequency of occurrence of low, medium and high streamflows. Streamflows with an exceedence probability below 0.1% are usually considered as extremely high or flood flows for many planning or design applications. Comparisons for the four test catchments

all showed close agreements for exceedence probabilities of 0.1% and above. Minor differences exist between analytical FDCs and those constructed from continuous simulation results for exceedence probabilities below 0.1%. This probably indicates that the simplifying assumptions adopted for the derivation of analytical flow-duration relationships are largely acceptable for many applications. To include more possibilities in the validation study, a wide range of catchment characteristics are represented by the four test catchments. In addition, in the continuous simulation of the fourth test catchment, a variable baseflow condition was specified, the magnitude of this baseflow variation was determined according to typical baseflow variations observed in small southern Ontario streams. Good agreement for the fourth test catchment seems to suggest that use of an average baseflow rate would generally not result in unacceptable errors if the interest is in FDCs of small streams.

Implemented in a spreadsheet, the analytical expressions derived in this paper can be a useful tool for water resources engineers. For the many urban stream restoration projects where measured streamflow data are scarce, the expressions can be used to generate FDCs which incorporate the effects of land use and development in the upstream catchment. The closed-form nature of the analytical equations makes numerical solution algorithms unnecessary and minimizes the computational burden. Upon further testing, e.g., comparison with FDCs constructed using observed streamflow data from a specific location, these analytical expressions together with local rainfall statistics may be used in stream restoration studies. Caution should be used in applying the analytical expressions for drainage areas greater than $\approx 50\,\text{km}^2$ and in interpreting the analytical results for exceedence probabilities below 0.1%.

# References:


1. Adams, B.J., Fraser, H.G., Howard, C.D.D., Hanafy, M.S., (1986). "Meteorological Data Analysis for Drainage System Design." *Journal of Environmental Engineering*, 112(5), 827-847.

2. Adams, B.J., and Papa, F., (2000). *Urban stormwater management planning with analytical probabilistic models.* John Wiley Sons, Inc. Printed in the U.S.A.
3. Behera, P.K., Adams, B.J., and Li, J.Y., 2006. "Runoff quality analysis of urban catchments with analytical probabilistic models." *Journal of Water Resources Planning and Management*, 132(1), 4-14.
4. Benjamin, J.R., and Cornell, C.A., (1970) *Probability, Statistics and Decision for Civil Engineers*, McGraw-Hills, New York, U.S.A.
5. Brown, K., (2000). *Urban Stream Restoration Practices: An Initial Assessment.* The Center for Watershed Protection. Elliot City, MD, USA.
6. Chalise, S.R., Kansakar, S.R., Rees, G., Croker, K., and Zaidman, M., (2003). "Management of water resources and low flow estimation for the Himalayan basins of Nepal." *Journal of Hydrology*, 282, 25-30.
7. Chen, J. and Adams, B.J., (2005). "Urban stormwater control evaluation with analytical probabilistic models." *Journal of Water Resources Planning and Management*, 131(5), 362-374.
8. Cigizoglu, H.K., and Bayazit, M., (2000). "A generalized seasonal model for flow duration curve." *Hydrological Processes*, 14, 1053-1067.
9. Cordova, J.R., and Gonzalez, M., (1997). "Sediment yield estimation in small watersheds based on streamflow and suspended sediment discharge measurement." *Soil Technology*, 11, 57-65.
10. Eagleson, P.S., (1972). "Dynamics of Flood Frequency." *Water Resources Research*, 8(4), 878-897.
11. Fennessey, N. and Vogel, R.M. (1990). "Regional flow-duration curves for ungauged sites in Massachusetts." *Water Resources Planning and Management*, 116(4), 530-549.
12. Guo, Y. and Adams. B.J., (1998a). "Hydrologic Analysis of Urban Catchments with Event-based Probabilistic Models 1. Runoff Volume." *Water Resources Research*, 34(12), 3421-3431.
13. Guo, Y. and Adams. B.J., (1998b). "Hydrologic Analysis of Urban Catchments with Event-based Probabilistic Models 2. Peak Discharge Rate." *Water Resources Research,* 34(12), 3433-3443.

14. Guo, Y. and Adams. B.J., (1999a). "Analysis of detention ponds for stormwater quality control." *Water Resources Research*, 35(8), 2447-2456.
15. Guo, Y. and Adams. B.J., (1999b). "An analytical probabilistic approach to sizing flood control detention facilities." *Water Resources Research*, 35(8), 2457-2468.
16. Howard, C. D. D., (1976). "Theory of storage and treatment plant overflows." *Journal of Environmental Engineering, ASCE,* 102( EE4), 709-722.
17. Male, J.W., and Ogawa, H., (1984). "Tradeoffs in water quality management." *Journal of Water Resources Planning Management*, 110(4), 434-444.
18. Mimikou, M. and Kaemaki, S. (1985). "Regionalization of flow duration characteristics." *Journal of Hydrology*, 82, 77-91.
19. Ness, R., and Joy, D.M. (2002). "Performance of natural channel designs in southwestern Ontario." *Canadian Water Resources Journal*, 27(3), 293-315.
20. Petts, G.E., Bickerton, M.A., Crawford, C., Lerner, D.N., and Evans, D., (1999). "Flow management to sustain groundwater-dominated stream ecosystems." *Hydrological Processes*, 13, 497-513.
21. Quimpo, R.G., Alejandrino, A.A., and McNally, T.A. (1983). "Regionalized flow duration for Philippines." *Journal of Water Resources Planning and Management*, 109(4), 320-330.
22. Scholz, J.G., and Booth, D.B. 2001. "Monitoring urban stream: strategies and protocols for humid-region lowland systems." *Environmental Monitoring and Assessment*, 71, 143-164.
23. Searcy, J.K. (1959). "Flow-duration curves." *Water Supply Paper* 1542-A, U.S. Geological Survey, Weston, VA.
24. Singh, K.P. (1971). "Model flow duration and streamflow variability." *Water Resources Research*, 7(4), 1031-1036.
25. Singh, R.D., Mishra, S. K., and Chowdhary, H. (2001). "Regional flow-duration models for large number of ungauged Himalayan catchments for planning microhydro projects." *Journal of Hydrologic Engineering*, 6(4), 310-316.
26. Smakhtin, V.U., (2001). "Low flow hydrology: a review." *Journal of Hydrology*, 240, 147-186.

27. Smakhtin, V.Y., (1999). "Generation of natural daily flow time-series in regulated rivers using a non-linear spatial interpolation technique." *Regulated Rivers: Research and Management*, 15, 311-323.
28. Smakhtin, V.Y., and Masse, B., (2000). "Continuous daily hydrograph simulation using duration curves of a precipitation index." *Hydrological Processes*, 14, 1083-1100.
29. Strevens, A.P., (1999). "Impacts of groundwater abstraction on the trout fishery of the River Piddle, Dorset: and an approach to their alleviations." *Hydrological Processes*, 13, 487-496.
30. U.S. Army Corps of Engineers (USACE), (2000). *HEC-HMS Technical Reference Manual*, CPD-74B. Published by the U.S. Army Corps of Engineers, Davis, Calif.
31. Vogel, R.M., and Fennessey, N.M., (1994). "Flow-duration curves. I: new interpretation and confidence intervals." *Journal of Water Resources Planning and Management*, 120(4), 485-504.
32. Vogel, R.M., and Fennessey, N.M., (1995). "Flow duration curves II: a review of applications in water resources planning." *Water Resources Bulletin*, 31(6), 1029-1039.
33. Yu, P-S and Yang, T-C. (1996). "Synthetic regional flow duration curve for southern Taiwan." *Hydrological Processes*, 10, 373-391.
34. Yu, P-S., and Yang, T-C, (2000). "Using synthetic flow duration curves for rainfall-runoff model calibration at ungauged sites." *Hydrological Processes*, 14, 117-133.
35. Yu, P-S., Yang, T-C., Liu, C-W., (2002). "A regional model of low flow for Southern Taiwan." *Hydrological Processes*, 16, 2017-2034.
36. Zaidman, M.D., Keller, V., Young, A.R., Cadman, D., (2003). "Flow-duration-frequency behavior of British Rivers based on annual minima data." *Journal of Hydrology*, 277, 195-213.

## NOTATIONS

The following symbols are used in this paper:

$A_1, A_2, A_3, A_4, A_5, A_6$ = the designation of these symbols are explained in section 2.4.

b = interevent time (hr)

$D[Q > q]$ = the expected value of duration of a runoff event (hr)

E(t+b) = expected value of runoff event/ interevent cycle (hr)

$f_c$ = ultimate infiltration capacity of the soil (mm/hr)

h = degree of imperviousness (%)

K = storage coefficient (hr)

$P[Q > q]$ = the probability of exceedence of a specific flow rate q during the period of interest per year

$P_{e_1}[Q > q]$ = the first part of the probability of exceedence per runoff event/interevent cycle

$P_{e_2}[Q > q]$ = the second part of the probability of exceedence per runoff event/interevent cycle

Q = average flow rate (mm/hr)

q = a specific flow value, greater than zero (mm/hr)

$q_{abf}$ = the difference between q and $q_b$ (mm/hr)

$q_b$ = constant rate of baseflow (mm/hr)

$S_d$ = summation of the area-weighted depression of the impervious and pervious area, respectively (mm)

$S_{dd}$ = difference between $S_{il}$ and $S_{di}$ (mm)

$S_{di}$ = depression of the impervious area (mm)

$S_{dp}$ = depression of the pervious area (mm)

$S_{il}$ = initial loss in the pervious area (mm)

$S_{iw}$ = initial soil wetting infiltration volume (mm)

t = duration of a rainfall event (hr)

$t_c$ = time of concentration (hr)

$t_*$ = the x coordinate of the point of intersection of the three lines in the v-t plane

v = volume of a rainfall event (mm)

$v_r$ = volume of runoff per rainfall event(mm)

$v_*$ = the y coordinate of the point of intersection of the three lines in the v-t plane

$\theta$ = the total number of runoff event/interevent cycles within each hydrologic year

$\zeta$ = inverse of the average rainfall volume from a series of rainfall events ($mm^{-1}$)

$\lambda$ = inverse of the average rainfall duration from a series of rainfall events ($hr^{-1}$)

$\psi$ = inverse of the average interevent time from a series of rainfall events ($hr^{-1}$)

# Chapter 7

## Conclusions and Future Research

## 7.1 Conclusions

Channel-forming discharge plays an important role in stream restoration. Accurate estimation of effective discharge or other types of channel-forming discharge is the key in carrying out a successful rehabilitation project. Because of the problems associated with the transport effectiveness curve approach of determining $Q_e$, this research focuses primarily on the analytical approach of determining $Q_e$ for small urban catchments. The accuracy of the analytical approach of determining $Q_e$ is dependent on the goodness-of-fit between the frequency distribution pattern of the flow series and the assumed pdf. At the same time it is also dependent on the accurate depiction of sediment transport mechanics. Whether analytical techniques or the transport effectiveness curve approach is used, the determination of $Q_e$ is data intensive. To accurately determine $Q_e$, significant hydrologic and sedimentological data are required. In the following, the major contributions of this thesis through each of its papers and how each of the papers effectively deals with some of the issues/concerns associated with $Q_e$ are presented.

- The major conclusions from the first paper about the analytical investigation of $Q_e$ from mixed exponential distribution are as follows:
  1. Below drainage areas of 10 $km^2$, the conventional lognormal pdf does not approximate the frequency distribution pattern of the flow series that well. Therefore, for small streams below the critical drainage area, the conventional lognormal pdf is not the best choice for analytically determining $Q_e$.
  2. Goodness-of-fit tests indicate that the mixed exponential distribution better represents the frequency distribution pattern of the flow series. This implies that for those small streams this proposed distribution works better than the

conventional lognormal distribution and ultimately aids in improving the estimation of $Q_e$.

3. $Q_e$ values determined from the mixed exponential distribution were compared with those determined from the transport effectiveness curve approach. The results show a good and even better conformance than the $Q_e$ values determined from lognormal distributions.
4. $Q_e$ values determined from the mixed exponential distribution model were found to be more accurate than those determined from lognormal distribution function not only for small streams but for large streams as well.

- Encouraged by the improvement of accuracy in $Q_e$ values determined from mixed exponential distributions, the mixed gamma distribution was introduced in the research. The mixed exponential is actually a special type of gamma distribution. Therefore, if the mixed exponential distribution improved the results, the mixed gamma distribution would have a similar outcome and would be even more generally applicable. Instead of investigating streams of widely varying range of sizes, this paper primarily focused on small streams that had a definite percentage of zero flows. The major conclusions from the paper investigating the analytical estimation of half discharge from a mixed gamma distribution were as follows:

1. Goodness-of-fit tests of selected southern Ontario streams with a definite percentage of zero flows revealed that they are better approximated by gamma than the conventional lognormal distributions. Therefore, the mixed gamma distribution was introduced and it was found that this distribution also outperformed the lognormal distribution.
2. In this paper, $Q_{1/2}$ and f-load discharges were analytically determined for the first time from the mixed gamma distribution. Before this, the only analytical solution of $Q_{1/2}$ that existed was derived from a lognormal distribution. This analytical derivation has in some way broadened the applicability of the analytical estimation of half discharge, which can now be applied to small streams that have a definite percentage of zero flows.

3. A comparison of $Q_f$ with $Q_e$ for the selected streams for a wide range of exponent of sediment rating curve (b) values revealed that when $b \geq 2$, $Q_e$ values can be used analogously with $Q_{0.6}$. This indicates that if it becomes difficult in graphically determining $Q_e$, the f-load discharge, corresponding to an f value of 0.6 can be used as a reasonable substitute. However this substitution can only be made under the circumstances where b values are greater or equal to 2.

- The effective discharge at the catchment outlet or at a particular stream reach is dependent on upstream catchment characteristics and the sediment transport mechanics. These upstream catchment characteristics involve degree of imperviousness, drainage area, infiltration capacity of the soil, etc. In the paper the most critical hydrological and sedimentological parameters pertaining to $Q_e$ were investigated. The major findings from the third paper are:

1. The effective discharge is sensitive firstly, to the exponent of the sediment rating curve, secondly, to the storage coefficient of the catchment and thirdly, to the time of concentration.
2. The exponent to the sediment rating curve is 4 and 2 times more important than the storage coefficient and the time of concentration, respectively, for $Q_e$.
3. Discharges corresponding to return periods of 1.5 and 2.5 years ($Q_{1.5}$ and $Q_{2.5}$) were found to be highly sensitive to the degree of imperviousness, moderately sensitive to the storage coefficient and least sensitive to the time of concentration.
4. It was found that $Q_e$ and $Q_{1.5}$ or $Q_{2.5}$ can be used analogously when b is within the range of 3.5 and 5. Below this limit usage, of these two types of discharge indices analogously can cause deleterious effect in restoration projects.

- In spite of the significant development in the analytical estimation of $Q_e$ and $Q_{1/2}$ values, the applicability of these discharge indices in the case of degraded streams is often not possible because of the lack of data pertaining to streamflow and

sediment transport. The analytical probabilistic approach can in some way compensate for this shortcoming as the resulting probabilistic expressions are only dependent on catchment and rainfall characteristics. However, before applying this analytical probabilistic approach in a real stream, it is necessary to verify how this procedure performs in a practical design problem. The major conclusions from the paper are:

1. The case study demonstrated that peak discharges estimated by the analytical probabilistic stormwater model (APSWM) were generally in good agreement with those from the design storm approach.
2. Discrepancies caused by subcatchment aggregation and the difference in rainfall data analysis are of the same order of magnitude (25%).
3. This study also shows that a constant time of concentration may still be used in APSWM to better conform to the original assumption invoked in the derivation of equations forming the backbone of the analytical probabilistic approach. The reduction in discrepancy resulting from the use of variable time of concentration in APSWM is insignificant.

- Encouraged by the good performance of the analytical probabilistic approach for determining peak discharge in practical design problems, the analytical probabilistic approach was applied for the determination of flow duration relationships. The major conclusions from the paper are:

1. Closed form analytical expressions of the probability of exceedence of streamflow rate were determined. This probability of exceedence of streamflow is the same as the percentage of time that a particular flow is exceeded, which can be used to determine the flow duration curves.
2. The resulting flow duration curves from the derived analytical probabilistic expressions do not require streamflow information. Instead the curve can be plotted solely from the catchment and meteorological information that is more readily available.
3. Flow duration curves were determined from the derived closed-form analytical expressions, which were compared to those obtained from simulated streamflow data (data generated from continuous simulation). The

flow duration curves from closed form analytical equations conformed well to those constructed using simulated streamflow data. The analytical flow-duration relationships can be used together with a sediment rating curve for the estimation of the effective discharge.

## 7.2 Concluding Remarks

In today's socioeconomic perspective, sustainability is a key point in public policy making. The objective of stream rehabilitation/restoration is to make the stream ecologically sound and sustainable. A stream can sustain the natural and artificial loading if it is designed from a holistic point of view. This means that the hydrological, hydraulic, sedimentological and climatological factors associated with the study area should be carefully considered during stream rehabilitation. The conventional notion of bankfull discharge as the channel-forming discharge is unable to computationally or figuratively take all these important factors into consideration. As a result, streams rehabilitated based on the bankfull discharge are grossly over designed or under designed, which does not allow the adequate development of flood plains. The effective discharge provides the opportunity of utilizing different environmental factors in the rehabilitation process, resulting in a more reliable design scheme.

## 7.3 Recommendations for Future Research

These are exciting times as there appears to be a growing interest in stream rehabilitation, particularly as it relates to the existence and estimation of channel-forming discharge. The restoration community is gradually realizing that determining the channel-forming discharge for urban streams is a complicated but important process. Therefore, firstly, for these urban streams the conventional notion of bankfull discharge as the channel-forming discharge needs to be abandoned. Secondly, other discharge indices, e.g., $Q_e$ and $Q_{1/2}$ should be carefully evaluated for accurate estimation of the true channel-forming discharge. In spite of the work that has been conducted so far, there still remains room for additional research on this topic. The following research work can be undertaken to improve our understanding of the effective discharge even further.

1. In addition to the lognormal and gamma pdf, the daily streamflow data have been found to be well approximated by the generalized Pareto (GP) distribution (Vogel and Fennessey 1993). This special pdf can be used for determining discharge indices such as $Q_e$ and $Q_{1/2}$. The results can be used for comparing with those values obtained from the mixed exponential and gamma pdfs.
2. The global sensitivity analysis results revealed that $Q_e$ is most sensitive to the exponent of the sediment rating curve (b). The latter term b depicts the mobilization phenomenon of bedload and the ease of transport of suspended sediment load. However, the transport phenomenons of each type of sediment load is different and are dependent on various sediment characteristics ranging from the specific weight, ratio of grain shear stress for bedload to the average sediment concentration for suspended sediment load. Alongside these sedimentological characteristics, hydraulic parameters of the stream, e.g., average velocity of flow, slope, etc. are also involved in the process of sediment transport. As a part of future research, global sensitivity analysis can be applied for determining the most critical sedimentological or hydraulic parameters associated with the exponent of the sediment rating curve. This would allow restoration engineers to put more emphasis on those critical hydraulic and sediment characteristics which may include, mean diameter of sediment particles, angularity or even grain size distributions.
3. In deriving the analytical probabilistic flow duration relationship, the generated average runoff resulting from a rainfall event was assumed to have a rectangular distribution. Assuming a triangular distribution as the generated runoff would be physically more representative of the runoff generation and depletion process. At the same time, it should be remembered that the triangular distribution would be mathematically more complicated. Derivation of the analytical probabilistic flow duration relationship based on a triangular distribution can be an interesting and challenging research direction.
4. The fourth recommended research direction is also related to the analytical probabilistic flow duration relationship. To reduce the mathematical complexity in the rainfall-runoff relationship, in-between precipitation events it was assumed

that the stream is sustained by a constant baseflow. However, in real streams the baseflow between precipitation events does not remain constant, especially if the IETD is significantly long. Under most circumstances the reduction of baseflow between precipitation events is expressed by a baseflow recession curve. The baseflow recession curve often takes the form of an exponential decay, as shown in Eqn. (7.1).

$$Q(t) = Q_0 e^{-(t-t_0)/k} \tag{7.1}$$

In Eqn. (7.1) $Q_0$ is the flow at the time of $t_0$ and k is the exponential decay constant. Eqn. (7.1) with certain modifications can be used in determining the analytical flow duration relationship. This is another research direction where there is possibility for improvement of the accuracy of the results.

5. Finally, although the initial goal was to apply the analytical probabilistic approach for determining $Q_e$, combining the sediment rating curve with the pdf determined from Eqns. (6.4) to (6.7), the resulting transport effectiveness term becomes mathematically cumbersome. Afterwards, the differentiation of the effectiveness term does not improve the situation either. Therefore, a more efficient mathematical scheme should be investigated for determining $Q_e$ from the analytical flow duration relationship derived in this research. The solution procedure adopted by Vogel et al. (2003) for determining $Q_{1/2}$ could be a good starting point for future research.

# References:


1. Vogel, R. M., Stedinger, J. R., Hooper, R. P., (2003) "Discharge indices for water quality loads." *Water Resources Research*, 39(10), doi: 10.1029/2002WR001872, 2003.
2. Vogel, R.M. and Fennessey, N.M. (1993) "L-Moment diagrams should replace product moment diagrams." *Water Resources Research*, 29(6), 1745-1752.

# *Appendix A*

## Thesis Related Paper

Quader, A., Guo, Y., and Bui, T., 2006. Discussion of 'Analytical Estimation of Effective Discharge', Peter Goodwin (2004), ASCE Journal of Hydraulic Engineering, 132(1), 112-114.

Urbanization has altered the physical, chemical and biological characteristics of many streams. Urban stream restoration is necessary but challenging. There is still no consensus on the overall methodology, the selection of restoration techniques, the selection of the design discharge (bankfull discharge, effective discharge, or discharge with a particular recurrence interval), and the design of the meandering characteristics. This paper deals with a critical issue in stream restoration projects, i.e., the estimation of effective discharge, $Q_e$. Although a number of issues related to $Q_e$ have been systematically described and discussed by the author in this paper, the discusser feels that a few additional points related to $Q_e$ must be addressed and clarified.

## A.1 Analytical Solution of $Q_e$

The analytical solution developed by the author for estimating $Q_e$ is based on the differentiation of the term $\Phi$ [product of $Q_s$ and f(Q)] with respect to Q and equating it to zero. Solution of equation (4), provides the maxima of $\Phi$, which is the discharge transporting the maximum amount of sediment load. The author investigates six types of frequency distributions and determines the corresponding $Q_e$ for each type. One of those frequency distributions is the two-parameter lognormal (LN). Nash (1994) estimated $Q_e$ for a LN distribution using the same methodology. However, the analytical solution derived by Nash (1994) over predicted $Q_e$, as he omitted the Q term in the denominator of the LN distribution [equation (1), in Nash (1994)]. The author of this paper has rectified that error.

Nash (1994) also concluded that $Q_e$ is independent of the coefficient $\alpha$ in the sediment rating curve [equation (2)], similar to the findings of this paper. The fact that $\alpha$ does not influence $Q_e$ has been strengthened by this paper even further as the analytically estimated $Q_e$ values for all six types of frequency distributions are independent of $\alpha$.

## A.2 Sediment Rating Curve

To investigate the influence of the variability of b, the author estimated $Q_e$ based on Brownlie and Mayer-Peter Mullar's equations. The Mayer-Peter Mullar's equation was based on laboratory experiments on sediment particles ranging from 6.4 to 30 mm

and more applicable to coarse sediment (Chang, 1988). Whereas, Brownlie's equation was derived from laboratory experiments on sand bed followed by multiple regression analysis, using a data source where the mean sediment particle size ranged from 0.088 to 2.8 mm (Brownlie, 1981). Both the Russian river (Klamt et al., 2000) and the Red river are gravel-bed streams. Therefore there is a high probability that the Brownlie's equation may not be applicable for both these rivers. The discusser feels that additional information on the range of the sediment particle size would have allowed the reader to better understand the applicability of the empirical coefficients and the two bedload transport equations.

From the analytical solutions for different forms of frequency distributions it is clear that $Q_e$ is strictly a function of the frequency distribution parameters and $\beta$. The author reports that the values of $\beta$ for bedload is higher than suspended bed material load, resulting in a higher $Q_e$ value for bedload rating curve in comparison to the suspended load rating curve for the Red River. However, no information on the $\beta$ value of bedload for the Russian River is provided in the paper. Therefore, the discusser feels that a general conclusion about the values of $\beta$ for different types of sediment loads cannot be reached from this paper. Furthermore, Nash (1994) concluded from a brief literature review that the value of $\beta$ for the suspended load and the bedload are the same. This difference in conclusion may need further investigation.

## A.3 Best Fit Analysis

From this paper it can be inferred that the accuracy of the estimation of $Q_e$ depends on the goodness of fit between the observed flow record and the assumed frequency distribution. The author concludes that for the Red River and the Russian River, the LN and G distribution provide the best fit with the observed flow record, while the N distribution produces the poorest fit. However, it would have been more helpful, if the author provided some information on the $R^2$, residual values or $\chi^2$ test performed at a certain confidence interval between the assumed theoretical frequency distributions and the observed flow record.

## A.4 Drainage Area

A literature review of urban stream restoration projects indicates that the drainage area of the restored urban streams is usually very small, significantly lower than the drainage basins of the Red River and the Russian River. A number of stream restoration projects have reported drainage areas even below 1 $km^2$. A preliminary study shows that the frequency distribution of very small drainage areas may not be any of the six types of frequency distributions that have been studied in this paper. As the accuracy of the analytical approach depends on the goodness of fit between the observed flow record and the assumed frequency distribution, for very small urban catchments, the derived analytical solutions for $Q_e$ may not be applicable. Furthermore, most stream restoration designs are for future conditions of the watershed. Under the changing hydrologic conditions of the watershed, the flow frequency distribution will change as well.

## A.5 Recurrence Interval of $Q_e$

Papers dealing with $Q_e$ have always given the approximate recurrence interval of the estimated $Q_e$ for ease of reference. In this paper, the author does not provide any information on the recurrence interval of the estimated $Q_e$ values. The author could have used an annual flow or a partial duration series to estimate the recurrence interval of $Q_e$. According to Nash (1994), the recurrence interval of $Q_e$ is the inverse of $P(Q \geq Q_e)$. $P(Q \geq Q_e)$ can be estimated by integrating a particular frequency distribution from $Q_e$ to $\infty$. For the six types of frequency distributions the definite integration can prove to be very complicated. Nash (1994) in his paper did not show the final mathematical form of the recurrence interval for the LN distribution. From the six types of frequency distributions, for the N distribution, the recurrence interval ($T_R$) of $Q_e$ can be estimated from the following two equations, which have been derived by the discusser.

$$P(Q \geq Q_e) = 0.5\left[\mathrm{Sgn}(\sigma) - \mathrm{erf}\left(\frac{Q_e - \mu}{\sqrt{2}\sigma}\right)\right] \tag{1a}$$

$$T_R = \frac{1}{P(Q \geq Q_e)} \tag{2a}$$

In Eqn. (1a) Sgn and erf are the signum and the error function, respectively; $Q_e$ is the effective discharge; $\mu$ and $\sigma$ are the mean and standard deviation of the observed flow record, respectively. The value of Sgn($\sigma$) is equal to 1, and 0 corresponding to a positive, and zero value of $\sigma$. In Eqn. (2a) $T_R$ is the recurrence interval of $Q_e$. Eqn. (1a) has been derived for the simplest form of frequency distribution, i.e., the N distribution. For the LN, LN3, G, P3 and LP3 frequency distributions, the form of Eqn. (1a) will be even more complicated. For a hypothetical test catchment, where the flow series is normally distributed, the variation of $T_R$ for different values of $\mu$ and $\sigma$ is determined based on Eqns. (1a) and (2a) and presented in Table 1.A.

**Table 1.A:** Variation of $T_R$ for different values of $\mu$ and $\sigma$

| $\mu$ ($m^3$/sec) | $\sigma$ ($m^3$/sec) | $Q_e$ (N distribution) | $T_R$ (yr) |
|---|---|---|---|
| 0.9 | 1.287 | 2.32 | 7.45 |
| 2.12 | 0.1 | 2.13 | 2.16 |
| 8.94 | 10.74 | 20.3 | 6.89 |

Table 1.A indicates that for a N frequency distribution, changing the values of $\mu$ and $\sigma$ causes a large variation in the analytically estimated [Eqns. (1a) and (2a)] $T_R$ values, ranging from 2 to 8 years. Whereas, the commonly assumed recurrence interval of $Q_e$ is 1.5 to 2 years.

The analytical framework for estimating $Q_e$ as presented in this paper depends on the frequency distribution pattern and the sediment rating curve. The accuracy of the analytical approach strongly depends on the goodness of fit between the assumed frequency distribution and the observed flow record. To cover the wide range of flow distribution pattern in different climatic and geographic regions, additional frequency distributions need to be taken into consideration for the estimation of $Q_e$.

## References:


1. Brownlie, W.R., 1981. "Prediction of Flow Depth and Sediment Discharge in Open Channel", Rep. No. KH-R-43A, W.M. Keck Laboratory of Hydraulics and Water Resources, California Institute of Technology, Pasadena, Calif., 232.
2. Chang, H.H., 1988. "Fluvial Processes in River Engineering", Krieger Publishing Company, Florida.
3. Klamt, R., Otis, P., Seymour, G., Blatt, F., 2000. "Review of Russian River Water Quality Objectives for Protection of Salmonid Species Listed under the Federal Endangered Species Act", Prepared by Regional Water Quality Control Board, North Coast Region, 5550 Skylane Boulevard, Suite A, Santa Rosa California 95403.
4. Nash, D.B., 1994. "Effective Sediment-Transporting Discharge from Magnitude-Frequency Analysis", Journal of Geology, Vol. 102, pp. 79-95.